Tumoral and peri-tumoral vascularization in NeuroOncology: the approach of MRI

Zhen Jiang

Université de Grenoble & Université de Soochow

THÈSE COTUTELLE

Spécialité: Biotechnologie, Instrumentation, Signal et Imagerie pour la Biologie, la Médecine et l'Environnement

Docteur de l'Université de Grenoble: **Zhen JIANG**

Approche par IRM de la Vascularisation Tumorale et Peri-tumorale en Neuro-Oncologie

Soutenue le 23 septembre 2010, à Suzhou

COMPOSITION DU JURY:

Pr. Jean-François LE BAS *Clinique Universitaire de Neuroradiologie et IRM, CHU de Grenoble, France*	Codirecteur
Pr. Alexandre KRAINIK *Clinique Universitaire de Neuroradiologie et IRM, CHU de Grenoble, France*	Codirecteur
Pr. Chun-feng LIU *Service de Neurologie, Hôpital sino-français de Suzhou (CHU de Suzhou), Chine*	Codirecteur
Pr. Xin-sheng DING *Université de Nankin, Chine*	Rapporteur Président
Pr. Jean-Claude FROMENT *Service de Neuroradilogie, Hôpital Neurologique de Lyon, France*	Rapporteur
Pr. Qing LAN *Service de Neurochirurgie, Hôpital sino-français de Suzhou (CHU de Suzhou), Chine*	Examinateur

---

中国·苏州大学 – 法国·格勒诺布尔大学

联合培养博士学位论文

脑肿瘤及瘤周血管生成的磁共振成像研究

（Tumoral and peri-tumoral vascularization in NeuroOncology: the approach of MRI）

姓　　名：　蒋震

专业名称（中方）：　神经病学

专业名称（法方）：　医学、生物学信号与成像

研究方向：　神经影像学

中方导师：　刘春风　教授

法方导师：　Alexandre KRAINIK　教授

Jean-François LE BAS　教授

Remerciements

Ce travail de thèse s'inscrit dans une collaboration institutionnelle entre l'Hopital Universitaire Sino-Français de Suzhou et le CHU de Grenoble, collaboration qui s'inscrit elle même dans le cadre d'un jumelage entre nos deux villes.

Je tiens tout d'abord à remercier le professeur **Jean-François LE BAS**, co-directeur de ma thèse, pour m'avoir accueilli au sein de l'unité IRM de CHU Grenoble et pour son soutien tout de long de ma thèse pendant ces deux années de séjour en France.

Je remercie sincèrement le professeur **Alexandre KRAINIK**, co-directeur de ma thèse, dont la grande disponibilité et la patience m'ont permis de travailler dans les meilleures conditions et pour l'ensemble du savoir pratique et théorique qu'il m'a transmis.

Cette thèse n'aurait pas du aboutir sans les soutiens du professeur **Chun-feng LIU**, co-directeur chinois de ma thèse, qui m'a encouragé et donné l'occasion de faire des études en France.

J'adresse un grand merci à tous les membres de l'unité IRM de CHU Grenoble et de l'équipe 5 de l'unité U836, en particulier à **Irène TROPRÈS**, **Caroline SALON**, **Nadine MICOUD**, **Sylvie GRAND**, pour leurs aides amicales.

Je remercie l'UJF (bourse EIFFEL), le CHU de Grenoble et la Région Rhône-Alpes (Programme MIRA) qui m'ont aidé financièrement pendant mes séjours en France.

Pour finir, tout ce travail n'aurait pas pu avoir lieu sans le soutien inconditionnel de ma femme, de mes parents, et de ma chère fille. Ils m'ont soutenu depuis le 1er jour de cette thèse. Ils ont toujours été derrière moi à m'encourager, par téléphone et méls lorsqu'ils n'étaient pas à mes cotés.

À mes parents, Hui-ren et Feng-lin

À ma femme Sha-fei, et à ma fille Ning

致谢

首先感谢我的法国导师 **Jean-François LE BAS** 教授，能接受我在格勒诺布尔附属医院磁共振室进行博士论文的研究工作。在法国总共两年的时间里，他不仅在生活上给予了我无微不至的关怀，还在临床与科研工作中给予了悉心的指导。

真诚地感谢我的法国导师 **Alexandre KRAINIK** 教授。他渊博的学识与耐心为我创造了良好的研究工作环境，开拓了我在磁共振功能成像领域的视野。他传授给我的知识让我受益匪浅。

由衷感谢我的中方导师**刘春风**教授。没有他的鼓励与支持，这项论文研究工作将无法圆满完成。

十分感谢格勒诺布尔大学附属医院磁共振室的同事们以及法国国家卫生与健康研究院 836 研究所第 5 研究团队成员们的热忱帮助，特别是 **Irène TROPRÈS**, **Caroline SALON**, **Nadine MICOUD**, **Sylvie GRAND**。

非常感谢约瑟夫·傅立叶大学为我争取到法国外交部 ÉGIDE“埃菲尔精英”博士奖学金以及 Rhône-Alpes 地区奖学金。

最后，感谢我的妻子、父母和可爱的女儿给予了我无私的奉献与支持，尽管这三年来很多时候我们只能通过电话与电子邮件互勉。

此论文也献给我亲爱的父母与妻女

Contents

Introduction

Primary brain tumors are one of the top 10 causes of cancer-related deaths [Wrensch *et al.* 2002]. In France, about 15 to 16 per 100,000 persons are diagnosed with these tumors each year [Bauchet *et al.* 2007]. Recent epidemiological studies revealed that the incidence rate of primary brain tumors has increased over the past few decades, in both developed and developing countries [Chakrabarti *et al.* 2005; 宋冰冰 *et al.* 2008; 翟秀伟 *et al.* 2008; Nasseri *et al.* 2009]. Although the population with primary brain tumors accounts for a relative small percent of all malignant cancers, the aggressive nature of some types of these tumors and tumoral location in/near functional brain areas can impair patients in their daily life, and leads to a high fatality.

Epidemiological survey has indicated that glioma is the most frequent primary brain tumor in adults[Bauchet *et al.* 2007]. In order to survive and proliferate, the gliomas are strongly dependent on the development of a new vascular network that occurs primarily by angiogenesis[Jouanneau 2008]. And the latter was considered as an important factor which is highly related to the tumoral malignancy[Daumas-Duport *et al.* 1997a; Daumas-Duport *et al.* 1997b].

However, due to the over-expression of proangiogenic cytokines, these new tumor vessels are frequently dilated, tortuous, and hyperpermeable[Jain *et al.* 2007]. This abnormal tumor vascular network may results in heterogeneity of blood flow in different areas within tumor. With tumor proliferation and its disorganized vascularization, the perfusion status and the vascular function both in tumor and in adjacent brain tissues will change. Thus, for development of individualized therapy to improve outcome in patients with gliomas, the characterization of tumoral tissue and pathophysiological changes in tumoral vicinity is undoubtedly crucial.

Nowadays, besides anatomic and structural information, physiologic status of brain tumors and adjacent parenchyma can also be noninvasively investigated by modern

magnetic resonance imaging (MRI) techniques. These imaging advances have improved the diagnostic, the guiding of surgical resection, the planning of radiotherapy, and the outcome evaluation in patients with gliomas[Young 2007]. For example, tumor vascularity and its neighboring cortical function, which are very important for tumor growth and treatment, can be characterized respectively using dynamic susceptibility contrast (DSC) perfusion MRI and blood oxygenation level-dependent functional MRI (BOLD fMRI).

DSC perfusion MRI relies on the measurement of the T2 or T2* decrease during the first pass of an exogenous endovascular tracer through the capillary bed, using the ultrafast imaging technique, most commonly the echo plannar imaging (EPI), to record the changes of tracer concentration[Grandin 2003]. The tracer is gadolinium chelate, which is also for use as the conventional MR imaging contrast agents, injected as tight intravenous boluses using a power injector[Rosen *et al.* 1990]. By means of developed medical image processing software, parameters about brain hemodynamic can be calculated in a few minutes from the time-intensity curves measured in each pixel. The most commonly calculated parameters are: time-to-peak (TTP), mean-transit-time (MTT), cerebral blood volume (CBV) reflected the area under the curve, and cerebral blood flow (CBF), equaling to CBV/MTT. The corresponding parametric maps are then reconstructed. They do not give the quantitative measurements of brain hemodynamics, but can be interpreted visually or semi-quantitatively by calculating the ratio between the values in a ROI placed in the abnormal area and a mirror ROI placed in the contralateral area considered as a normal reference, providing very useful information for clinical settings.

As angiogenesis is a requirement for tumor growth, these aforementioned perfusion parameters have been utilized as MRI surrogate markers of angiogenesis for characterizing gliomas. The correlation between elevated CBV and increased vascular density has been investigated in mouse glioma models as well as in human tissue [Aronen *et al.* 2000; Pathak *et al.* 2001]. And the heterogeneity in the distribution of CBV has been revealed by some studies of CBV in gliomas, which may likely reflect the known underlying heterogeneity in tumor vasculature. Therefore, DSC perfusion MRI has contributed to the

differentiation of the tumor grade, generally speaking, high-grade gliomas with neovascular proliferation and high CBV values, with respect to low-grade gliomas with low CBV values. DSC can also offer the complementary information to evaluated the response to treatment, differentiate tumor recurrence from radiation necrosis, and distinguish tumor from some glial-tumor mimic pathological changes such as untypical infection, tumefactive multiple sclerosis lesions.…[Cha *et al.* 2002; Akella *et al.* 2004; Holmes *et al.* 2004]. With an optimized threshold value of relative CBV (rCBV), DSC has been considered as a valuable technique to evaluate the clinical outcome of patients with gliomas[Law *et al.* 2006a; Law *et al.* 2006b; Hirai *et al.* 2008; Law *et al.* 2008].

Of all gliomas, oligodendrogliomas represent approximately 20%. They originate from oligodendrocytes and affect preferentially young adults (mean age: 35 years) [Daumas-Duport *et al.* 1997b]. In a comparative analysis of rCBV in patients with low-grade astrocytoma or other low-grade oligodendroglioma, Cha *et al.* reported that rCBV values were significantly higher in patients with oligodendroglioma in comparison to those with astrocytoma[Cha *et al.* 2005]. Up to now, there are few studies about the aspect of diagnosis and prognostic using DSC MR imaging just focusing on a large sample group of patients with oligodendrogliomas. **It then became the first objective of the study for this doctoral thesis (See Chapter II).**

To map functional brain regions, BOLD fMRI uses deoxyhemoglobin as an intrinsic contrast agent. Its paramagnetic property can shorten T2* relaxation time. During brain activation, the increased cerebral blood flow (CBF) in the capillary bed of the cortex associated with neural activity results in a localized decrease of deoxyhemoglobin-to-oxyhemoglobin ratio. This change in the concentration of deoxyhemoglobin leads consequently to an increase in the signal intensity in the local brain area using T2* sensitive MRI sequences[Ogawa *et al.* 1990; Ogawa *et al.* 1992; Kim *et al.* 1999]. Owing to its contribution of physiologic information and noninvasive characteristic, BOLD fMRI has become probably the most widely-used neuroimaging technique to map eloquent brain areas before surgical resection of brain tumors and to investigate lesion-induced cortical

reorganization[Atlas *et al.* 1996; Maldjian *et al.* 1997; Schulder *et al.* 1998; Roux *et al.* 1999; Krainik *et al.* 2003; Krainik *et al.* 2004].

However, several clinical studies showed that the fMRI activations were decreased in the vicinity of brain tumor when compared to the homologous activation in the contralateral hemisphere[Holodny *et al.* 2000; Schreiber *et al.* 2000; Fujiwara *et al.* 2004; Krainik *et al.* 2004; Ulmer *et al.* 2004; Liu *et al.* 2005; Hou *et al.* 2006; Ludemann *et al.* 2006; Chen *et al.* 2008]. Because these changes may provide false negative results and simulate false hemispheric dominance for language, as well as pseudo lesion-induced cortical reorganization, the reliability of fMRI application in these patients has been debated[Inoue *et al.* 1999; Fujiwara *et al.* 2004; Ulmer *et al.* 2004].

In fact, BOLD fMRI reflects an incompletely understood coupling of neural activity, oxygenation, and basal perfusion[Logothetis *et al.* 2004]. Despite a roughly linear relationship between neural activity and the BOLD signal, experimental and clinical evidences showed that hemodynamic response vary across physiological and pathological conditions according to different populations, cortical areas and brain lesions[D'Esposito *et al.* 2003]. Changes in basal perfusion may explain impaired peritumoral activation in the vicinity of hypervascularized brain tumors[Hou *et al.* 2006; Ludemann *et al.* 2006]. Altered functional mechanisms of brain perfusion have been also suggested in patients with brain tumors[Ulmer *et al.* 2004; Liu *et al.* 2005; Hou *et al.* 2006; Ludemann *et al.* 2006; Chen *et al.* 2008], as well as in patients with vascular risk factors and stroke[Rother *et al.* 2002; Hamzei *et al.* 2003; Rossini *et al.* 2004; Krainik *et al.* 2005; Girouard *et al.* 2006].

Although different physiological mechanisms are engaged, experimental changes of brain perfusion using vasoreactivity were used to estimate the vascular component related to neural activity detected by BOLD fMRI[Kastrup *et al.* 2001; Cohen *et al.* 2002; Rother *et al.* 2002; Hamzei *et al.* 2003; Krainik *et al.* 2005; Haller *et al.* 2008]. Experimental calibration of the vascular response during CO_2 or O_2 challenge allows quantitative fMRI of oxygen consumption[Stefanovic *et al.* 2005; Chiarelli *et al.* 2007]. Actually, quantitative

fMRI remains difficult in clinical practice because of technical requirements for data acquisition and analyses. However functional MRI of brain perfusion would be helpful to better identify brain regions with impaired vascular function and to improve image interpretation[Hamzei *et al.* 2003; Krainik *et al.* 2005]. **Thus, the second objective of the study for this doctoral thesis was performed to identify morphological, pathological, and perfusion parameters that may account for the impaired motor-related fMRI activations in patients with brain tumor (See Chapter III).**

This thesis consists of 4 chapters: Chapter I contains summarizations of several important conceptions as well as research backgrounds, followed by Chapter II and Chapter III which present two studies focusing on the DSC and BOLD MRI technique applications in patients with brain tumor, respectively. Finally, the chapter IV presents the perspectives of MRI approaches in pre-therapeutic assessment and in anti-angiogenic treatment follow-up.

Chapter I: Conceptions & research backgrounds

1.1 Brain tumors and their vascularization

1.1.1 The tumoral angiogenesis

Three distinct mechanisms, vasculogenesis, angiogenesis, and arteriogenesis implement the vascular network development in vivo. Vasculogenesis refers to the spontaneous blood-vessel formation at the embryonic stage, when angioblast differentiation into endothelial cells to form blood vessels. Angiogenesis, which occurs later in embryogenesis and after birth, is a physiological process involving the growth of new blood vessels from pre-existing ones, such as wound healing. Arteriogenesis is the term used for an enlargement of the arteriolar network, induced by higher metabolic demands during vascular stenosis or occlusion occurs, for instance[Jouanneau 2008].

Angiogenesis is thought to be the main mechanism in tumoral vascularization. Similar to extracranial tumors, all brain tumors rely on blood vessels for survival and growth, regardless of different biological characteristics across different brain tumor types. The relationship between tumoral growth and new vessel formation has been proven in animal models using cancer treatment of anti-angiogenic agent[Jain *et al.* 2007; Jouanneau 2008].

Along with tumor growth, tumor-cells will migrate along blood vessels that can be subsequently compressed and destabilized, leading to vessel regression and reduced perfusion[Padera *et al.* 2004]. Hypoxia and tumor-cells death then take place [Holash *et al.* 1999]. Hypoxia and mutations in tumor-cells induce the secretion of growth factors that recruit new blood vessels through angiogenesis[Jain *et al.* 2007] (Figure I-1). Although the mechanism of angiogenesis has not been incompletely understood, by the time of diagnosis and/or surgery in patients, tumors have often already induced aggressive angiogenesis.

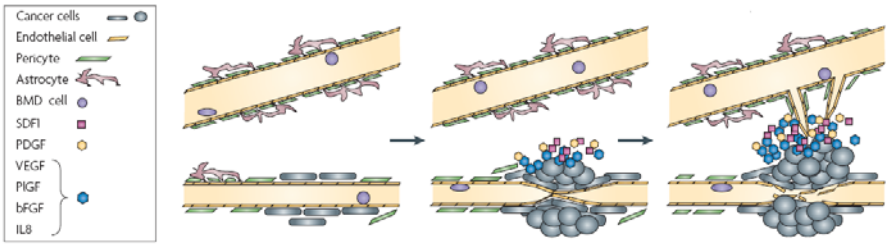

Figure I-1: Process of angiogenesis in tumoral vascularization. After tumor-cells migrating and proliferation along blood vessels, hypoxia then take place due to vessel regression and reduced perfusion. The secreted growth factors, such as vascular endothelial growth factor (VEGF), basic fibroblast growth factor (bFGF), interleukin (IL8) and stromal-cell-derived factor (SDF1) can recruit new blood vessels[Jain et al. 2007].

1.1.2 Angiogenesis in tumoral evolution

It is widely accepted that absence of neovascularization would prevent tumor mass from growing beyond 1 to 2 mm^2. Obviously, the new vessels network induced by angiogenesis in or surrounding tumors bring adequate nutrient and oxygen, supplying for tumoral proliferation [Carmeliet 2000; Carmeliet *et al.* 2000]. This neovascularization has been reported to be correlated to tumor aggressiveness [Leon *et al.* 1996].

Besides, an interesting phenomenon called “angiogenic switch”, plays an important role in the progression from a low-grade astrocytoma to a highly vascularized glioblastoma. Glioblastomas may arise de novo (primary glioblastoma), or arise from malignant progression of low-grade astrocytoma (secondary glioblastoma). Differences of the two groups became apparent by genetic analysis of tumor biopsies. In secondary glioblastoma, the progression of a low to high grade tumor involves a sequence of genetic events in tumor cells which accumulate over a long period of time, whereas patients with primary glioblastoma rapidly accumulate lots of genetic changes. For example, most of the secondary glioblastoma and giant glioblastomas has mutated p53, whereas amplification of epidermal growth factor receptor (EGFR) gene is common in primary and small cell glioblastoma [von Deimling *et al.* 1993]. The epidermal growth factor (EGF) is one of the growth factors that can modulate the expression of vascular endothelial growth factor (VEGF). The latter has been suggested as a molecule that is primarily responsible for brain

tumor angiogenesis [Jouanneau 2008].

1.1.3 Vascularization in tumoral classification and grading

The 2007 WHO classification classifies gliomas on the basis of their histological features in three types as astrocytomas, oligodendrogliomas, and oligoastrocytomas, respectively. Analysis of the most malignant region in tumoral parenchyma enables grading gliomas in four levels (grade I to grade IV), depending on four main features: nuclear atypia, mitoses, microvascular proliferation, and necrosis[Behin *et al.* 2003; Louis *et al.* 2007b; Ducray *et al.* 2010]. For example, types of astrocytomas are usually ranged by the order of increasing anaplasia as: pilocytic astrocytoma (grade I), diffuse astrocytoma (grade II), anaplastic astrocytoma (grade III), and eventually glioblastoma (grade IV), which is the most frequent subtype.

Here, the microvascular proliferation has been considered to necessary for tumoral grading, because proven evidences of the highly relationship between tumoral malignancy and angiogenesis have been investigated[Daumas-Duport *et al.* 1997a; Daumas-Duport *et al.* 1997b]. Histological examinations of high grade gliomas showed features of tumor cell invasion along vessels consisting in pericapillary infiltrates of tumor cells in the periphery of glioblastoma[Schiffer *et al.* 1997]. Experimental studies also demonstrate that angiogensis is an essential process in gliomas development and is strictly associated with tumor cell invasion of adjacent brain tissue[Friedlander *et al.* 1996; Zagzag *et al.* 2000; Vajkoczy *et al.* 2002].

According to the WHO classification guidelines that are currently most used, oligodendrogliomas and mixed oligoastrocytomas are classified in two grades: low grade (grade II) and anaplastic (grade III). However, the histopathologic grading of oligodendrogliomas remains controversial, because of accumulating evidence that a third group should be added, consisting of glioblastoma with an oligodendroglial component. It remains to be established whether or not these tumors carry a better prognosis than standard glioblastomas[He *et al.* 2001; Louis *et al.* 2007b].

Besides, Daumas-Duport and coworkers proposed a complementary grading system (also called St. Anne classification) for oligodengrogliomas combined with survival analysis. If the tumor presents endothelial hyperplasia and/or contrast enhancement, corresponding to the more malign grade B in St.Anne classification, worse clinical outcome could be suggested. In fact, these two features, endothelial hyperplasia on a microscopic level, and contrast enhancement on a macroscopic level, are both referring to a same phenomenon: tumroal angiogenesis[Daumas-Duport *et al.* 1997a]. However, with the impact of new imaging biomarker such as rCBV calculated using DSC, the prognostic value of contrast enhancement in patients with gliomas remains discussion[Lev *et al.* 2004; Hirai *et al.* 2008; Ducray *et al.* 2010]. The first study for this thesis has also touched upon this issue (see Chapter II).

1.1.4 The blood-brain barrier (BBB) rupture in brain tumor

The blood-brain barrier is a structure that selectively restricts the exchange of molecules between the intracerebral and extracerebral circulatory systems. It is composed of three cell types: endothelial cells, pericytes and astrocytes. The very tight junctions between endothelial cells prevent any hydrophilic molecule over 500 kDa from passively entering the brain parenchyma[Jain *et al.* 2007]. The astrocytes and pericytes may be hardly involved to the function of BBB directly. With enveloping the BBB by their foot processes, astrocytes and pericytes may give structural and chemoinductive support to maintain integrity of the endothelium[Rebeles *et al.* 2006].

With the stimulation of numbers of growth factors activated by angiogenesis process, the neovasculatures are abnormally formed in tumors. The integrity of endothelium in these neovasculatures is broken down because of the tight junctions lost (open endothelial gaps), whereas fenestration appears. In addition, during the angiogenesis process, the increased expression of the endothelial water channel molecule can also be found. So, all of these cellular changes leads to increased tumoral BBB permeability [Rebeles *et al.* 2006].

The disruption of BBB by tumors may result in vasogenic oedema surrounding the tumor due to the accumulation of fluid and plasma proteins. Moreover, it can change heterogenously the blood flow within/around the tumors, because of the heterogeneous leakiness of tumoral vessels [Jain *et al.* 2007].

This leakiness of tumoral neovasculature cans be detected by conventional medical imaging techniques, such as computed tomography (CT) or MRI, because of the intravascular injected contrast agent (iodine or gadolinium) leaking into extravascular space through the damaged BBB. It's definitely useful to identify the size of the tumor. However, the contrast agent leakage may be heterogeneous in some gliomas due to the heterogeneous formation of tumoral vessels, and determination of tumor size becomes difficult [Gerstner *et al.* 2008].

Studies showed that increased vascular permeability has been correlated with higher grades of tumor suggesting higher permeability in more aggressive lesions, and permeability has also been correlated with elevated mitotic index [Gerstner *et al.* 2008]. However, it seems that the contrast enhancement due to the abnormal vascular permeability in tumor should not be considered as the unique factor reflecting tumoral malignancy. Indeed, accounting for 30% of gliomas that have no contrast enhancement are the high grade gliomas, whereas 16% of low grade gliomas present the contrast enhancement[Ducray *et al.* 2010].

1.1.5 Functional imaging techniques in current diagnosis and treatment in brain tumor

Up to now, conventional medical imaging still plays an important role in brain tumor diagnosis by offering global tumoral morphology such as the lesion localization and the lesion size, which can guide the biopsy in reducing error sampling risks for histopathological analysis. However, morphological information can hardly reflects all of the most bioactive area in tumors. So the confused results of tumoral classification and grading due to the imprecise biopsy are occasionally taking place.

Since last two decades, functional imaging techniques were developed to allow ones

measure and analyze the information characterizing the metabolism and the perfusion in brain tumors. With this complementary functional information, the diagnosis and treatment for brain tumors have been progressed.

For example, the perfusion imaging techniques can characterize the brain tumor by quantitatively or qualitatively measuring cerebral vasularization. With the analysis of perfusion parameters (CBV, CBF, K_{trans} (constant of BBB permeability)), the mechanism of neovasculature proliferation and abnormal cerebral perfusion due to gliomas has been more and more interpreted. For instance, relative CBV measured by MR perfusion imaging correlates closely with angiographic and histologic markers of tumor vasculature[Aronen *et al.* 1994; Sugahara *et al.* 1998; Maia *et al.* 2005], and are more elevated in high-grade than in low-grade gliomas[Sugahara *et al.* 1998; Law *et al.* 2003; Lev *et al.* 2004]. A correlation between rCBV and the expression of vascular endothelial growth factor has been demonstrated by using immunohistochemical staining of surgical specimens[Maia *et al.* 2005].

CBV measurements also allow to estimate the efficacy of delivery of chemotherapy agents. Because areas of tumor with high CBV may respond better to drugs than areas with low CBV due to poor perfusion limits exposure of tumor cells to a drug. Meanwhile, the supervise of the degree of permeability of the BBB in brain tumor may not only be used to understand the underlying histopathological process of progression or recurrence taking place in the gliomas, but also to identify the BBB maximally open time point which allows penetration of chemotherapy agent into the normally impenetrable brain to optimize tumoral combination therapy[Gerstner *et al.* 2008].

Concerning brain tumor surgical resection, the most important issue is maximally removing the lesion and minimally injuring perilesional functional brain areas for reducing the risks of post-operation neurological deficit. BOLD fMRI is useful to map eloquent brain areas before surgical resection. Besides, the lesion-induced cortical reorganization can also be investigated by means of the analysis of BOLD signal elicited indirectly by neural activation based on the neurovascular coupling, the processes by which neural

activity influences the hemodynamic properties of the surrounding vasculature[Atlas *et al.* 1996; Maldjian *et al.* 1997; Schulder *et al.* 1998; Roux *et al.* 1999]. Indeed, the exact mechanisms that underlie neurovascular coupling are not completely understood. There is empirical evidence that hemodynamic response might be altered in normal ageing and disease. So, interpretation of BOLD fMRI studies of individuals with abnormal vasculature pathology might be more challenging than is commonly acknowledged[D'Esposito *et al.* 2003].

1.2 MR imaging techniques for cerebral perfusion

1.2.1 DSC MR imaging

1.2.1.1 Micro-vascularization

The macro-cirulation system in vivo is consisted of relative big blood vessels whose diameter is superior to 1 mm, including arteries (carrying oxygenated blood and nutritive elements such as glucose) and veins (carrying deoxygenated blood with products of metabolism such as carbon dioxide). These macro-vessels can be visualized using conventional angiographic technique. The blood flow in these vessels could be measured by Doppler velocimeter.

The micro-vascularization refers to vessel distal branching including arterioles, capillaries and veinules. Arteries extend into arterioles and terminated by capillaries that irrigate local tissue. The venous blood evacuates from the capillaries though veinules that converge into veins. As a basal structure of tissue irrigation system, the micro-vascularization forms undoubtedly in cerebral vascularization. The perfusion study that refers to the cerebral micro-vascularization, allows to obtain essential physiological information on cerebral tissue status.

1.2.1.2 Perfusion parameters

1.2.1.2.1 Cerebral blood volume (CBV)

The cerebral blood volume (CBV) involves only the microvaculature (i.e. arterioles,

capillaries, and venules)[Barbier *et al.* 2001]. It is defined as the volume of blood in a cerebral voxel divided by the mass of the voxel: $CBV = \frac{Volume\ of\ blood\ in\ a\ voxel}{Mass\ of\ the\ voxel}$.

Due to CBV is frequently expressed in milliliters per 100 gram of tissue, or in microliters per gram (μLg^{-1}), then it can be defined as a volume fraction: $CBV(\%) = 100\frac{Volume\ of\ blood\ in\ a\ voxel}{Volume\ of\ the\ voxel}$.

To convert between the two quantities, one can use the following relationship, which considering the mean density of brain tissue: $CBV(\%) = 0.104\, CBV(\mu Lg^{-1})$. Van Zijil and co-workers reported that the arteriolar, capillary, and venular volumes were about 21%, 33%, and 46% of the total microvascular blood volume, respectively[van Zijl *et al.* 1998].

The CBV may vary functionally according to the physiological or pathological conditions. For instance, in human being, hypercapnia increases CBV with approximate 1.8%/mmHg; hypocapnia reduces CBV with 1.3%/mmHg[Ito *et al.* 2003]. The CBV increasing may be due to the local vasodilatation, the recruitment of dysfunctional capillaries or angiogenesis phenomenon.

1.2.1.2.2 Cerebral blood flow (CBF)

The cerebral blood flow (CBF) is defined as the net blood flow passing through the voxel divided by the mass of the voxel:

$$CBF = \frac{Net\ blood\ \ flow\ through\ the\ voxel}{Mass\ of\ the\ voxel}.$$

Commonly, the units used for CBF are milliliters per 100 gram of tissue per minute and microliters per gram per second (μLg^{-1} $second^{-1}$). Combined with measurements of CBV, the CBF can provide complementary information of tissue irrigation as well as the local hemodynamic property.

1.2.1.2.3 Mean transit time (MTT)

According to the central principle, the mean transit time (MTT) presents the average

amount of time that takes water molecule or contrast agent particle to pass through the voxel vasculature:

$$MTT = \frac{CBV}{CBF}.$$

The general unit expressed for MTT is seconds.

1.2.1.3 DSC MR imaging techniques

The commonly used MR imaging contrast agents are gadolinium chelates with high magnetic susceptibility. Given their size and low lipophilicity, they are constrained to the intravascular space by intact BBB.

Besides their common clinical practice that is to visualize the parenchymal enhancement occurs in regions of broken BBB, these agents can be also used as "tracers" by injecting them as intravenous boluses with high injection rates (generally ≥ 4ml/s), and then imaging their initial passage through the brain vasculature using repeated rapid cine imaging technique (for instance, echo-planar imaging (EPI)).

When the bolus passes through the voxel, the signal intensity on gradient-echo (GE) T2*-weighted image drops (Figure I-2). Thus, one can acquire a curve of the signal intensity change according to the time course for those voxels recruited within a region of interest (ROI) (Figure I-3).

The reason of this signal-intensity-drop is that the contrast agent is confined to intravascular space, which elicits microscopic variation in the local magnetic field, which directly leads to decreased signal intensity. In addition, intravascular contrast agent also establishes magnetic field gradients around the vessels, which cause signal-intensity loss when protons diffuse in these gradients [Fisel *et al.* 1991]. The change in transverse relaxivity (ΔR_2^*) at each time point and in each voxel could be quantified as:

$$\Delta R_2^*(t) = \frac{-1}{T_E} \ln\left(\frac{S(t)}{S_0}\right) \quad \text{Equation 1}$$

where $S(t)$ is the signal intensity in the voxel at time t and S_0 is the baseline signal intensity before the bolus arrives, and T_E is the echo time. This relaxivity change is

assumed to be linearly proportional to the tissue contrast agent concentration and confined within the intravascular space without leakage (Figure I-4)[Barbier *et al.* 2001].

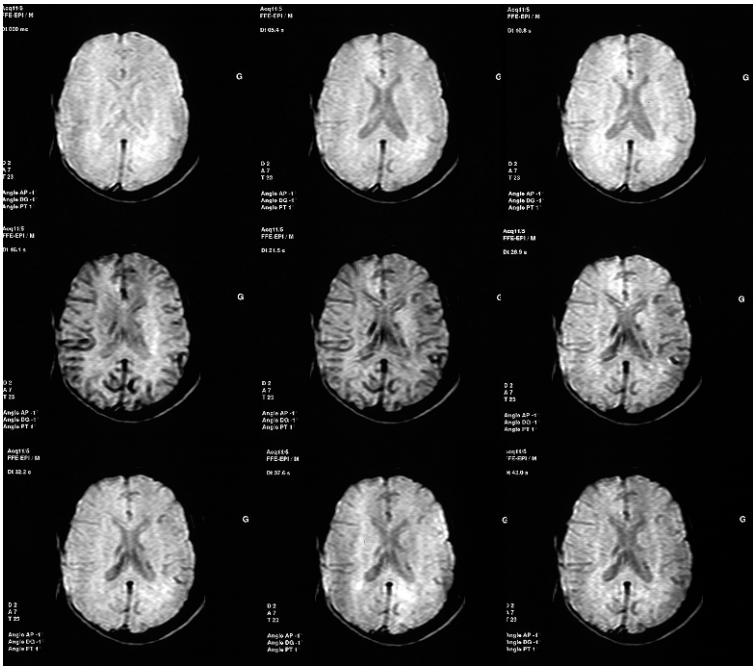

Figure I-2: A series of GE-EPI T2*-WI dynamic images acquired immediately during gadolinium bolus injection demonstrates that signal decreasing during the contrast agent first pass, which is due to the microscopic magnetic-field-strength variations and water diffusion through gradients elicited by the intravascular contrast agent.

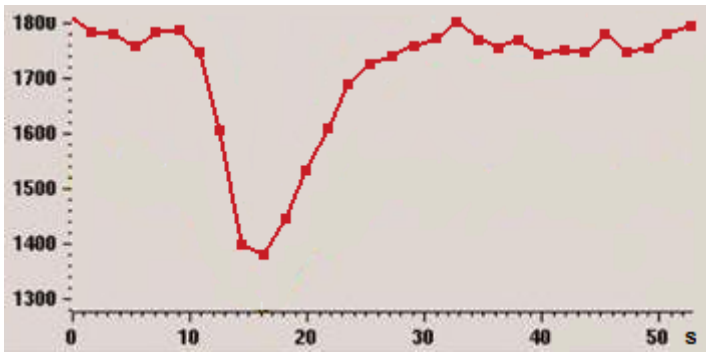

Figure I-3: Signal intensity versus time for a region of interest based on a series of dynamic images.

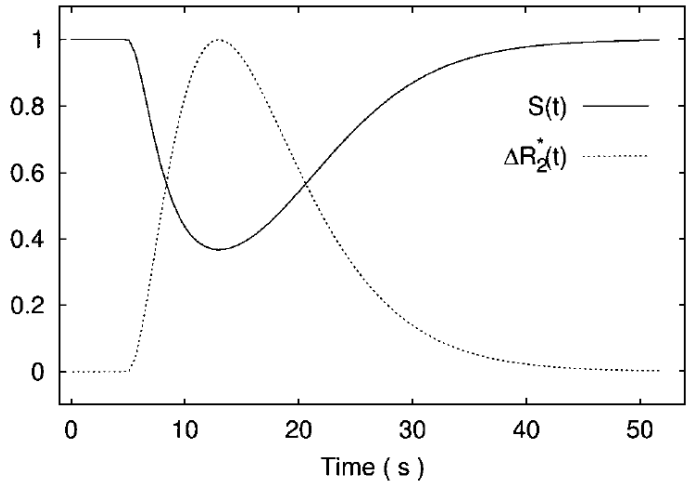

Figure I-4: Signal intensity S(t) is converted to the transverse relaxivity (ΔR_2^*) curve (according to the Equation 1), which is assumed to be proportional to that of the tissue contrast agent concentration[Barbier et al. 2001].

1.2.1.4 Measurements of perfusion parameters with DSC MRI [Barbier *et al.* 2001]

1.2.1.4.1 Quantitative measurements of perfusion parameters

The measurements of absolute value of perfusion parameters rely on tracer kinetic theory. If knowing the input and the output of a tracer from a voxel, one can determine the volume of distribution (i.e. CBV, or more strictly, the plasma volume, because the contrast agent is excluded from the red blood cell) and the clearance rate (CBF) by using conservation of mass mathematics. However in imaging, the only information that we have is the signal-intensity changes in all the voxels, from which we can estimate the plasmatic and tissular concentrations of the tracer .

Supposing no recirculation effects in the model, the measurement of plasma volume (v_p = CBV • [1- hematocrit (Hct)]) can be expressed as the integral of the tissue concentration time curve:

$$v_p \propto \int_0^\infty C_{tissue}(t)dt \quad \text{Equation 2}$$

Relative CBV can be determined simply by measuring the area under the contrast concentration time curve (see below), but absolute CBV measurement requires the arterial input function (AIF(t)) that describes a time-dependent arterial concentration of the contras agent triggered by a bolus of non-diffusible tracer. Thus, CBV is given by:

$$CBV \propto \frac{\int_{-\infty}^{+\infty} C_{tissue}(t)dt}{\int_{-\infty}^{+\infty} AIF(t)dt}$$ Equation 3

The most traditional method consists in measuring a global AIF as a time-concentration curve (or signal change curve) inside a large feeding artery at the base of the brain, such as the middle cerebral artery or anterior cerebral artery, and then to apply this AIF to all of the voxel in the brain.

The measuring CBF needs to insight into the components of the tissue concentration curve. The latter is a combination of the effects of the AIF and the inherent tissue properties (modeled as a "residue function", R(t)) that represents the fraction of tracer still present in the tissue at time t after an ideal bolus injection. As such, it has a maximal value of 1 at t=0 and monotonically decreases to zero. Thus, one can write the relationship between the tissue concentration and AIF as:

$$C_{tissue}(t) = CBF \cdot AIF(t) \otimes R(t) = CBF \int_0^t AIF(\tau)R(t-\tau)d\tau$$ Equation 4

where $\otimes$ means the convolution process.

to estimate tissular perfusion by the CBF, the effects of AIF on the tissue concentration curve should be removed using mathematical process of deconvolution.

1.2.1.4.2 Relative measurements of perfusion parameters

The individual measurements of absolute CBV, CBF, and MTT values are difficult. However relative values obtained by comparing ipsi- and controlateral measurements are relevant and remain commonly performed in clinical practive.

From acquired dynamic images during contrast agent first passage, $\Delta R_2^*(t)$ curves, which assumed proportional to $C_{tissue}(t)$, can be calculated in all brain voxels by Equation 1. To eliminate contribution of tracer recirculation, a gamma–variate function is generally fitted to these curves. In the hypothesis of a constant AIF to the entire slice, a relative CBV index can be calculated as:

$$CBV_{index} = \int_0^t \Delta R_2^*(\tau)d\tau$$ Equation 5

Although without knowledge of AIF, a MTT index can also be calculated using the nondeconvolved $\Delta R_2^*(t)$ curve as:

$$MTT_{index} = \frac{\int_0^t \tau \Delta R_2^*(\tau) d\tau}{\int_0^t \Delta R_2^*(\tau) d\tau} \quad \text{Equation 6}$$

Then, a CBF index is given by:

$$CBF_{index} = \frac{CBV_{index}}{MTT_{index}} \quad \text{Equation 7}$$

1.2.1.5 Cautions for measurements of perfusion parameters by DSC MRI

1.2.1.5.1 DSC MRI sequence

Up to now, two imaging sequences, gradient-echo (GE) and spin-echo (SE) perfusion-weighted imaging (PWI) sequences have been used to measure perfusion parameters. The GE PWI includes contributions from all the vessels within the voxel [Fisel *et al.* 1991; Weisskoff *et al.* 1994]. With approximate a threefold lower signal-to-noise (SNR) than that of GE PWI, SE PWI is relatively more sensitive to capillary vessels. Thus, SE PWI permits to discern processes on the microvascular level while suppressing the effects of larger vessels. Experimental evidence showed that CBV measurements deriving from these two imaging sequences are different [Dennie *et al.* 1998; Zaharchuk *et al.* 1999; Zaharchuk *et al.* 2000].

1.2.1.5.2 Permeability of BBB

What should be noted is that all methods for absolute perfusion parameters measurements mentioned above are based on the intact BBB. These algorithms were derived according to the intravascular tracer kinetic model. The disrupted BBB may leads to definite errors in CBV and CBF measurements. The investigators suggested that the effects of extravasation may be minimized with the application of a preloading dose of contrast agent or by using multiecho methods [Miyati *et al.* 1997; Barbier *et al.* 1999; Donahue *et al.* 2000; Paulson *et al.* 2008]. Besides, more complex modeling with the number of parameters has been applied to analyze the separate effects of BBB permeability,

and some of these methods drove the development of permeability imaging techniques.

1.2.1.5.3 AIF determination

Determination of AIF is critical for absolute CBF measurements. As mentioned above, the AIF can obtain by measuring the signal change inside or around a major blood vessel and to apply this AIF to all of the brain voxels. In fact, one should be aware that AIF is different for every voxel. The determination of true AIF is always challenged because of difficulties due to inflow effects, partial volume averaging, vessel-orientation-dependent relaxivity, and possible differences in relaxivity between tissue and bulk blood. Recently, some investigators have attempted to determine more local AIFs[Lorenz *et al.* 2006].

1.2.2 Blood-oxygen-level-dependent (BOLD) signal and cerebral perfusion

1.2.2.1 The innervation of cerebral vessels and neurovascular unit

The brain perfusion relies heavily on neuronal activity. This conjunction rests on perivascular innervation and neurovascular unit. Thus, the perfusion measure attracts more attention in neuroscience as well as in clinical medicine because it is a direct reflection of interaction between the vessels and the neurons.

As shown in the Figure I-5[Hamel 2006], the nerves that control cerebral perfusion may be approximately categorized in two levels according to the histological structure: the “extrinsic” innervation and the “intrinsic” innervation.

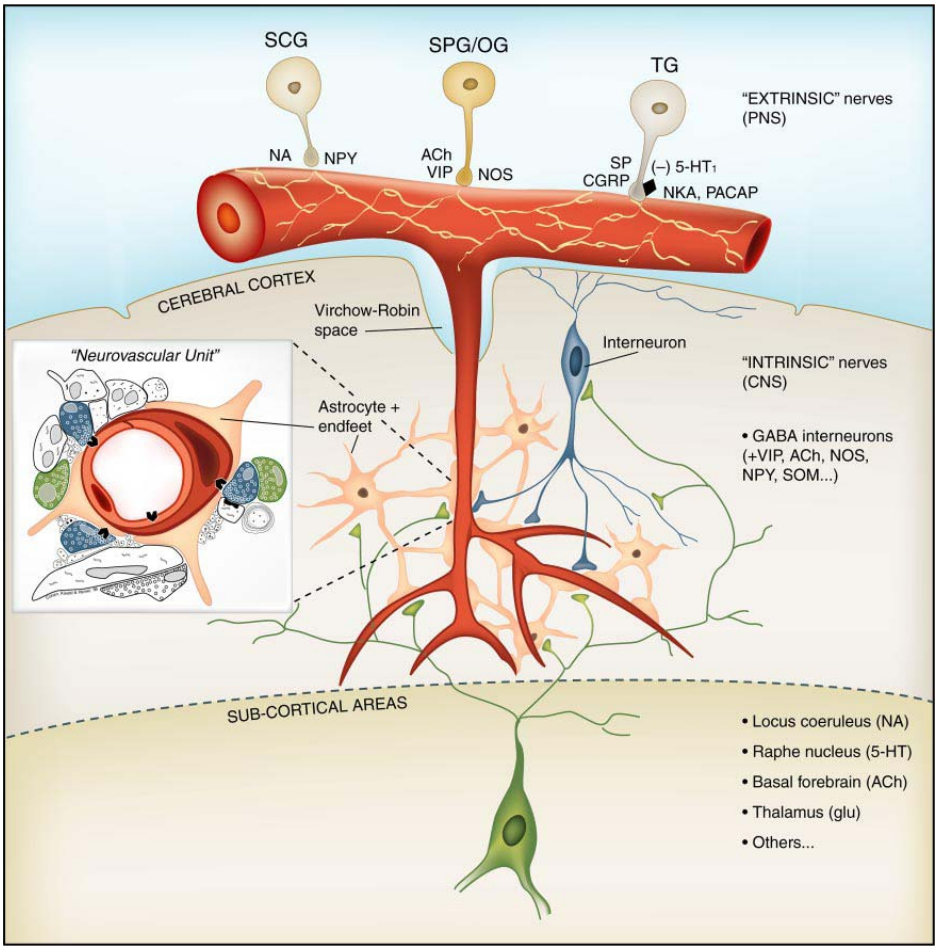

Figure I-5: Schematic representation of the cerebral vascular innervation. *The "extrinsic" innervation of the brain surface vessels arises from the peripheral nervous system (PNS), including the superior cervical ganglion (SCG) delivered noradrenalin (NA), the neuropeptide Y (NPY); the sphenopalatine or otic ganglion (SPG/OG) delivered acetylcholine (Ach), vasoactive intestinal peptide (VIP), nitric oxide (NO) activated by NO synthetase (NOS); the trigeminal ganglion delivered 5-HT, P substance(SP), neurokinine (NK), calcitonin gene-related peptide (CGRP), ... The "intrinsic innervation" of the arterioles located in cerebral parenchyma is dominated by central nerve system (CNS) via GABAergic cortical interneurons and the efference of sub-cortical neurons came from locus coeruleus, raphe nucleus, orbito-frontal region[Hamel 2006].*

The "extrinsic" innervation of the cerebral pial arteries comes from the peripheral nervous system, including the superior cervical, sphenopalatine, trigeminal or otic ganglions that transmit the nerve impulse from peripheral baroreceptors. The function of the "extrinsic" innervation is sympathic vasoconstriction (with neurotransmitters such as noradrenalin, 5-HT, neuropeptide Y) and parasympathic vasodilatation (with

neurotransmitters such as acetylcholine, nitric oxide, vasoactive intestinal peptide). The arteries divide progressively into arterioles that penetrate in cerebral parenchyma. When their entry deeper, once the Virchow-Robin space has vanished, the vascular basement membrane comes into direct contact with the astrocytic end-feet. The vessels then loose their peripheral nerve supply, and receive neural input from neurons located within the brain itself, hence the appellation of "intrinsic innervation" of the brain microcirculation.

The "intrinsic innervation" of the intra-parenchyma arterioles originates from the central nervous system via cortical interneurons and sub-cortical neurons originating from Meynert basal nucleus, orbito-frontal region (acetylcholine), locus coeruleus (noradrenaline), and raphe nucleus (5-HT). The effect of the GABAergic cortical interneurons can contract or dilate the vessels. Although the GABA is a vasodilatator, the activation of these interneurons is modulated by a specific sub-cortical innervation. The sub-cortical efference innervates directly the vascular wall and the astrocytes.

At capillary level, the pericytes bordered by astrocytic end-feet which are innervated by cortical interneurons or subcortical neurons constitute a "neuronal – astrocytic - vascular" tripartite unit. This structural association is commonly called "neurovascular unit", which is referred as the basis of neurovascular coupling. The metabolic mechanisms inducing the neurovascular coupling are illustrated in Figure I-6 [Iadecola 2004].

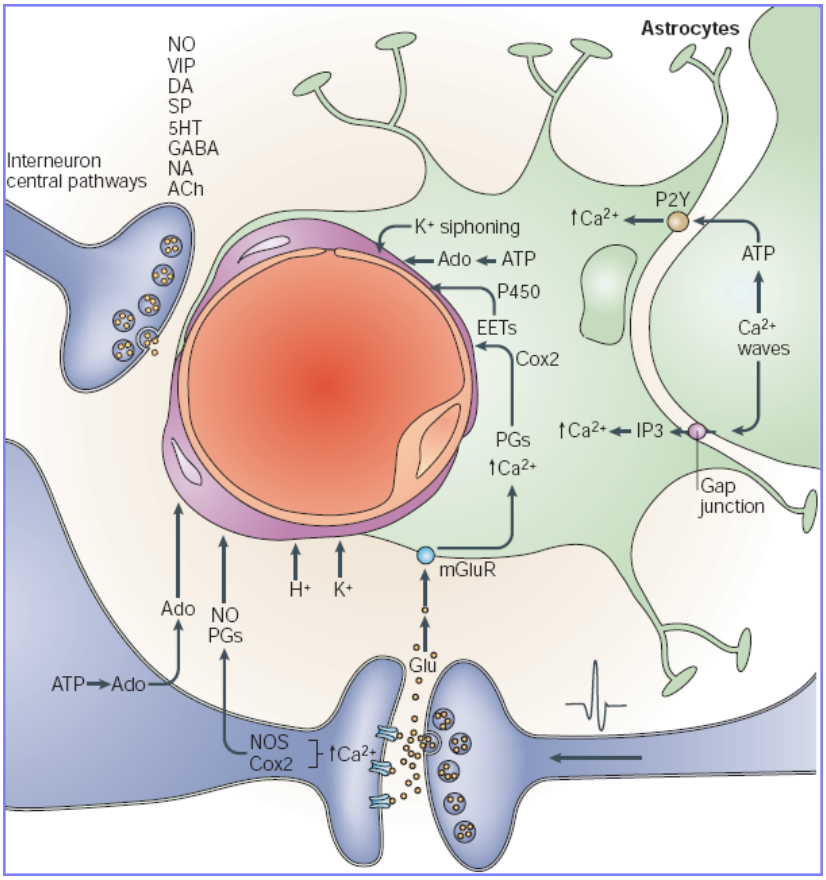

Figure I-6: Schematic representation of neurovascular unit. *The liberation of glutamate (Glu) from the axonal ending increases intracellular concentration of Ca^{2+} in neurons and glia, which results in the production of NO, prostaglandins(PGs), epoxyeicosatrienoic acids (EETs). A calcic wave propagates between the astrocytes through gap junctions. During synaptic transmission, the neurons liberate ions (H^+ and K^+), adenosine (Ado). The K^+ ions are subsequently eliminated by astrocytic end-feet. These substances can lead to vasodilatation, associated with axonal ending of the vasomotor pathways of sub-cortical neurons and interneurons[Iadecola 2004].*

The increase of cerebral perfusion relates tightly to the energetic activation of brain. In human, the post-synaptic activity consumes about 75% of the energetic supply [Attwell *et al.* 2002]. The neuronal energetic metabolism, especially the active or inhibited synaptic activity, is based on consumption of oxygen and glucose which is delivered by the blood in surrounding capillary[Drake *et al.* 2007].

1.2.2.2 BOLD signal and neurovascular coupling

The BOLD signal relies on the blood-flow mediated relationship between neural activity and the concentration of deoxyhaemoglobin in the surrounding microvasculature.

When activated by corresponding tasks (for example, hand movement activates the neurons in the controlateral motor cortex), neurons require more oxygen and glucose which results in a dilation of the neighboring vessels, and the blood flow in these vessels will increase. But the increase of neuronal oxygenic consumption is less than the increase of blood flow, thus, a relative decrease in the concentration of deoxyhaemoglobin takes place. The process by which neural activity influences the haemodynamic responses of the surrounding vasculature is referred to as "neurovascular coupling" (Figure I-7).

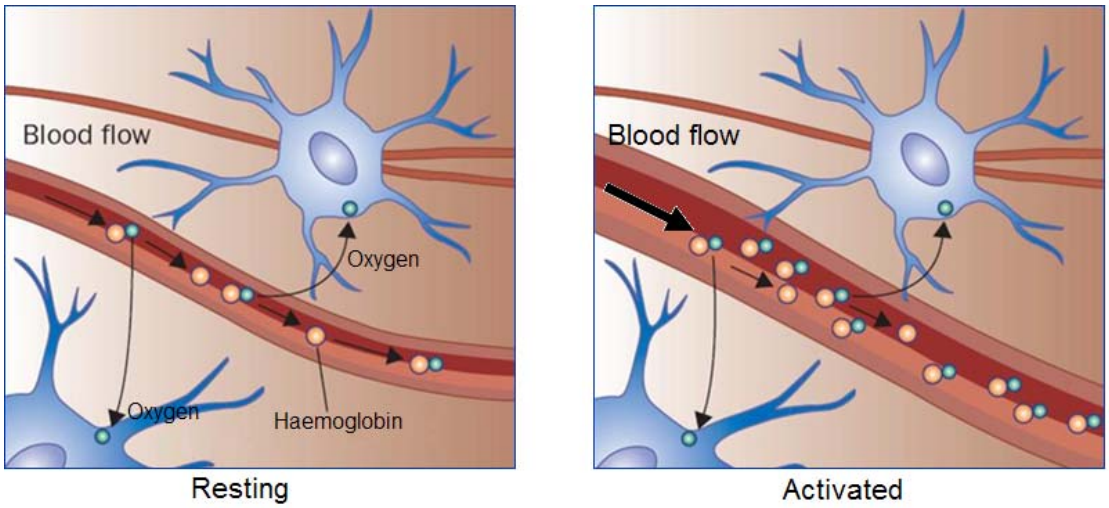

Figure I-7: Schematic of neurovascular coupling. *When neurons become active, they require more oxygen and glucose, but their oxygen consumption increase less than the increase in perfusion; this results in a relative decrease in the concentration of deoxygenated haemoglobin in the surrounding microvasculature. Because of the paramagnetic property of deoxyhaemoglobin, this change, even if it is very small, can be detected by T_2* MR imaging sequence [Rossini et al. 2003].*

With the paramagnetic property, the deoxyhaemoglobin can alter the homogeneity in intra- or peri-vascular magnetic field which leads to shorten the T_2* relaxation time. Although the change in the ratio of oxyhaemoglobin to deoxyhaemoglobin via neurovascular coupling is very small, it can be also detected by T_2* sensitive MR imaging sequence on which the signal intensity increases according to the neural event occurs[Ogawa *et al.* 1992].

The estimation of neural activity by analysis of BOLD signal is based on the hypothesis that the relation between them is approximately linear, without any non-linear

complexes or interactions in the process of neurovascular coupling. This hypothesis has been supported by several experiments combining fMRI with different electrophysiologic methods[Logothetis and Wandell 2004]. Although estimating approximately, the localization of neural activity using BOLD fMRI has been experimentally validated not only in animals[Logothetis and Wandell 2004] but also in clinical practice by comparison with magneto-encephalography[Stippich *et al.* 1998], pre- and perioperative stimulations[Lehericy *et al.* 2000] and cerebral lesion studies[Krainik *et al.* 2001; Krainik *et al.* 2003].

1.2.2.3 The problem of neurovascular coupling and its influence on the BOLD signal

Indeed, the relation between neural activity and BOLD signal is quite indirect, because neural activity influences the BOLD signal by multiple physiological factors depending one by one (Figure I-8)[Arthurs *et al.* 2002; D'Esposito *et al.* 2003]. Obviously, any physio-pathological change that affects these factors can also induce the variation of BOLD signal subsequently.

Studies have indicated that the BOLD signal is impressible to the quality and intensity of neuronal responses to stimulus[Logothetis *et al.* 2001], to basal perfusion conditions [Cohen *et al.* 2002; Brown *et al.* 2003; Stefanovic *et al.* 2006], and to the vasoreactivity [Hamzei *et al.* 2003; Rossini *et al.* 2004; Krainik *et al.* 2005]. Moreover, there are other general factors that can induce the variation of BOLD signal, including the age[Hesselmann *et al.* 2001; D'Esposito *et al.* 2003; Restom *et al.* 2007], the sex [Kastrup *et al.* 1999c], as well as uptakes of some chemical substance such as caffeine [Liu *et al.* 2004] and alcohol[Seifritz *et al.* 2000].

In pathological condition, the modification of BOLD signal has been investigated on subjects with arterial stenosis[Rother *et al.* 2002; Hamzei *et al.* 2003], microangiopathy [Hund-Georgiadis *et al.* 2003], Alzheimer disease[Restom *et al.* 2007], and even with the macroscopic lesion such as stroke[Rossini *et al.* 2004; Krainik *et al.* 2005] and brain tumor[Holodny *et al.* 2000; Schreiber *et al.* 2000; Fujiwara *et al.* 2004; Krainik *et al.* 2004; Ulmer *et al.* 2004].

So, the variation of BOLD signal assumed that the physio-pathological changes have globally or locally influenced the basal CBF, neurovascular coupling and vasomotricity. With BOLD signal from neurovascular fMRI, it is impossible to distinguish the pure effect of neuronal activity from the variation of haemodynamic response, neither the eventual interaction between them. For better interpreting the variation of BOLD signal of neurovascular coupling, it needs to estimate the functional variation of cerebral perfusion.

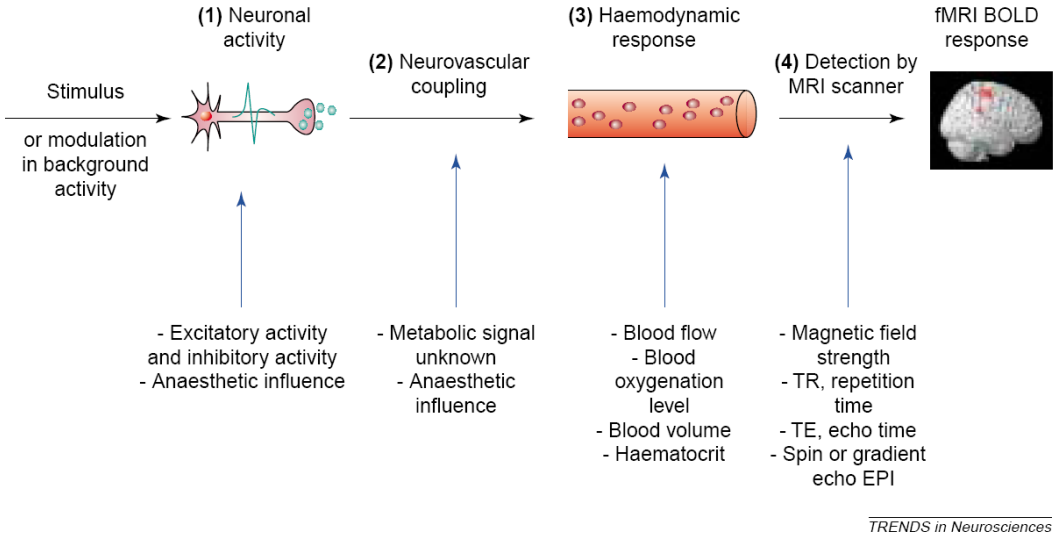

Figure I-8: Haemodynamic response and fMRI BOLD signal. *The principal parameters that influence the BOLD signal are: (1) the quality and intensity of neuronal response to a stimulus ;(2) the integrity of neurovascular coupling; (3) basal perfusion parameters; (4) the characteristic of haemodynamic response; (5) the imaging parameters of MR scanner to detect the BOLD signal[Arthurs and Boniface 2002].*

1.2.2.4 The imaging of cerebral vasoreactivity

The imaging of cerebral vasoreactivity is one of functional imaging approaches that allows to estimate functional characteristics of the cerebral perfusion. Contrary to the imaging of neurovascular coupling that gives preference to study the neural activity, the imaging of cerebral vasoreactivity gives preference to study vasomotricity which is independent of neural activity, using stimulation of vascular activity by means of vascular stimulation, such as vascular motricity drugs (acetazolamide) injection or modulation of blood carbonation.

1.2.2.4.1 Approaches of vascular stimulation

Acetazolamide is widely used in clinical practice as a diuretic to treat intracranial hypertension. After intravenous injection, a vasodilatation occurs with a CBF increase about 20-30%[Brown *et al.* 2003; Grandin *et al.* 2005]. Because of several contraindication (renal insufficiency, hepatic insufficiency, allergy, etc.) as well as some secondary effects (hydro-electrolytic unbalance, diabetes, nephritic colic, etc.), the application of acetazolamide is limited in fMRI[Brown *et al.* 2003].

Hyperventilation during at least one minute induces hypocapnia in association with vasodilatation reflecting a CBF decrease about 25%[Rostrup *et al.* 2002; Rostrup *et al.* 2005] and with a drop of BOLD signal about 1-5%[Cohen *et al.* 2002; Naganawa *et al.* 2002; Krainik *et al.* 2005]. Besides, hyperventilation could induce tachycardia without modulation of arterial blood pressure[Lavi *et al.* 2006].

Contrarily, apnea over 20 seconds can lead to a CBF increase about 60% in association with a 1-5% increase of BOLD signal[Kastrup *et al.* 1999a; Kastrup *et al.* 1999b; Kastrup *et al.* 2001; Liu *et al.* 2002]. However, 20 seconds of apnea results in blood pressure elevation, secondary hyperventilation, and a transient hypocapnia. The time for return to basal state needs 45 seconds.

Although performing simply and reliably, both hyperventilation and apnea can induce head movement during imaging which could subsequently affect the analysis of image data. Both of them also depend on performance, sometimes altered, by subjects or even by patients[Krainik *et al.* 2005].

The vasodilatation induced by inhalation of 5-7% CO_2 during 2-3 minutes is accompanied by an increase with 6%/ mmHg in CBF and with 1.8%/mmHg in CBV[Ito *et al.* 2003]. The BOLD signal varies progressively to reach a plateau after 30-60 seconds of CO_2 inhalation. It needs equally 30-60 seconds to return to basal level when stopping CO_2 administration[Kim *et al.* 1999; Kastrup *et al.* 2001; Riecker *et al.* 2003]. Among the inconvenient of CO_2 inhalation, some minor secondary effect that will recover rapidly, including slight headache, air thirsty, anxiety, and fatigue, have been reported[Jensen *et al.*

2005].

The inhalation of carbogene, a gas mixture of CO_2/O_2 with 7%/93%, is a potential alternative, because neither contraindication nor undesirable effect was reported. Indeed, carbogene is not considered as a drug, and has been readily used in clinical patients[Hamzei *et al.* 2003; Rauscher *et al.* 2005; Lavi *et al.* 2006]. Carbogene inhalation can induce vasodilatation in association with an increase of CBF[Lavi *et al.* 2006] that leads subsequently to an increase of BOLD signal about 4-6% in gray matter[Vesely *et al.* 2001; van der Zande *et al.* 2005].

1.2.2.4.2 Advantages of cerebral vasoreactivity imaging

The cognitive functional imaging technique, such as BOLD fMRI, is heavily based on neurovascular coupling. Although the obvious modulation of BOLD signal occurs in patients, few studies have involved in intra- and inter-individual variation of physiological mechanism that originate signal measured. It is necessary to find a technique to better interpreting the fMRI results from these patients[D'Esposito *et al.* 2003].

With vascular stimulation mentioned above, combined with BOLD contrast fMRI technique, one can measure the BOLD signal and cerebral blood flow simultaneously. The obtained parameters enable, by hypercapnic calibration of biophysical model of BOLD signal, relative quantification of oxygen consummation in cerebral parenchyma[Hoge *et al.* 1999; Stefanovic *et al.* 2004].

Hence, in cognitive neuroscience, the cerebral vasoreactivity imaging allows comparison the data intra- and interindividually for better estimating the modification induced by aging, neuro-degenerative pathology, etc. In clinical practice, this method may enable better interpretation the functional maps, especially in patients before surgical intervention, considering the alteration of the vasoreactivity in lesion vicinity.

Measuring either directly testing the vascular reactivity to vasomotor stimulation (acetazolamide or CO_2), or indirectly via the neurovascular coupling induced by cognitive tasks, the global and regional variation of cerebral vasoreactivity observed in patients has indicated the modifications of the basis of cerebral perfusion[Cohen *et al.* 2002; Rostrup *et*

al. 2005], of vascular mechanic property[Kalaria 1996; Lacombe *et al.* 2005], of the concentration of vasomotrial substance in perivascular environment, of the relations between vessels, astrocytes and neighboring neurons [D'Esposito *et al.* 2003].

So, the cerebral imaging of vasoreactivity enables one to investigate the cerebral abnormality in infra-centimetric spatial aspect combining with functional modulation of cerebral perfusion. It is possible to estimate the sensibility and the specificity of these abnormalities in comparison with the results from the healthy controls. This imaging technique for microvascular function and the interactions with metabolic, neuronal and glial perivascular environment may offer a better phenotypic characterization of neurological and psychiatric disease even an estimation of the individual vulnerability to these affections before the appearance of clinical signs or of the identifiable macroscopic lesions in imaging.

Chapter II: Prognostic value of DSC MRI in patients with oligodendroglioma

RÉSUMÉ

OBJECTIF : L'objectif de cette étude était de valider les mesures de volume sanguin cérébral, obtenues en imagerie IRM de perfusion, comme marqueur pronostique pour la survie de patients présentant un oligodendrogliome ou une tumeur mixte oligoastrocytaire.

MATERIEL ET METHODE : Entre 1998 et 2004, 54 patients (23 femmes et 31 hommes) âgés de 21 à 73 ans, porteurs d'un oligodendrogliome ou d'une tumeur mixte, ont été examiné, avant tout traitement, en IRM de perfusion (Imagerie de susceptibilité magnétique dynamique au cours d'une injection de Gadolinium). Le volume sanguin cérébral relatif (rVSC) était calculé à partir du rapport entre une mesure dans la tumeur et une mesure dans la substance blanche controlatérale. Les patients ont été classés en 2 groupes A et B, selon la classification de Ste Anne.. Un suivi clinique et par IRM a été réalisé jusqu'au décès du patient ou sur un minimum de 5 ans.Tous ces patients ont été classés aussi selon la classification OMS et ont fait l'objet d'une analyse de groupes entre les grades II et les grades III. L'âge, le sexe, le traitement, le grade tumoral, la prise de contraste et le rVSC ont été testés en utilisant les courbes de suivi par la méthode de Kaplan- Meier, et des analyse uni et multivariées.

RESULTATS : Dans cette population pour laquelle la médiane de survie était de 3 ans, une valeur seuil de rVSC à 2,2 est validée par l'analyse de ROC, comme facteur pronostique pour la survie de 3 ans. Le rVSC, l'âge, le sexe, la prise de contraste, et le grade tumoral constituent des facteurs pronostiques de la survie dans une analyse univariée. Dans une analyse cette fois multi variée, les facteurs ci-dessous le grade tumoral, le rVSC, l'âge du patient, et le sexe, apparaissent, dans cet ordre, comme des facteurs indépendants du pronostic qui ont été sélectés dans le Cox model, sauf la prise de contraste. La

classification OMS aboutit aussi à la conclusion que le grade (II versus III) est lui aussi un facteur independant du pronostic

CONCLUSION : Le rVSC avant toute thérapeutique, mesuré en imagerie de perfusion de premier passage, apparait comme un facteur pronostique pour la survie des patients présentant un oligodendrogliome (ou une tumeur mixte), en utilisant la classification de St Anne , qui sépare les IIA des IIB.

Mots Clés : IRM de perfusion ; Tumeur cérébrale ; Oligodendrogliome ; Pronostic

摘　要

目的：探讨磁共振灌注成像（perfusion MRI）测定局部相对脑血容量（rCBF）在少突胶质细胞瘤（oligodendroglioma，OG）（含少突胶质细胞-星形细胞混合胶质瘤（mixed oligoastrocytoma，OA））患者生存评价中的价值。

方法：回顾性分析 1998 年-2004 年之间，经病理证实的 54 例（女 23 例、男 31 例；年龄：21-73 岁）OG（含 OA）患者的临床资料。所有患者在临床干预前均进行 MRI 常规检查及 perfusion MRI 检查。对于 perfusion MRI 影像数据，运用专业影像工作站进行图像后处理，测量并计算肿瘤瘤体脑血容量指数与对侧正常脑白质脑血容量指数的比值，得到每位患者脑肿瘤的 rCBV。随后经神经外科活检或手术切除获取肿瘤标本进行病理学检查，并依照 St. Anne 医院分类法将肿瘤分类为 A 组与 B 组。所有患者确诊后根据具体情况给予相应治疗，定期随访并进行磁共振复查，直至死亡或至少期满 5 年。另按照 WHO 标准将患者分成 II 级组和 III 级组用以检测该分类方法的预后效能。采用 ROC 方法界定预测中位生存时间的 rCBV 阈值。记录如下指标并对其进行单因素及多因素生存分析：患者年龄、性别、是否接受肿瘤切除、是否接受放疗、是否接受化疗、肿瘤分类、首次 MRI 检查肿瘤有否增强、rCBV 值。

结果：本组患者中位生存时间为 3 年。当阈值取 2.2 时，rCBV 能对本组患者 3 年的生存状态进行最佳判断。在单因素分析中，肿瘤的分类、是否增强、rCBV，以

及患者的年龄、性别均作为生存预测因子被检出。其中，除肿瘤是否增强外，其余的指标均被选择进入多因素 Cox 回归模型。WHO 分类方法（II 级/III-IV 级）也被检测为独立的生存预测因子。

结论：临床干预前运用磁共振灌注成像测定的 rCBV 值，能够预测 OG 或 OA 患者的预后。与肿瘤是否有强化相比，rCBV 测定对此类肿瘤恶性程度的分类（IIA 级/IIB 级）及生存预后更具价值。

关键词：磁共振灌注成像；脑肿瘤；少突胶质细胞瘤；预测因子

2.1 Introduction

Oligodendrogliomas represent approximately 10% of primary cerebral tumours and 20% of gliomas. They originate from oligodendrocytes and affect preferentially young adults (mean age: 35 years)[Daumas-Duport *et al.* 1997b]. An epileptic seizure or non-specific neurological symptoms such as headaches are the usual mode of presentation of these tumours. Oligodendrogliomas are more responsive to chemotherapy than the other glial tumours[Engelhard *et al.* 2003], especially in the case of 1p/19q codeletion. Upon MRI imaging, low-grade lesions typically show homogenous low signal intensity on T1-weighted and high signal intensity on T2-weighted /FLAIR of cortical-subcortical topography; cystic and calcified components may be present. Higher-grade lesions correspond to either low grade lesions that have progressed and present a localised high grade area, or to lesions that were aggressive at initial examination with necrotic areas[Brami-Zylberberg *et al.* 2005].

During perfusion first-pass MRI obtained during an intravenous bolus injection of gadolinium, tumoral neovascularisation[Aronen *et al.* 1994; Kremer *et al.* 2002] may be estimated using the relative cerebral blood volume measurement (rCBV) calculated by dividing the cerebral blood volume measurement of the pathological region by that of the corresponding healthy region. This neovascularisation has been reported to be correlated to tumour aggressiveness[Leon *et al.* 1996].

A few published research papers[Lev *et al.* 2004; Law *et al.* 2006a; Mills *et al.* 2006; Law *et al.* 2008] have investigated the prognostic value of rCBV in patients with glioma. A recent long-term follow-up study[Hirai *et al.* 2008] has shown that rCBV at pre-treatment perfusion MRI is a useful prognostic biomarker for survival in patients with high-grade astrocytoma. In our study, factors affecting survival were assessed in patients with oligodendroglioma. To this end, a retrospective analysis of the medical records of 54 consecutive patients with oligodendroglioma (or mixed tumours) was conducted; patients were followed up until death or for at least 5 years.

The purpose of this study was to evaluate retrospectively whether cerebral blood volume measurement based on pretreatment perfusion MRI is a prognostic biomarker for survival in patients with oligodendroglioma or mixed oligoastrocytoma.

2.2 Material and methods

2.2.1 Patients

Between 1998 and 2004, 54 patients (23 females and 31 males, aged 21 to 73 years (mean: 46.4 years)) were included in this retrospective study when they met the following inclusion criteria: 1) histopathologically proven oligodendroglioma or mixed tumour; 2) no history of brain tumour; 3) performance of perfusion MRI prior to any surgery (stereotactic biopsy or resection); 4) no chemotherapy or radiotherapy prior to perfusion MRI; 5) survival time of at least 2 months after perfusion MRI.

Following diagnosis, patients were followed up every 4 to 6 months by the neurosurgeon (after tumour resection), neuro-oncologist, or radiation oncologist depending on the initially proposed treatments, secondarily conducted treatments, or the progression of the lesion. Follow-up was both clinical and radiological, systematically including a control MRI. Follow-up was ensured within the multidisciplinary “brain tumour” team comprised of neuropathologists, neurosurgeons, neuro-oncologists, and radiation oncologists. The team met on a weekly basis, and all therapeutic decisions were based on consensus following analysis of the patient’s medical record.

2.2.2 Imaging

All MRI examinations were performed using a 1.5 Tesla scanner (Philips Medical System).

Standard MRI work-up systematically comprised at least one series of T2-weigthed images (turbo spin echo, repetition time msec (RT)/echo time msec (ET) =6235/120; numbers of signals averaged (NAS) =2; turbo factor=15) and T1-weigthed images (spin echo, RT/ET=500/10; NAS=2) obtained prior to and after gadolinium injection.

DSC perfusion MRI was carried out using T2*-weighted gradient echo - echo planar images (T2* GE-EPI) with the following parameters: RT/ET/α=1500/70/45; field of view=220mm, matrix=128x256, and slice thickness=7mm. Twelve axial slices parallel to the anterior commissure – posterior commissure (AC-PC) plane, covering the entire cerebral parenchyma were acquired every 2 seconds during 1 minute. A bolus injection of gadolinium (0.1 mmol/kg of Gd-DTPA) was started simultaneously to the data acquisition, at a rate of 6 ml/sec, using an automatic injector (Spectris MR Injector; Medrad Inc.). After injection of the contrast agent, 20 ml of physiological saline solution were administered at a rate of 6 ml/sec[Le Bas *et al.* 2005; Le Bas *et al.* 2006].

2.2.3 rCBV measurement

DSC perfusion MRI was processed on a workstation using dedicated software (Philips Medical System). By using modelling related to the gamma function, the software reconstructs parametric maps of cerebral blood volume (CBV) for each slice. On the different slices passing through the tumour, the regions of interest (ROI) of about a square centimeter were drawn in pathological and healthy areas according to the following rules, respectively:

- in pathological areas: 1) the ROI was drawn in the area where CBV was the highest[Wetzel *et al.* 2002] on the respective map, in confrontation with the T1-weighted images obtained after contrast injection at the same level to match with contrast agent uptake by the tumour; 2) outside of the large vessels and the choroid plexus; 3) at a distance from the skull base and meningeal structures to avoid susceptibility artefacts.

- in healthy areas: a ROI was drawn on the contralateral white matter on the same slice in most of the cases. For the lesions located in the convexity, both ROIs were drawn in cortical/subcortical matter.

The ratio between maximum CBV in tumour tissue and CBV in the healthy contralateral hemisphere was established. The maximum rCBV ratio, equal to CBVmax/CBVnormal, was considered representative of the lesion.

2.2.4 Histopathological analysis

Histopathological analysis was conducted on either biopsies taken in stereotactic conditions or surgical resection specimens. Tumour samples obtained by biopsy or surgical resection were analysed according to both the World Health Organisation (WHO)[Louis *et al.* 2007a] and the St. Anne Hospital classifications [Daumas-Duport *et al.* 1997a]. The latter classification distinguishes two prognostic groups based on histological (endothelial hyperplasia) and imaging (contrast uptake on MRI or X scan) criteria: oligodendrogliomas grade A without endothelial hyperplasia and contrast uptake; oligodendrogliomas grade B with endothelial hyperplasia or contrast uptake on imaging. Anaplastic oligodendrogliomas (grade III in WHO classification) with nuclear atypia belong to grade B category in St. Anne Hospital classification. No cytogenetic study was conducted to investigate 1p/19q deletion status.

2.2.5 Statistical analysis

To assess the predictive value of perfusion indices for survival, the 54 patients were classified firstly in two groups, grade A and grade B in St. Anne Hospital classification, and then grade II and grade III-IV in WHO classification.

Taking into account the non-normal distribution of data, the Mann-Whitney U test, a non-parametric method, was conducted to evaluate the relationship between rCBV and the different tumour grades (grade A/ grade B). Survival time was defined as the time period between the initial radiological investigation, including the perfusion study, and the date of death or last follow-up, taking into account that the follow-up period for surviving patients was at least 5 years, at July 31, 2009.

Receiver Operating Characteristic (ROC) curve analysis allowed us to establish an optimal threshold value for rCBV when accounting the median survival time.

Several clinical and MRI factors were tested for their prognostic value relating to survival time, including age (<50/≥50 years), sex (male/female), type of treatment received (neurosurgical resection (absent/present), chemotherapy (present/absent), radiotherapy

(present/absent)), tumour grade (grade A/ grade B), contrast agent uptake (present/absent), and rCBV (below or above the optimal threshold value given by the ROC curve analysis).

For each of these factors survival curves were assessed using the Kaplan-Meier method, and their differences were analysed using the log-rank test. Cox proportional multivariate hazard model analysis was performed after adjusting for prognostic factors. A chi-squared test was used to estimate between-group differences in 3-year survival rates. Statistical analyses were performed using SPSS version 15. $P<0.05$ was considered statistically significant.

All of the analysis mentioned above was performed again after using the WHO classification, i.e. regrouping the grade IIA and grade IIB into a same group (grade II), and the grade III or IV into another one (grade III-IV).

2.3 Results

2.3.1 Pathological and Clinical data

Tumour samples were obtained by biopsy or surgical resection. According to the WHO classification[Louis *et al.* 2007a], tumours were classified in 31 oligodendrogliomas (or mixed tumour) grade II and 23 oligodendrogliomas (or mixed tumour) grade III-IV. According to the St. Anne Hospital classification [Daumas-Duport *et al.* 1997a], same samples were classified in 21 oligodendrogliomas (or mixed tumour) grade A (IIA) and 33 oligodendrogliomas (or mixed tumour) grade B (10 grade IIB and 23 grade III-IV)

In total, 20 patients underwent immediate neurosurgical resection, of which 16 patients received complementary chemotherapy, two were treated with complementary radiotherapy, and the remaining two did not receive complementary treatments. Among the 34 patients who did not undergo surgical resection, 17 received chemotherapy, 5 radiotherapy, 9 chemotherapy and radiotherapy, while three patients did not receive these treatments.

On conventional images, contrast uptake by the tumour was present in 26 of the 33

patients from grade B group, whereas it was absent in 7 patients from grade B group (4 grade IIB and 3 grade III-IV). In the entire study population, the rCBV varied from 0.7 to 9.9 (median ±standard deviation: 1.7±1.6), and the rCBV of grade A group (1.2±0.4) was significantly lower than that of grade B group (2.5±1.8; Mann-Whitney U=168; p=0.001). Similarly, when taking the WHO classification, the rCBV of grade II group (1.2±0.6) was significantly lower than that of grade III-IV group (2.7±2.0; Mann-Whitney U=147; p=0.000).

2.3.2 Survival analysis

Of the 54 patients, 21 were still alive at the end of the study, at July 31, 2009, all presenting a survival time of more than 5 years (1,845 days). The median survival was 3,800 days for the grade A group and 393 days for the grade B group, with a median survival of 1,100 day (approximately 3 years) for the entire group. ROC analysis revealed that the optimal rCBV threshold value predicting 3-year survival was 2.2 (sensitivity=89%; specificity=59%), as shown in Figure II-1. The relation between rCBV and survival time is illustrated in Figure II-2a and Figure II-2b.

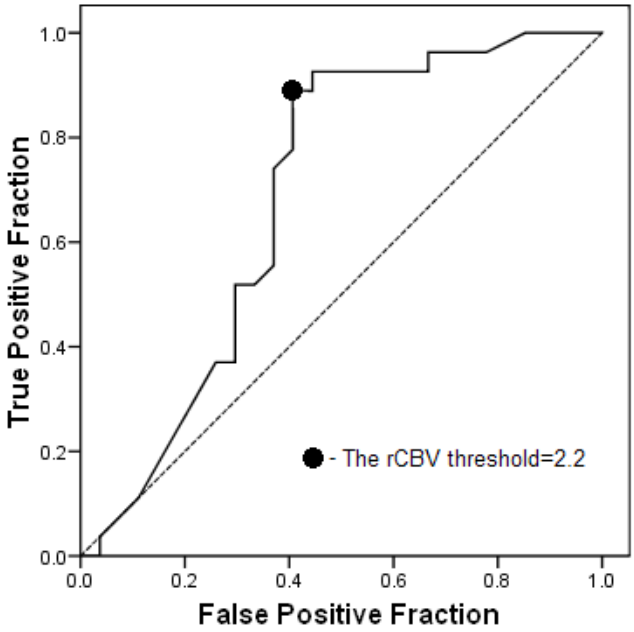

Figure II-1: *ROC curve to determine the optimal threshold value of rCBV in predicting 3-year survival. With a threshold value of 2.2 for rCBV, sensitivity as well as specificity for distinguishing 3-year survival (89% and 59%, respectively) are optimal. The area under the curve is 0.689 (p=0.017).*

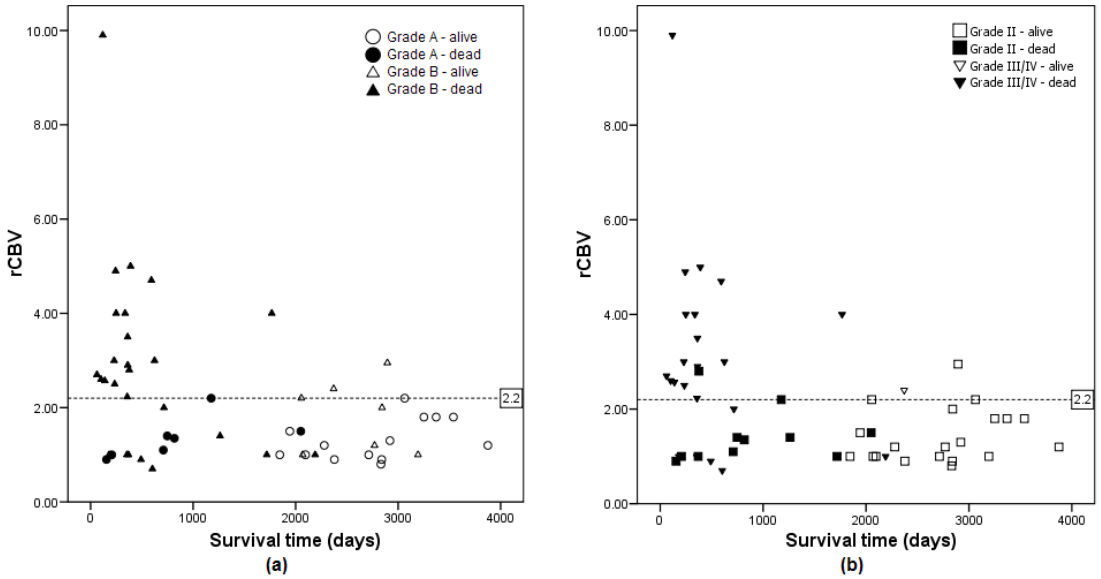

Figure II-2: *Relation between rCBV and survival time in 54 patients with oligodendroglioma. The threshold value of 2.2 for rCBV (dotted line) was determined based on best results obtained by ROC analysis enabling discrimination between patients with/without 3-year survival. (a) Concerned the population investigated in terms of the classification of St. Anne Hospital. (b)Concerned the same population presented in terms of the WHO classification.*

In the entire study population, the percentage of patients surviving 3 years was 50% (n=27); the percentage of patients from grade B group surviving 3 years (11/33; 33.3%) was found to be significantly lower than that of patients from grade A group (16/21; 76.2%) (χ^2=9.43; p=0.002). A similar statistical difference was found between patients with high rCBV (≥2.2) (6/22; 27.3%) and those with low rCBV (<2.2) (21/32; 65.6%) (χ^2=7.67; p=0.006). These differences remained significant even after using the log-rank test that takes into account survival times at study end.

The survival curves in relation to tumour grade and rCBV are presented in Figure II-3. For grade B group tumours, survival had a trend towards a difference between patients with low rCBV and those with high rCBV (log-rank χ^2=3.73; p= 0.053). Contrarily, for grade A group tumours, rCBV had no significant effect on survival.

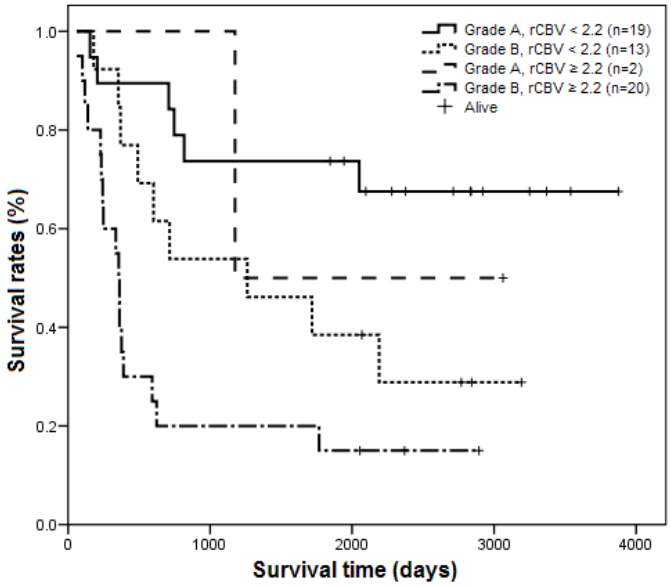

Figure II-3: *Survival curves for grade A and grade B patients according to the rCBV value. For grade B tumours, survival tended to be differ in patients with low rCBV in comparison to those with high rCBV (p=0.053). Contrarily, for grade A tumours, rCBV had no significant effect on survival.*

With respect to clinical findings and MRI data, prognostic factors identified in univariate analysis are listed in Table II-1. These factors are: patient age (p=0.004), patient sex (p=0.005), tumour grade (p=0.001), contrast uptake by the tumour (p=0.003), and rCBV (p=0.001).

Table II-1 : Prognostic factors in patients with oligodendroglioma

Prognostic factors	Number of patients (total N=54)	Survival rates* (%)	P value†
Âge (years)			
<50	31	64.5	0.004
≥50	23	30.4	
Sex			
Male	31	38.7	0.005
Female	23	65.2	
Tumour grade			
grade A	21	76.2	0.001
grade B	33	33.3	
Neurosurgical resection			
Present	20	60.0	0.291
Absent	34	44.1	
Chemotherapy			
Present	42	54.8	0.216

Absent	12	33.3	
Radiotherapy			
Present	19	36.8	0.162
Absent	35	57.1	
Contrast uptake by tumour			
Present	26	34.6	0.003
Absent	28	64.3	
rCBV			
<2.2	32	65.6	0.001
≥2.2	22	27.3	

* Calculated in regard to a 3-year survival

† Analyses based on Log-rank test

The results of multivariate Cox regression analysis are presented in Table II-2. Of the aforementioned factors, tumour grade (grade A/ grade B) was the most important prognostic factor (risk ratio=2.70), followed by rCBV (risk ratio=2.15), patient age (risk ratio=2.10), and patient sex (risk ratio=0.45). Contrast uptake was not found to be a prognostic factor in multivariate analysis.

Table II-2 : Multivariate analysis (Cox regression) of prognostic factors

Prognostic factors	Risk ratio* (95.0% IC)	P value
Selected		
Tumour grade: B	2.701(1.132 – 6.443)	0.025
rCBV ≥ 2.2	2.154(1.044 – 4.447)	0.038
Âge ≥50 years	2.102(1.032 – 4.284)	0.041
Sex: male	0.453(0.208 – 0.986)	0.046
Excluded		
Contrast uptake by tumour: present	Not applicable	0.753

* Risk ratio was not calculated when p≥0.05

When regrouping the patients using the WHO classification, only tumour grade (grade II/ grade III-IV) and patient sex were found to be the independent prognostic factors by Cox regression analysis, with the risk ratio as 6.12 and 0.46 respectively. rCBV, patient age and contrast uptake by the tumour were washed out.

Illustrative cases are presented in Figures II- 4-7.

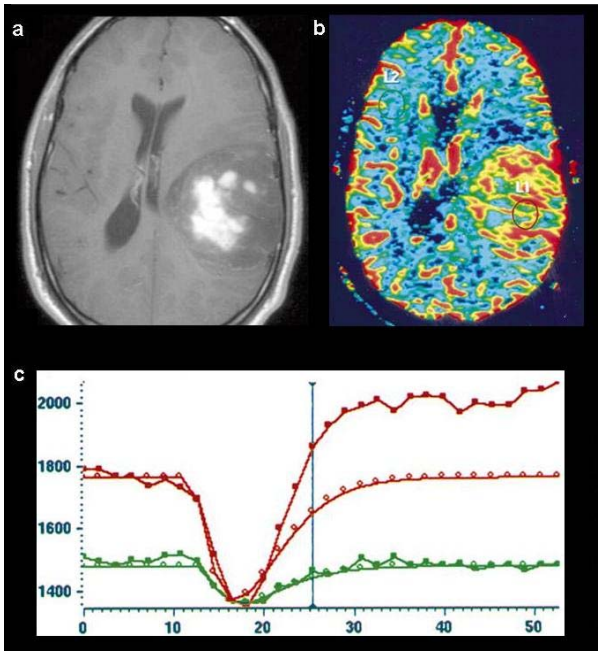

Figure II-4: *40-year-old man: well-circumscribed lesion in left frontal lobe, with non-homogeneous contrast uptake, with no signs of necrosis (a); rCBV=3.4 in the selected ROI. Grade B (grade III according to the WHO classification) oligoastrocytoma (biopsy). On the parametric map for CBV, the neovascularisation areas do not match the areas of maximum contrast uptake (b). Contrast enhancement essentially corresponds to lesions of the haemato-encephalic barrier, which manifest themselves by exceeding the first passage curve beyond the baseline (c).*

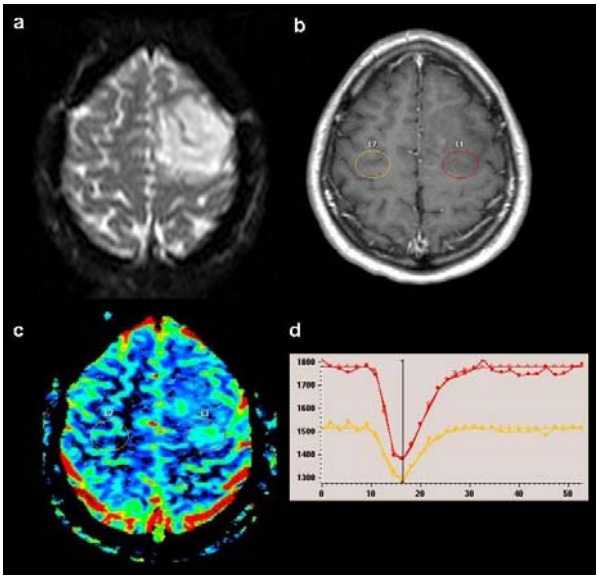

Figure II-5: *23-year-old man: lesion in the left frontal premotor area, without significant contrast enhancement (a, b). On the parametric map for CBV, focal regions with increased cerebral blood volume are observed; rCBV=1.8 (c, d). Grade A oligodendroglioma (resection specimen). A moderate increase in rCBV is not always associated with tumour aggressiveness.*

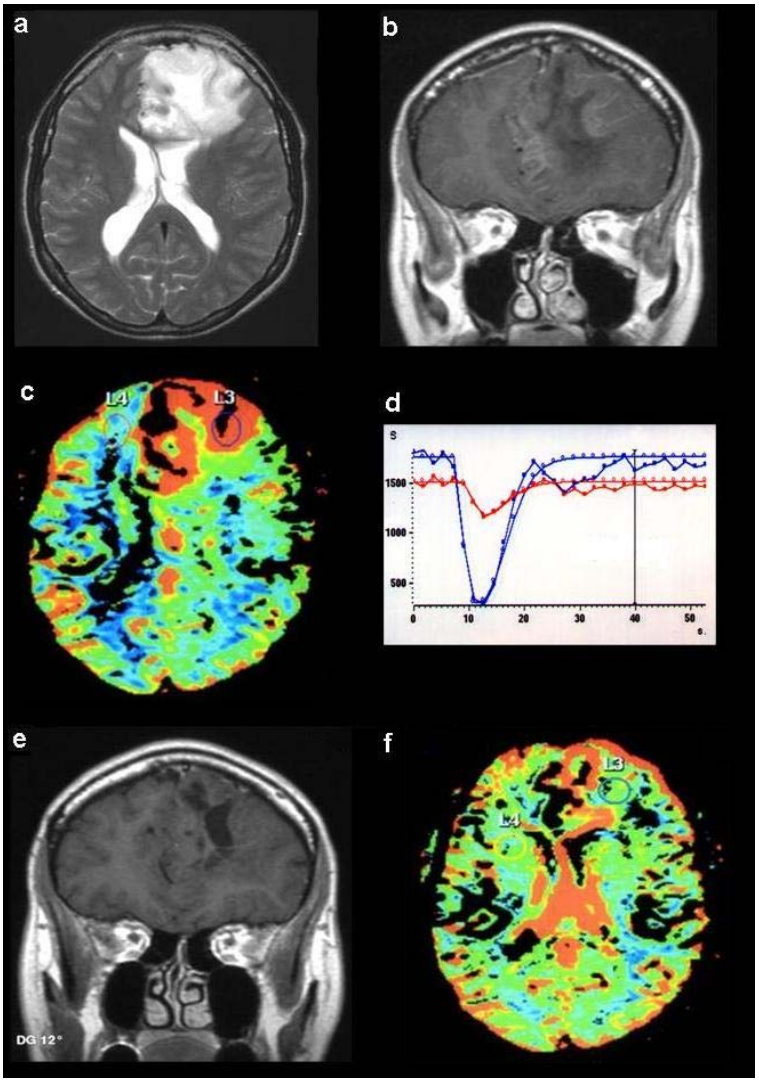

Figure II-6: *42-year-old women: left anterior and paramedian frontal lesion extending into the corpus callosum, with moderate focal contrast enhancement (a, b). On the parametric map for CBV, there is significant angiogenesis; rCBV=2.8 (c, d). Grade B (grade II according to the WHO classification) oligodendroglioma (biopsy). Following chemotherapy, a marked regression of the lesion is noted, with contrast enhancement and signs of neovascularisation (e, f).*

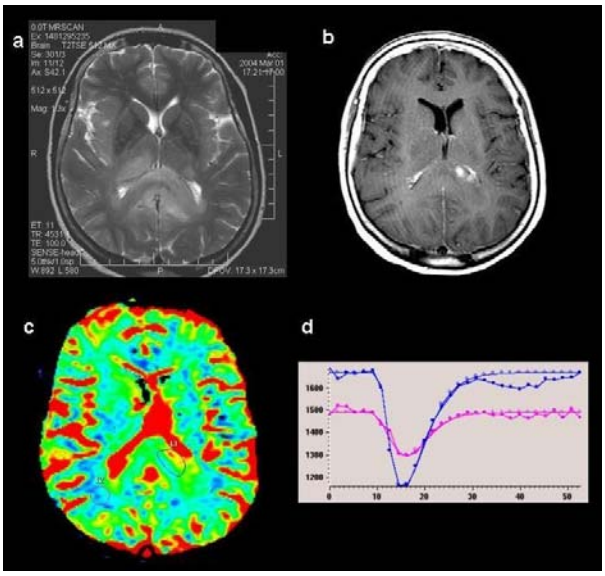

Figure II-7: *64-year-old women: ventricular lesions with nodular contrast enhancement at the left corpus callosum level (a, b). On the parametric map for CBV, significant angiogenesis is observed at the level of the small nodule (rCBV=2.8) and a general increase in rCBV at the level of the corpus callosum splenium (c, d). Grade B (grade II according to the WHO classification) oligodendroglioma (biopsy). Rapid tumour progression occurred during the following months.*

2.4 Discussion

Based on this study results, rCBV at pre-treatment perfusion MRI appears to be an independent prognostic biomarker for survival in patients with oligodendroglioma. In accordance with previous studies, we reported that rCBV was a more relevant prognostic factor for survival than contrast uptake by tumour tissues in a population of gliomas of a different nature and different grades[Lev *et al.* 2004; Hirai *et al.* 2008]. In a recent study, T. Hirai *et al.*[Hirai *et al.* 2008] established that rCBV, with a threshold value of 2.3, was a useful prognosticator for survival in patients with high-grade astrocytoma. A more recent study [Brasil Caseiras *et al.* 2009] revealed that rCBV was found to have a prognostic value in a 20-patient series with low-grade astrocytoma. Even in a study population including 189 patients with high-grade glioma or low-grade glioma, rCBV was also detected as an independent predictor for clinical outcome [Law *et al.* 2008]. In this context, we thought it might be interesting to evaluate whether rCBV was a useful prognostic factor

for survival in patients with oligodendroglioma (oligodendroglioma and mixed oligoastrocytoma), using a similar statistical approach than that used in the study by T. Hirai *et al.*

Median survival time significantly differed in grade A group patients (3,800 days or approximately 11 years) in comparison to that in grade B group patients (393 days or approximately 1 year). For grade A group patients, the median survival of 11 years observed in our study is very close to that observed by C. Daumas-Duport [Daumas-Duport *et al.* 1997a]. Because more than 60% of the patients in grade A group were survival at the end of this study, the median survival time for this group was then estimated as a mathematic extrapolation.

When taking the WHO classification, the median survival time for patients of grade II group was 3,800 days, which was significantly longer than that of grade III-IV group (342 days).

In a comparative analysis of rCBV in patients with low-grade astrocytoma or other low-grade oligodendroglioma, Cha *et al.* reported that rCBV values were significantly higher in patients with oligodendroglioma in comparison to those with astrocytoma [Cha *et al.* 2005]. These high values observed in patients with so-called low-grade oligodendroglioma (grade II according to WHO classification) suggest the fact that grade II tumours with endothelial proliferation should not be mixed up, in terms of prognosis, with oligodendroglioma without proliferation or contrast agent intake.

Considering the 3-year survival for our patient population, ROC curves allowed us to establish a rCBV threshold value of 2.2, which is very close to that reported by T. Hirai for high-grade astrocytomas[Hirai *et al.* 2008]. This result again suggests that all oligodendrogliomas with high rCBV value should be regarded as high grade tumours. As shown in Figure II-2a, all the patients with rCBV superior to 2.2 were in grade B group, while there were some grade B oligodendrogliomas whose initial rCBV was inferior to such threshold. None of grade A group patient had a tumoral rCBV superior to the threshold value of 2.2. When using the WHO classification (Figure II-2b), there were 2

gliomas from grade II group with rCBV superior to 2.2; and some gliomas from grade III-IV group with initial rCBV inferior to 2.2.

The univariate analysis conducted on age, sex, contrast uptake, tumour grade, and rCBV provided remarkable results. Independent from rCBV, which was found to be a prognostic factor, tumour grade and contrast uptake were identified as prognostic factors for survival. In our study, patient age was found to be a significant prognostic factor, which was not the case in T. Hirai's study on astrocytomas. Contrarily, as was the case in Hirai's study, sex was also identified as a significant prognostic factor for survival, with women having a longer survival than men, reflected by a median survival of 3,800 days for women and 550 days for men. The similar difference was also indicated in other studies of high-grade gliomas and may be explained by hormonal or X chromosome-genic factors[Burton *et al.* 2002; Shinojima *et al.* 2004], but it was not suggested in patients with low-grade gliomas[Law *et al.* 2006a; Law *et al.* 2008]. So this issue remains further research.

The different administered treatments, often given in association (surgery and chemotherapy), were not found to be discriminators in terms of survival. It should be mentioned, however, that our patient population was not well suited for this type of analysis as patients received several complementary treatments, often given concomitantly during patient follow-up.

Multivariate analysis determined the following independent factors of prognosis by order of importance: tumour grade (with a distinction between grade A and grade B), rCBV (with a threshold value of 2.2), patient age (with a threshold value of 50 years), and sex (female/male). Contrast uptake was not found to be an independent prognostic factor in multivariate analysis.

2.5 Limitations for design and image analysis

This study has a number of limitations regarding design and image analysis.

Therapeutic treatment options and their chronology were not taken into account. In fact, the entire study population was seen by our multidisciplinary "brain tumour team" comprising neuroradiologists, surgeons, radiation oncologists, and neuro-oncologists. This team decided on the best therapeutic strategy to be implemented for each patient at the initial stage and following tumour progression.

It should also be mentioned that there are always possibilities of error regarding the tumour grading based on biopsies, which do not necessarily reflect the entire lesion [Jackson *et al.* 2001]. In our series, seven lesions were graded as B on histological examination, which revealed endothelial proliferation, whereas MRI did not reveal any significant contrast uptake.

For these 7 lesions from grade B group without tumoral contrast uptake, 4 of which were graded as IIB, the rest 3 were graded as III-IV. As Ginsberg *et al.* already indicated that some grade II oligodendrogliomas enhance and some grade III lack contrast enhancement[Ginsberg *et al.* 1998].

From a methodological perspective, the positioning of the region of interest (ROI) may be subject to discussion, as it was shown to be operator-dependant. However, there appears to be consensus that ROI, of a square centimetre, positioned at the level of maximum CBV in the pathological region and the contralateral apparently healthy white matter allows for the rCBV measurement which is considered representative and reproducible for tumoral neovascularization[Wetzel *et al.* 2002]. In the study on oligodendrogliomas, which tumoral topography is often cortical or subcortical, it sounds appropriate to draw the ROI on the mirrored region in contra-lateral hemisphere, which should also include the cortex. And it has been well respected in our series, sometimes when the lesion located at the convexity level (shown in Figure II-5). The operator's experience, the accomplishment of parametric map of CBV as well as the MR imaging,

which may undoubted influence the measurements according to the ROI position, were taken into accounted.

Regarding rCBV measurement, several authors propose correction methods for extravasion of contrast medium[Boxerman *et al.* 2006; Spampinato *et al.* 2006] or recommend another model than that derived from gamma function, using the deconvolution of the first pass curve by the arterial entry function[Wirestam *et al.* 2000]. However, deconvolution methods are highly sensitive to arterial input function (AIF) selection, i.e. location and acquisition type[Bleeker *et al.* 2009a]. In fact, relative estimation of brain perfusion using interhemispheric ratios on perfusion maps calculated without AIF selection, is a well-known method, demonstrated to be robust and reproducible[Wetzel *et al.* 2002]. In clinical practice and research, many studies in neuro-oncology were conducted using gamma-variate fitting correction, even recently [Law *et al.* 2008].

2.6 Conclusion

In conclusion, this long-term follow-up study (5 years or more for patients who were still alive 5 years after diagnosis) involving 54 patients with oligodendroglioma or mixed oligoastrocytoma demonstrated that the rCBV was a useful independent prognostic biomarker for survival in this patient population while using the St. Anne Hospital classification. Moreover, our study findings support the usefulness of this classification, which separates in terms of survival oligodendrogliomas grade A and oligodendrogliomas grade B.

Contrast uptake was not found to be an independent prognostic factor in the multivariate analysis. Thus in accordance with previous studies, we reported that rCBV was a more relevant prognostic factor for survival than contrast uptake[Lev *et al.* 2004; Hirai *et al.* 2008]. It may suggest revising Saint-Anne classification using rCBV rather than contrasting uptake.

Chapter III Impaired fMRI Activation in Patients with Primary Brain Tumors

RÉSUMÉ

OBJECTIF : Estimer les mécanismes physio-pathologiques des altérations du signal BOLD à proximité des tumeurs cérébrales primitives.

MATERIEL ET METHODE : 25 patients porteurs d'une tumeur frontale ou pariétale (gliome de bas grade (GBG) (n=8), gliome de haut grade (GHG) (n=7), méningiome (n=10)) sans infiltration tumorale macroscopique du cortex sensorimotrice primaire (SM1) ont été examinés par IRMf BOLD lors d'une tâche motrice simple avant la résection chirurgicale. Une imagerie de la vasoréactivité lors d'inhalation de carbogène (CO_2 7% / O_2 93%) a été réalisé pour évaluer la qualité du signal BOLD. Les paramètres de perfusion, volume sanguin cérébral (CBV), débit sanguin cérébral (CBF) et temps transit moyen (MTT), ont été estimés en IRM de perfusion de premier passage. Des régions d'intérêt de 1 cm^3 ont été placées dans le SM1 centrée sur la valeur T maximale obtenue lors de mouvements controlatéraux. L'asymétrie inter-hémisphérique a été évaluée par les rapports inter-hémisphériques des imageries BOLD et de perfusion.

Résultats : Lors de la tâche motrice controtumorale, les activations fonctionnelles SM1 ipsitumorales étaient diminuées chez les patients porteurs de GHG et méningiomes. Les asymétries étaient corrélées avec la distance entre la tumeur et SM1. Le CBV ipsi-tumoral était diminué pour les GHG, il était normal pour les méningiomes. Les variations de la perfusion basale ne pouvaient pas expliquer les altérations des activations SM1 ispitumorales. La diminution du rapport inter-hémisphérique de la réponse BOLD au carbogène était le plus meilleur paramêtre pour modeliser l'asymétrie de l'activation motrice (R=0.51). De plus, 94.9±4.9% des activations motrices étaient inclus dans la réponse BOLD au carbogène.

Conclusion : Les cartographies BOLD au carbogène seraient utiles pour mieux interpréter l'altération des activations sensorimotrices chez des patients porteurs de tumeurs cérébrales.

Mots Clés : Tumeur cérébrale ; Vasoréactivité cérébrale ; IRMf BOLD ; IRM de perfusion

摘 要

目的：探讨原发性脑肿瘤患者肿瘤侧主动运动区（SM1）BOLD 信号减弱的病理生理学机制。

方法：SM1 皮层未见肿瘤侵犯的 25 名额叶或顶叶原发性脑肿瘤患者（低级别胶质瘤（LGG）（n=8），高级别胶质瘤（HGG）（n=7），脑膜瘤（n=10））术前行简单运动任务的 BOLD fMRI 检查。随后给予 Carbogen 气体（二氧化碳/氧混合气体）吸入检测患者全脑的 BOLD 反应信号。采用动态磁敏感造影剂首过磁共振灌注成像技术，检测脑血容量（CBV）、脑血流量（CBF）及平均通过时间（MTT）等血流灌注参数。在 SM1 具有最高 T 值的运动任务激活区内绘制 1cm^3 的感兴趣区（ROI），提取血流灌注及 BOLD 反应参数，采用两侧参数的比值考察其不对称性。

结果：HGG 及脑膜瘤患者肿瘤侧 SM1 运动任务激活程度显著下降，且与 SM1 到肿瘤的距离相关。肿瘤侧 SM1 的 CBV 在 HGG 患者较对侧下降，在脑膜瘤患者则保持正常。局部基础血流灌注的改变不能解释 SM1 区的激活程度下降。Carbogen 吸入激发的 BOLD 反应是 SM1 运动任务激活程度不对称性的最有价值的预测因子（R=0.51）。94.9±4.9%的运动任务相关的激活体积被纳入 Carbogen 吸入激发的 BOLD 反应区域内。

结论：Carbogen 吸入激发的 BOLD 反应参数图能更好地解释脑肿瘤患者功能区运动任务激活程度的改变。

关键词：脑肿瘤；脑血管反应；血氧水平依赖功能磁共振成像；磁共振灌注成像

3.1 Introduction

Besides anatomic and structural information, physiologic status of brain tumors and adjacent parenchyma is routinely investigated by MRI. Tumor vascularity and neighboring cortical functions can be characterized using dynamic susceptibility contrast (DSC) perfusion MRI and blood oxygenation level-dependent (BOLD) functional MRI (fMRI). In spite of the validation of fMRI in clinical practice by confrontations with invasive procedures such as intraoperative electrical stimulations and resections[Lehericy *et al.* 2000; Krainik *et al.* 2001], several clinical studies showed that fMRI activations were decreased in the vicinity of brain tumors when compared to the homologous activation in the contralateral hemisphere[Holodny *et al.* 2000; Schreiber *et al.* 2000; Fujiwara *et al.* 2004; Krainik *et al.* 2004; Ulmer *et al.* 2004; Liu *et al.* 2005; Hou *et al.* 2006; Ludemann *et al.* 2006; Chen *et al.* 2008]. Because these changes may provide false negative results and simulate false hemispheric dominance for language, as well as pseudo lesion-induced cortical reorganization, the reliability of fMRI application in these patients has been debated [Inoue *et al.* 1999; Fujiwara *et al.* 2004; Ulmer *et al.* 2004].

Experimental studies and clinical evidence showed that the hemodynamic response vary across physiological and pathological conditions[D'Esposito *et al.* 2003]. For instance, changes in basal perfusion may explain impaired peritumoral activation in the vicinity of hypervascularized brain tumors[Hou *et al.* 2006; Ludemann *et al.* 2006]. Altered functional mechanisms of brain perfusion have been also suggested in patients with tumor[Ulmer *et al.* 2004; Liu *et al.* 2005; Hou *et al.* 2006; Ludemann *et al.* 2006; Chen *et al.* 2008], as well as in patients with vascular risk factors and stroke[Rother *et al.* 2002; Hamzei *et al.* 2003; Rossini *et al.* 2004; Krainik *et al.* 2005; Girouard and Iadecola 2006]. Therefore, an evaluation of the hemodynamic response has been proposed to test functional properties of the brain vasculature using fMRI. Beside intravenous injection of acetazolamide that elicit whole-brain hyperperfusion[Brown *et al.* 2003; Grandin *et al.* 2005], capnic challenges

such as CO_2 inhalation, apnea, and hyperventilation have also been used to modulate perfusion using vasoreactivity to circulating gases. Although different physiological mechanisms are engaged, experimental changes of brain perfusion using vasoreactivity were used to estimate the vascular component related to neural activity detected by BOLD fMRI[Kastrup *et al.* 2001; Cohen *et al.* 2002; Rother *et al.* 2002; Hamzei *et al.* 2003; Krainik *et al.* 2005; Haller *et al.* 2008]. Experimental calibration of the vascular response during CO_2 or O_2 challenge allows quantitative fMRI of oxygen consumption[Stefanovic *et al.* 2005; Chiarelli *et al.* 2007]. Actually, quantitative fMRI remains difficult in clinical practice because of technical requirements for data acquisition and analyses. However functional MRI of brain perfusion would be helpful to better identify brain regions with impaired vascular function and to improve image interpretation[Hamzei *et al.* 2003; Krainik *et al.* 2005].

The purpose of this study was to identify morphological, pathological, and perfusion parameters that may account for the variance of motor-related activations using BOLD fMRI in patients referred for surgical treatment of primary brain tumor. Using carbogen inhalation, a gas mixture of CO_2 (7%) and O_2 (93%), BOLD signal could be estimated over the brain, independently of motor-related neural activity. Expected results would help to better interpret activation maps at the individual level.

3.2 Subjects and methods

3.2.1 Patients

Patients with a primary brain tumor referred for a surgical treatment at the university hospital of Grenoble were selected according to the following criteria: 1) presence of a primary tumor in the frontal or parietal region; 2) distance between the tumoral border and ipsitumoral primary sensorimotor cortex (SM1) superior to 5 mm; 3) absence of neurological deficit on clinical examination; 4) absence of cardiovascular risks factors or stroke history; 5) good comprehension and task performance during fMRI. All subjects

gave their informed consent according to the Declaration of Helsinki and the study was approved by the Ethical Committee of our institution.

Thus, 25 patients (women (n=11), men (n=14); age range: 22-76 years, mean: 43.4 years; right-handed (n=22), left-handed (n=3)) were included. Histological diagnoses were made on paraffin-embedded material using the current World Health Organization (WHO) classification[Louis *et al.* 2007a] and consisted of oligodendrogliomas (OG), glioblastomas (GB), and benign meningiomas. Gliomas were also classified according to the Saint-Anne classification in grade A OG (n=8), grade B OG (n=4), and GB (n=3)[Daumas-Duport *et al.* 1997a]. These tumors were further presented in 3 main groups: low grade glioma (LGG) for OG grade II/A (n=8); high grade glioma (HGG) for OG grade II/B, III/B, and GB (n=7), and meningioma (n=10 with meningioma grade I (n=5) and grade II (n=5)) (see details in Table III-1).

Table III-1: Clinical and pathological data in patients with primary brain tumor

Obs. Nr /Age/sex[1]/ handedness[2]	Histology (WHO/SA)[3]	Topography	Volume (cm^3)	Distance to Sensorimotor Cortex (mm)	rBOLD Motor in SM1	rBOLD Carbogen in SM1	rCBV in SM1	rCBF in SM1	rMTT in SM1	rTTP in SM1
1/45/M/R	OG II/A	Right parietal	18.2	13	1.08	0.91	0.95	1.00	0.93	0.99
2/37/F/R	OG II/A	Right frontal	21.9	7	0.45	0.89	0.85	0.90	0.95	1.02
3/37/M/R	OG II/A	Right frontal	4.1	32	1.11	1.25	0.73	0.69	1.01	1.03
4/22/M/L	OG II/A	Left frontal	4.1	34	1.03	1.00	0.83	0.75	1.12	1.08
5/31/F/L	OG II/A	Left frontal	12.6	12	1.05	1.03	0.95	0.96	0.99	0.98
6/38/M/R	OG II/A	Right frontal	36.9	24	1.15	0.93	0.58	0.62	0.99	1.04
7/26/F/R	OG II/A	Left frontal	16.2	6	1.02	0.86	1.07	1.03	1.03	1.05
8/25/M/R	OG II/A	Left frontal	44.2	15	1.06	0.93	0.87	0.88	1.01	1.00
9/30/M/R	OG II/B	Left frontal	64.5	6	0.67	1.24	1.06	1.21	0.84	0.92
10/25/F/R	OG III/B	Right frontal	31.4	17	0.61	0.81	0.69	0.70	1.01	1.02
11/31/F/R	OG III/B	Right frontal	108.1	31	1.23	1.46	0.79	0.81	0.99	1.04
12/59/F/R	OG III/B	Right parietal	14.5	6	0.24	0.77	0.68	0.61	1.13	1.09
13/30/F/R	GB IV	Right frontal	31.3	6	0.90	0.80	0.55	0.59	0.99	1.06
14/47/F/R	GB IV	Left frontal	35.8	7	0.47	0.49	0.71	0.73	0.88	0.90
15/51/M/R	GB IV	Left parietal	27.4	6	0.57	0.88	1.02	0.95	0.89	0.87
16/46/F/R	Meningioma I	Left parietal	11.7	17	0.72	0.82	1.01	0.95	1.07	1.04
17/58/M/R	Meningioma I	Left parietal	67.9	20	0.70	0.62	1.05	0.96	1.06	0.99
18/37/F/R	Meningioma I	Left frontal	18.8	14	0.72	1.28	0.78	0.74	1.13	1.08
19/63/M/R	Meningioma I	Right parietal	16.5	7	0.72	0.99	1.01	1.12	0.89	1.02
20/41/M/R	Meningioma I	Right parietal	75.8	12	0.94	0.77	1.13	1.12	1.00	0.99
21/60/M/R	Meningioma II	Right parietal	53.0	18	0.70	0.82	0.84	0.82	1.01	0.98
22/58/M/L	Meningioma II	Left frontal	22.1	8	0.37	0.84	1.28	1.18	1.10	1.08
23/53/M/R	Meningioma II	Left frontal	12.1	15	0.92	1.15	1.28	1.29	1.13	1.11
24/60/M/R	Meningioma II	Right frontal	30.4	29	0.53	0.64	0.85	0.87	0.99	0.94
25/76/F/R	Meningioma II	Left frontal	10.5	14	0.72	0.85	0.79	0.79	1.02	1.06

[1]M: male, F: female; [2]R: right-handed, L: left-handed; [3]according to WHO classification and Sainte-Anne classification; OG: oligodendroglioma; GB: glioblastoma

3.2.2 MR Imaging protocol

Image acquisitions were performed on a 1.5T whole-body MR scanner (Philips®). MR images were acquired parallel to the anterior commissure–posterior commissure (AC-PC) plane in the following order: functional, perfusion, and anatomical imaging.

3.2.2.1 Functional imaging:

Data acquisition was performed using single-shot gradient-echo echo-planar-imaging (GE/EPI) T_2* weighted-images (WI), covering the whole brain (time of repetition (TR)/time of echo (TE)/flip angle (α): 3000ms/45ms/90°; field of view: 256mm; acquired matrix: 64×64; slice thickness: 4mm; voxel size: 4×4×4mm^3; 32 slices; no gap; number of dynamic scans adjusted to the paradigm length (see below)).

3.2.2.2 Perfusion imaging:

Intravenous administration of Gd-DTPA (0.2 ml/kg) was performed using a power-injector pump at an injection rate of 6ml/s followed by saline flush. Simultaneously, multi-shot GE/EPI T_2* WI covering the cerebral tumor were acquired (TR/TE/α: 465ms/28ms/45°; field of view: 256mm; matrix: 64×64; slice thickness: 4mm; voxel size: 4×4×4mm^3; 12 slices; no gap; 30 dynamic scans with an interscan delay of 1.9s for an acquisition time of 57.5s).

3.2.2.3 Anatomical imaging:

A 3D T_1-weighted GE sequence covering the whole brain was performed to coregister functional data and to define regions of interest (ROI) (TR/TE/α: 7.65ms/3.7ms/8°; field of view: 256mm; matrix: 256×256; slice thickness: 1mm; no gap; voxel size: 1×1×1mm^3; 150 axial planes).

3.2.3 Tasks

Prior to MR examination, all patients were informed and trained to practice motor tasks appropriately. During functional imaging, the task instructions were visually cued by E-prime®, and presented using a pair of goggles customized for fMRI experiments (NordicNeuroLab®).

3.2.3.1 Motor tasks:

To detect primary sensorimotor activation during motor tasks, 2 schemes could be performed according to the location of the tumor: 1) when the tumor was located in the vicinity of the upper part of the central sulcus close to the hand knob[Yousry *et al.* 1997], sequential thumb-to-digits oppositions at 1hz of the right hand and of the left hand were performed successively; 2) when the tumor was located in the vicinity of the lower part of the central sulcus, bilateral lip contractions at 1hz were performed. Motor paradigms were block-designed with 4 cycles of alternating rest (36 seconds) and movements (36 seconds) during 96 dynamic scans, for duration of each run of 4 minutes 48 seconds. Task performance was visually monitored.

3.2.3.2 Carbogen inhalation:

To test the BOLD signal independently of neural activity engaged in motor tasks, all subjects had a BOLD fMRI during carbogen inhalation, a gas mixture of CO_2 (7%) and O_2 (93%). This task was conducted just after motor tasks and consisted of 3 cycles of alternating inhalation of air (60 seconds), carbogen (120 seconds), and air (60 seconds) during 240 dynamic scans, for a duration of 12 minutes. Gas administration was achieved using a nasal canula at 6 liters/min.

3.2.4 Data analysis

3.2.4.1 Functional data

The data was processed offline in MATLAB® with SPM5 software (Wellcome Department of Cognitive Neurology, UK). Preprocessing steps included in-plane motion correction, realignment and spatial smoothing (full-width half-maximum (FWHM): $6\times6\times6mm^3$). No spatial normalization was performed.

3.2.4.1.1 Motor tasks:

Statistical analyses were performed at the individual level, using a temporal cut-off of 128 seconds to filter subject-specific low frequency drift related mostly to the subject's biologic rhythms. Statistical maps were calculated for the movement condition using the canonical hemodynamic regressor and thresholded at $T>3.1$.

3.2.4.1.2 Carbogen inhalation:

To model the BOLD response to carbogen inhalation, 20 healthy right-handed volunteers (women/men: 8/12; age range: 21-37 years; mean: 27.4 years) were scanned during the carbogen task. In 6 subjects, arterial pressures in CO_2 ($aPCO_2$) and O_2 (aPO_2) were measured outside the MRI using a transcutaneous capnometer (TINA-TCM4®, Radiometer, Denmark). For comparison purposes, respiratory analyses, including end-tidal partial pressure ($etPCO_2$), respiratory frequency, but also heart pulse and O_2 saturation, were simultaneously obtained with a MR-compatible Maglife® device (Bruker Medizinteknik, Germany).

The response to hypercapnia was obtained as the mean BOLD signal over all healthy subjects and all brain voxels. It was demeaned and linearly detrended and then used to construct a model of response to carbogen inhalation. To allow a different model between ON/OFF and OFF/ON transitions (observed rise and fall times were different), the average response to each type of transition was fitted using a linear convolution technique between the stimulus function and a gamma function defined as follows: $h(t) = \frac{t}{\tau}\exp\left(-\frac{t}{\tau}\right)$, where t is time and τ is the hemodynamic time constant. A standard search (Nelder-Mead simplex) on parameter τ was performed to optimize the correlation between modeled and measured time series. Finally, the regressor of interest used in patient statistical analyses was obtained by concatenating each model response to ON/OFF or OFF/ON transitions according to the experimental design. Statistical analyses were performed at the individual level, using a temporal cut-off of 428 seconds. Statistical parametric maps were calculated using the dedicated regressor for the carbogen condition and thresholded at T>3.1.

3.2.4.2 Perfusion data

Dynamic susceptibility contrast was estimated using a dedicated software written in MATLAB® to perform first-pass analysis[Barbier *et al.* 2001]. Image preprocessing included: 1) realignment and spatial smoothing (FWHM=6×6×6mm^3), identical to fMRI pre-processing. Data analysis was performed using a voxelwise gamma-variate fitting with a Levenberg-Marquardt algorithm[Levenberg 1944; Marquardt 1963], to provide maps of cerebral blood volume (CBV), mean transit time (MTT), time to peak (TTP). Cerebral

blood flow (CBF) was calculated according to the central principle with CBF=CBV/MTT.

3.2.4.3 Regions of interest

Isometric regions of interest (ROI) of $1\times1\times1cm^3$ were drawn using MRIcroN software (http://www.sph.sc.edu/comd/rorden/mricron/), centered on the maximal T-value of the primary sensorimotor cortex (SM1) contralateral to the motor movement. In all cases but three, ROI were centered on the "hand knob" activated during contralateral hand movements. In patients 4, 15, and 19 who performed lips movements, SM1 activations were detected below "hand knobs".

Delineation of the tumoral border on anatomical 3D-T_1-WI corresponded to the abnormal hypointensity in intra-axial tumors (gliomas), and to the tumoral enhancement in extra-axial tumors (meningiomas). In patients with meningiomas, a peri-tumoral edema was detected in 6 patients out of 10 (Pts 16, 17, 18, 21, 22, 24). Among these patients, only 2 (Pts 18 and 24) had an edema within the ROI placed in SM1 in which fMRI and BOLD response at carbogen were measured. The mirror ROI of each tumor was saved as a contralateral reference. Thus for each patient, 4 ROI were obtained: ipsitumoral SM1 (iSM1), contratumoral SM1 (cSM1), tumor (Tumor), contratumoral (cTumoral). The distance between the center of ipsitumoral SM1 and the closest border of the tumor (distance "SM1-tumor") was measured. For both iSM1 and cSM1, T-values during contralateral motor movements (motor T-value) were extracted. Additionally for all 4 ROI, following parameters were extracted: T-value during carbogen inhalation (carbogen T-value), CBV, CBF, MTT, and TTP. To further facilitate interhemispheric and interindividual comparisons, an interhemispheric ratio was calculated as follows: rBOLD-motor in SM1 = (T-value in ipsitumoral SM1/T-value in contratumoral SM1) during respective contralateral movements. Additional similar ratios were calculated for BOLD signal to carbogen and perfusion parameters: rBOLD-carbogen, rCBV, rCBF, rMTT, rTTP in SM1 and in the tumor.

3.2.4.4 Statistical analysis

All results were analyzed using SPSS®. Intra-individual comparisons were conducted using paired t-test and Wilcoxon test when appropriate. To better understand the variance rBOLD-motor in SM1 across patients, the effect of the qualitative parameter of the tumor (tumor type) was tested using Kruskal-Wallis and follow-up Mann-Whitney tests.

Correlations were calculated using Pearson and Spearman coefficients when conducted on the whole group of patients and on subgroups according to the tumor type, respectively. A multiparametric linear regression analysis with backward selection and a probability value for exit the regression set at 0.10 was further conducted to estimate the predictability of rBOLD-motor among the following parameters: tumoral volume, distance "SM1-tumor", rBOLD-carbogen, rCBV-SM1, rCBF-SM1, rMTT-SM1, rTTP-SM1. Significance level was set at $p<0.05$.

3.3 Results

3.3.1 Primary sensorimotor activation

All patients performed appropriately motor tasks. During contralateral movements, activation expressed in T value was decreased in the ipsitumoral SM1 (m±sd=5.21±2.12) compared to the contratumoral SM1 (6.59±1.40) (*P*=0.001) (Figure III-1). This asymmetry expressed by the ratio rBOLD-motor (see statistical subsection above) ranged from 0.24 to 1.23 (0.79±0.27).

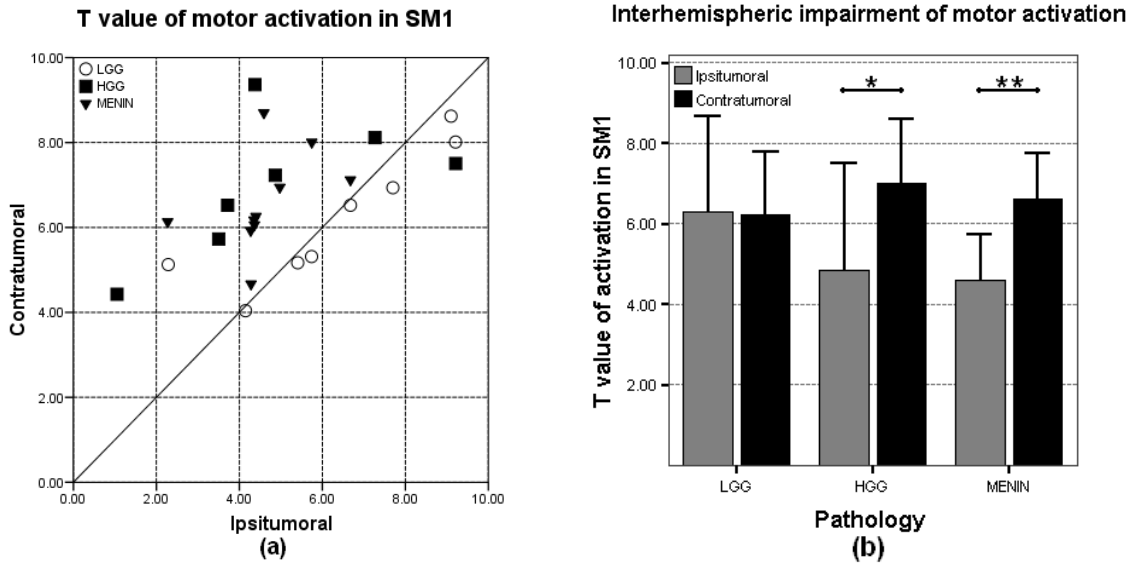

Figure III-1: Activation in contralateral SM1 during motor tasks. *In all patients with meningiomas and HGG but one, T-values measured in SM1 contralateral to the movements were decreased in the ipsitumoral SM1. In all patients with LGG but one, activations in SM1 were roughly symmetrical (a). Paired comparisons confirmed activation decreases in the ipsitumoral SM1 compared to the contratumoral SM1 (*P<0.05; **P<0.01) (b).*

3.3.2 Relationships with tumoral parameters

3.3.2.1 Pathology

Significant decreases of T-values in the ipsitumoral SM1 were detected in patients with HGG and meningiomas, but not with LGG (Figure III-1). This effect supported a decrease in the amplitude of motor-related BOLD signals in the affected hemisphere (Figure III-2). Indeed, rBOLD-motor, was related to the tumor type (P=0.03), due to a significant decrease in meningiomas (0.70±0.16) and in HGG (0.67±0.32) compared to LGG (0.99±0.22).

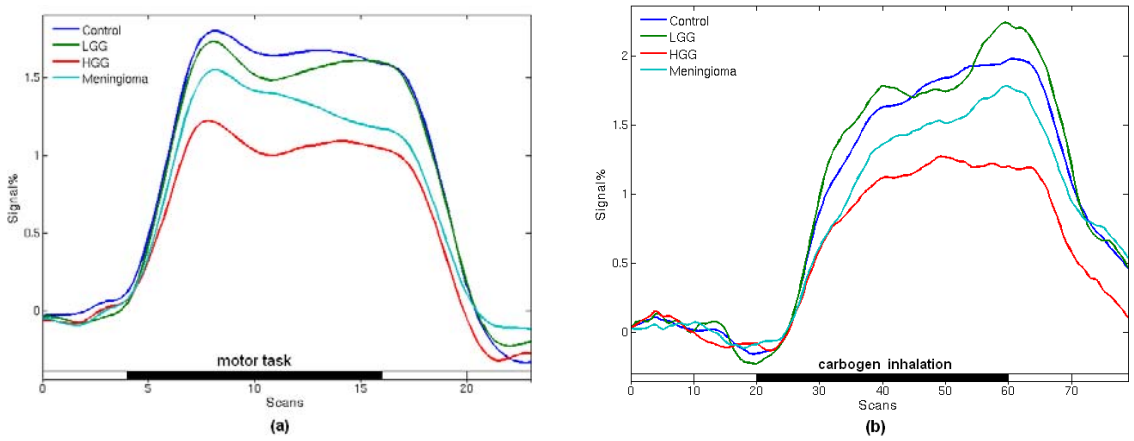

Figure III-2: Mean time courses of BOLD to motor task and carbogen inhalation in SM1*. For all tasks, onsets of BOLD responses were similar. However, BOLD amplitudes were decreased in the SM1 ipsilateral to HGG and meningiomas compared to LGG and healthy hemisphere, in both motor (a) and carbogen inhalation (b) tasks.*

3.3.2.2 Volume and distance "SM1-tumor"

Tumoral volumes were 19.8±14.4 cm^3 in LGG, 44.7±31.8 cm^3 in HGG, and 31.9±24.6 cm^3 in meningiomas, without difference across groups. The distance "SM1-tumor" was not significantly different across groups with 18±11 mm in LGG, 12±10 mm in HGG, 15±6 mm in meningiomas. rBOLD-motor was correlated to the distance "SM1-tumor" (R=0.48; P=0.02), not to the tumoral volume.

3.3.2.3 Tumoral perfusion

Tumoral perfusion was assessed semi-quantitatively using interhemispheric ratios (tumoral ROI/mirror ROI). Given by the interhemispheric CBV ratio, rCBV-tumor was increased in meningiomas (4.75±2.38), but not in HGG (0.84±0.28), neither in LGG

(0.78±0.18) (P<0.001). Similarly, rCBF-tumor was increased in meningiomas (4.25±2.11), not in LGG (0.80±0.23), neither in HGG (0.80±0.30) (P<0.001). rMTT-tumor tended to differ across groups (P=0.08), mainly due to an increase in meningiomas (1.18±0.17) compared to LGG (1.02±0.11) and HGG (1.07±0.06). No difference was detected for rTTP-tumor. rBOLD-motor, was not correlated to any perfusion parameter of the tumor.

3.3.3 Relationships with perfusion in SM1

In SM1, interhemispheric ratios were rCBV-SM1=0.89±0.19, rCBF-SM1=0.89±0.19, rMTT-SM1=1.00±0.08, rTTP-SM1=1.01±0.06. In fact, rCBV-SM1 tended to differ across tumor types (P=0.08), mainly because of a decrease in HGG (0.79±0.19) compared to meningiomas (1.00±0.19) (Mann-Whitney, P=0.04). rMTT-SM1 tended to differ across tumor types (P<0.1), because of an increase in meningiomas (1.04±0.07) compared to HGG (0.96±0.10) (P=0.05) (Figure III-3). No overall difference was detected for rCBF-SM1 and rTTP-SM1. No correlation was observed between rBOLD-motor and any perfusion ratios in the SM1.

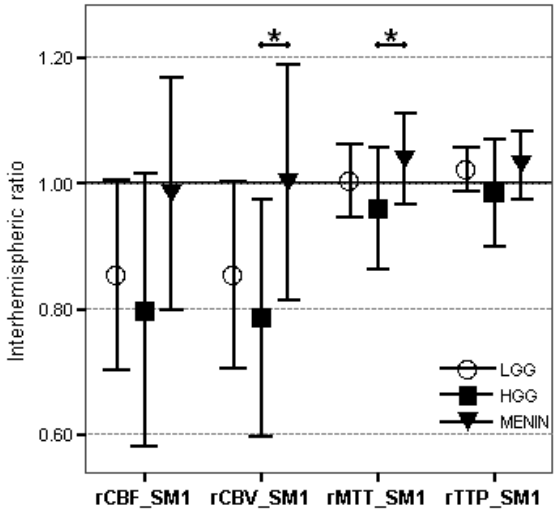

Figure III-3: Perfusion parameters in SM1. *For each perfusion parameter, an interhemispheric ratio (value ipsitumoral SM1/value in controtumoral SM1) was calculated. Overall trends were detected in rCBV-SM1 and rTTM-SM1, mostly because of changes between HGG and meningiomas (*P<0.05).*

3.3.4 Relationships with BOLD response to carbogen inhalation

3.3.4.1 BOLD response in healthy subjects

No adverse reaction, including anxiety, was detected during carbogen inhalation. In 6

subjects, physiological data was obtained outside the MR scanner using the same inhalation paradigm. Arterial PCO_2 increased by 4.8±0.8 mmHg, and arterial PO_2 increased by 51.2±11.6 mmHg, without significant change of heart pulse and respiratory frequency. Mean BOLD signal and its model (see Methods) are shown in Figure III-4.

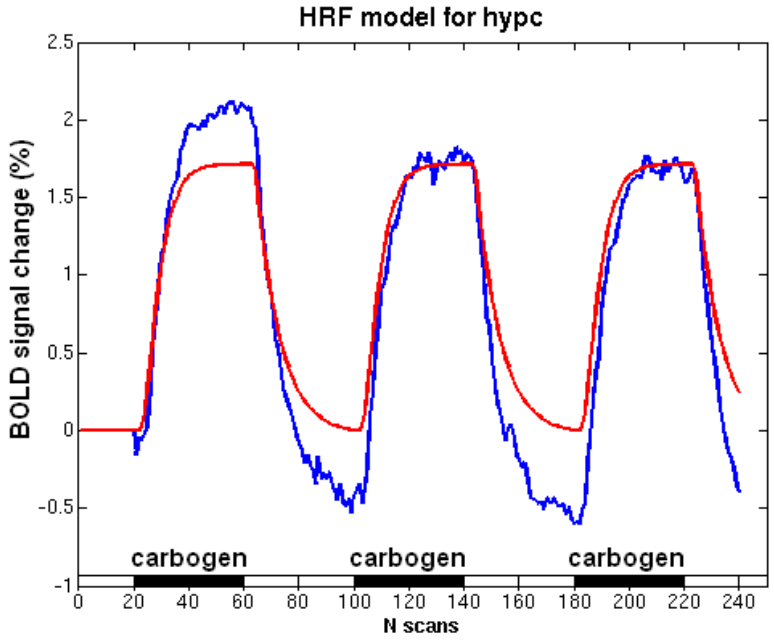

Figure III-4: Mean BOLD signal changes during carbogen inhalation in controls. *Mean percentage of BOLD signal changes in controls (blue line) elicited by alternating air and carbogen inhalation provided a dedicated regressor (red line), further used to analyze BOLD signal changes to carbogen inhalation in patients.*

3.3.4.2 Patients

The same gas inhalation paradigm was performed in all patients, without any adverse effect during or after the gas administration. Using the dedicated regressor, T-values were decreased in the ipsitumoral SM1 (12.3±4.9) compared to the contratumoral SM1 (13.5±5.1) (P=0.04). Despite a decrease in the amplitude of carbogen-related BOLD signals in the affected hemisphere in both meningiomas and HGG compared to LGG and the healthy hemisphere (Figure III-2), interhemispheric differences of T-values reached significance in patients with meningiomas, only (P<0.05). The interhemispheric ratio in SM1, rBOLD-carbogen, ranged from 0.49 to 1.46 (0.92±0.22), was significantly correlated to rBOLD-motor (R=0.51; P=0.01) (Figure III-5). For tumoral subgroups, rBOLD-

carbogen was correlated with rBOLD-motor in all gliomas (n=15; ρ=0.73; P=0.02), with a trend for HGG (n=7; ρ=0.71; P=0.07). Actually, 94.9±4.9% of all motor activations overlapped significant BOLD response to carbogen inhalation.

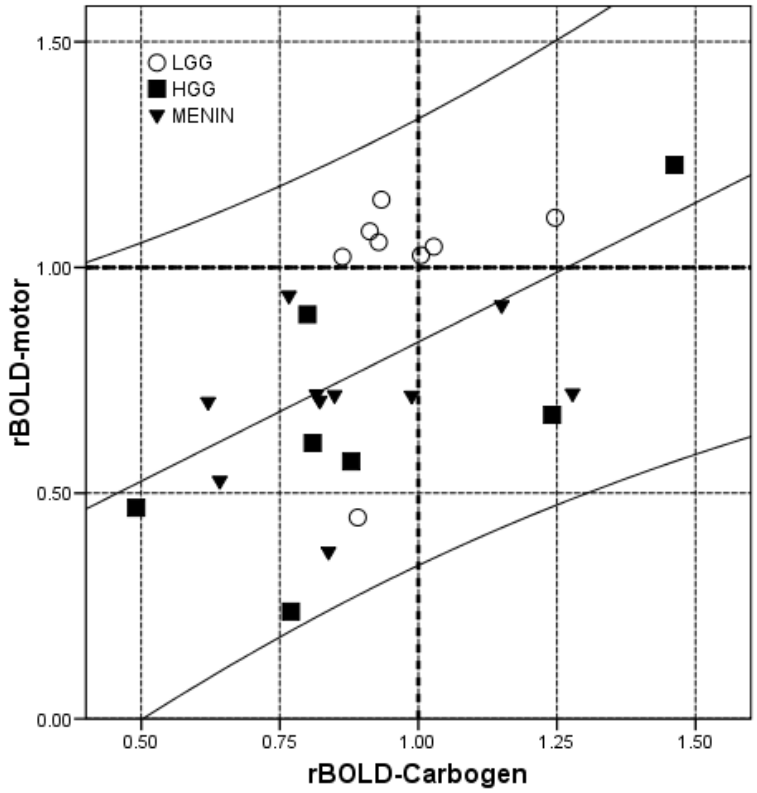

Figure III-5: Relationship between BOLD responses to carbogen inhalation and motor activation in SM1*In SM1, interhemispheric ratios of BOLD responses to carbogen inhalation (rBOLD-carbogen) and motor activation (rBOLD-motor) were correlated (R=0.51; P=0.01). The equation of the regression line expressed by rBOLD-motor = B·rBOLD-carbogen + C; with B=0.62±0.22 (β=0.51; p<0.01), and C=0.22±0.21 (P=0.3).*

3.3.5 Regression analysis

A multiparametric regression analysis was conducted to investigate which parameters among tumoral volume, distance "SM1-tumor", rBOLD-carbogen, rCBV-SM1, rCBF-SM1, rMTT-SM1, rTTP-SM1, may significantly account for the variance of the activation impairment in SM1 expressed by rBOLD-motor. Only rBOLD-carbogen was selected with an adjusted R^2=0.23 (p<0.01) (Figure III-5).

Illustrative cases are presented in Figures III-6-8.

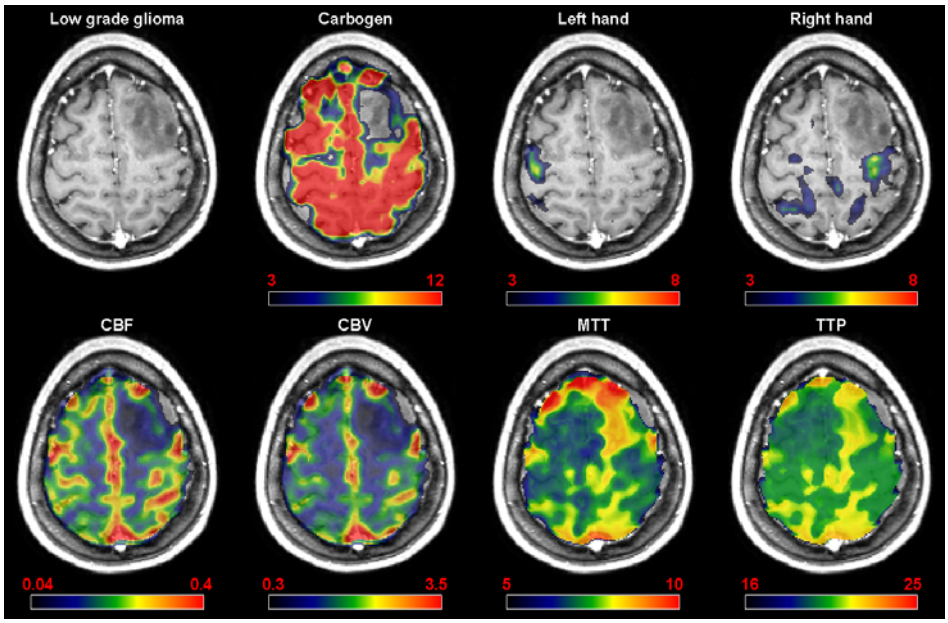

Figure III-6: Patient 5 with a low grade glioma of the left frontal lobe. *No abnormal perfusion was detected in both SM1. Hand movements elicited symmetric BOLD response in SM1 (rBOLD-motor=1.03). This symmetrical BOLD response was also detected after carbogen inhalation (rBOLD-carbogen=1.05). In SM1, rCBV=0.95, rCBF=0.96, rMTT=0.99, rTTP=0.98.*

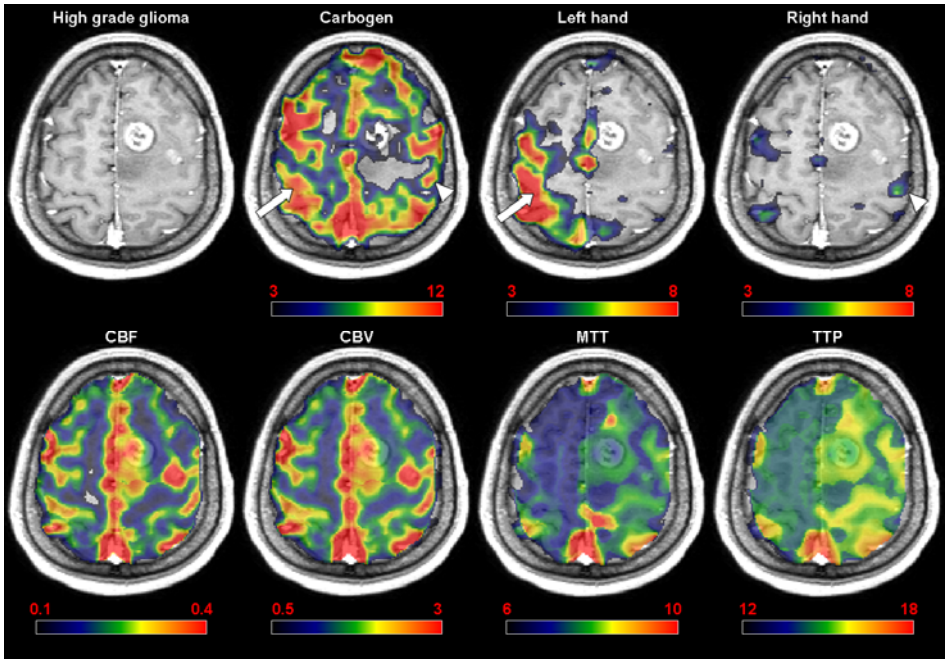

Figure III-7: Patient 14 with glioblastoma of the left frontal lobe.*Left hand movements elicited stronger activation in the right SM1 (arrow) than this detected during right hand movements in the left SM1 (arrowhead) (rBOLD-motor=0.47). This asymmetrical BOLD response was also detected after carbogen inhalation (rBOLD-carbogen=0.49). A mild hypoperfusion of the ipsitumoral SM1 was detected with rCBV=0.71, rCBF=0.73, rMTT=0.88, rTTP=0.90.*

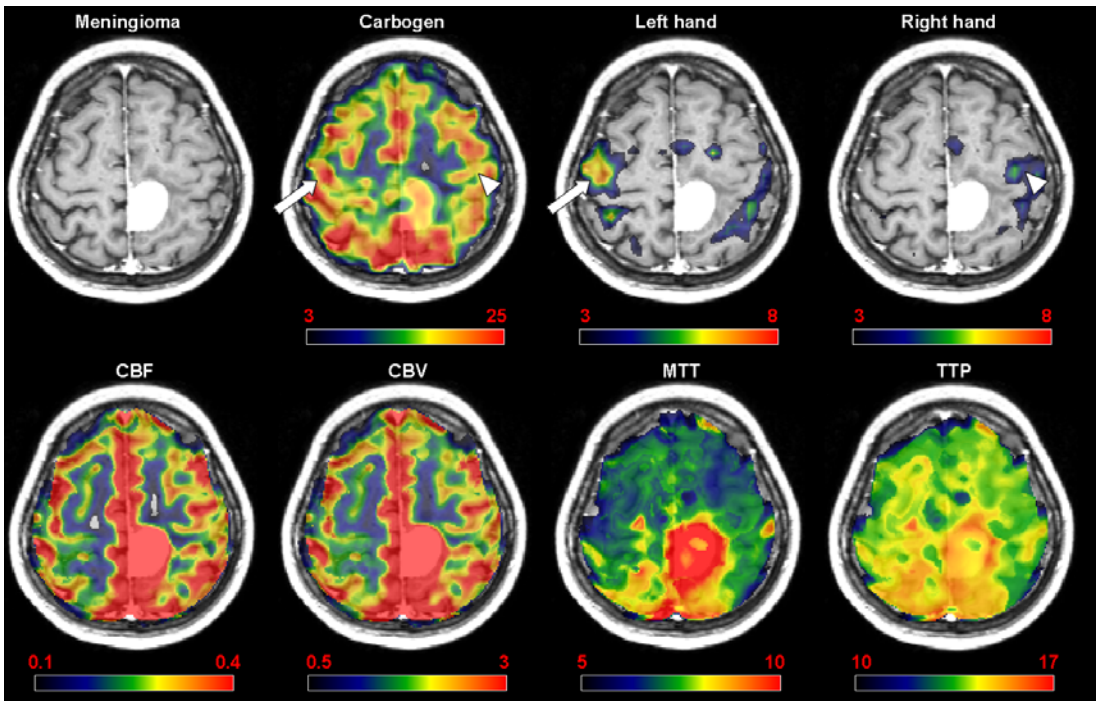

Figure III-8: Patient 16 with a meningioma of the medial aspect of the left paracentral lobule. *Left hand movement elicited a stronger activation in the right SM1 (arrow) than this detected during right hand movements in the left SM1 (arrowhead) (rBOLD-motor=0.72). This asymmetrical BOLD response was also detected after carbogen inhalation (rBOLD-carbogen=0.82). In SM1, perfusion was normal with rCBV=1.01 and rCBF=0.95, whereas as slight increase in transit time was detected with rMTT=1.07 and rTTP=1.04.*

3.4 Discussion

In this study on patients with brain tumor at initial admission, we have reported that motor-related activation in eloquent primary sensorimotor cortex was decreased in the ipsitumoral hemisphere. This impairment was detected in patients with meningiomas and high grade gliomas, but not with low grade gliomas. It was related to the vicinity of the lesion. Subtle changes in basal perfusion of adjacent parenchyma were detected across tumor types, but they could not solely account for the variance of activation asymmetry, suggesting different pathophysiological changes. An additional evaluation of the BOLD signal was performed using carbogen inhalation. This test that provided a broad BOLD contrast, independent of motor-elicited neural activity, showed a similar and significantly

correlated asymmetry in primary sensorimotor cortices.

3.4.1 Distance

Decreased ipsitumoral activation was correlated with the vicinity of the tumor, even for a distance greater than 10 mm, as previously reported[Liu *et al.* 2005; Hou *et al.* 2006; Ludemann *et al.* 2006]. In fact when the tumor is located within the SM1, the reliability of activation in the eloquent cortex elicited by motor tasks is highly questionable for several reasons.

First, poor performance during fMRI might explain decreased activation due to neurological deficit. Second, intratumoral hemorrhage and calcifications may be responsible of susceptibility artifacts and hypointensities on native T_2*-weighted images associated with abnormal activation. Similar artifacts may also be induced by prior surgery[Kim *et al.* 2005]. Third, intratumoral changes in oxygenation and hemodynamics can hardly guarantee appropriate physiological basis of the BOLD contrast. Thus, decreased activation may lead to false negative results[Holodny *et al.* 2000; Ulmer *et al.* 2003; Fujiwara *et al.* 2004; Ulmer *et al.* 2004].

To minimize the risk of inappropriate task performance during fMRI sessions such as different movement amplitude, rate, strength, and mirror movements, to avoid measuring tumoral tissue and artifacts due to hemorrhage or calcifications, and to estimate perfusion and BOLD signal within a morphologically normal eloquent parenchyma, patients were selected 1°) before any surgical procedure, 2°) without obvious tumoral involvement of the primary sensorimotor cortex (SM1) given by a normal neurological examination and a minimal distance of 5mm between SM1 and the border of the tumor delineated on anatomical 3D-T_1-WI corresponding to the abnormal hypointensity in intra-axial tumors (gliomas), and to the tumoral enhancement in extra-axial tumors (meningiomas).

However, we acknowledge that our assumption of functional and anatomical "normality" has several limitations. First, the normality of motor performance was assessed by clinical examination and visual monitoring. Second, the absence of tumoral

infiltration of the SM1 was assessed using conventional MRI, whereas neoplastic cells of gliomas could be detected in remote areas, without abnormality on conventional MRI[Giese *et al.* 1996]. Moreover, we did not exclude 2 patients with meningiomas and a peritumoral edema involving SM1 (Pts 18, 24). Advanced MR techniques such as Diffusion Tensor Imaging (DTI) seem more sensitive than conventional imaging to detect remote tumoral infiltration in gliomas, but not peritumoral edema in meningiomas [Provenzale *et al.* 2004].

Besides undetected parenchymal abnormalities, the effect of the distance could rely on several disorders in relation with the tumor type such as peritumoral changes in perfusion and metabolism. From a clinical perspective, the effect of vicinity which might mislead interpretation is an obvious issue as fMRI is particularly required as the tumor is closer to functional areas.

3.4.2 Tumor type and age

In line with several authors[Holodny *et al.* 2000; Schreiber *et al.* 2000; Ulmer *et al.* 2004; Liu *et al.* 2005; Chen *et al.* 2008], we found that BOLD signal impairment was mainly detected in patients with higher grade gliomas and meningiomas. Mainly because of patients with meningiomas were older than others, we found a relationship between the age and the interhemispheric activation impairment (R=-0.51, P<0.01). However, when conducted on pathological subgroups no correlation was detected between age and rBOLD-motor. In this particular context, the confounding effect of age on BOLD signal has been recently addressed, with a persistent lower BOLD signal in patients with glioblastoma even after controlling for age[Chen *et al.* 2008]. Thus, the effect of age on activation asymmetry seemed rather due to the incidence of tumor types with ageing, despite the fact that ageing may unveil pre-existing vascular disorders beside tumors.

In clinical practice, this result emphasizes indirectly the validity of preoperative fMRI in patient with low grade gliomas whose, among patients with gliomas, could expect a greater benefit of complete tumoral resection[Duffau *et al.* 2005].

3.4.3 Tumoral and peritumoral perfusion

In line with experimental data in healthy subjects showing that BOLD signal may decrease as CBV increases[Cohen *et al.* 2002], the influence of the tumor type on activation impairment might be explained by locoregional change in basal perfusion. Indeed, local hyperperfusion reported in patients with hypervascularized tumor such as HGG and meningiomas has been advocated to explain decreased activation[Hou *et al.* 2006; Ludemann *et al.* 2006]. This phenomenon was related to the vicinity of the lesion, and seemed critical when the motor cortex was located within the lesion[Hou *et al.* 2006].

We did not detect any significant relationship between activation and perfusion characteristics of the tumor. Contrary to previous studies[Hou *et al.* 2006; Ludemann *et al.* 2006], we selected patients without obvious tumoral involvement of the SM1 to avoid considering intratumoral activations which are hardly reliable for the reasons mentioned above.

Besides tumoral perfusion, we analyzed perfusion in functional SM1. A slight decrease in CBV in the ipsitumoral cortex of patients with gliomas was detected whereas CBV were symmetrical in patients with meningiomas (Figure III-3). In SM1, CBV and others parameters were not correlated with motor activations.

In patients with low-grade and high-grade gliomas, CBV and CBF were both reduced (Figure III-3). As a consequence of the vascular compression by the peritumoral infiltration and edema, CBV giving the blood fraction of the voxel, may decrease. Whereas a negative correlation between the distance and CBV (and CBF) has been previously described in HGG and meningioma[Bitzer *et al.* 2002; Uematsu *et al.* 2003; Hou *et al.* 2006; Lehmann *et al.* 2009], we detected this relationship in patients with LGG (ρ=-0.74, $P<0.04$), only. Actually, autoregulation allows vasodilatation to maintain a constant perfusion pressure and to compensate local increase in intracranial pressure. As previously suggested, autoregulation could be impaired in intra-axial tumors[Holodny *et al.* 2000; Chen *et al.* 2008]. In LGG, the preserved correlation of CBV with the distance could be interpreted as functional disorder of the autoregulation due to the mass effect, whereas the lost of this

correlation in HGG may suggest a deeper physiological impairment. In meningiomas, CBV was normal suggesting whether a preserved autoregulation or a poorly significant mass effect. To note that in patients 18 and 24 who harbored edema in the ipsitumoral SM1, rCBV was decreased.

Some limitations in our method to estimate perfusion might have dimmed the relationships with activation patterns. First, the tumoral CBV was likely underestimated, especially in necrotized high grade gliomas, because we used a whole-tumoral ROI that averaged important heterogeneities across the ROI, including neo-angiogenesis and necrosis foci. Second, we used a dynamic first-pass method, based on the integration of the signal drop using a voxelwise gamma-variate fitting. In case of brain-blood barrier (BBB) disruption, the extravascular leakage of Gd-DTPA results in an attenuation of the first-pass signal drop followed by an overshoot of the signal baseline. Thus in HGG, this phenomenon is known to underestimate CBV[Boxerman *et al.* 2006]. Several methods were proposed to better estimate perfusion including T1 mapping, pre-loading of contrast agent to saturate the interstitium. Such acquisitions were not performed at the time of fMRI examination. An alternative approach based on a bicompartimental model using a deconvolution of the arterial input function is now recommended to provide quantification of the brain perfusion[Ostergaard *et al.* 1996]. Indeed, advanced MRI allows characterizing tumoral neo-angiogenesis, vessel size and BBB disruption[Sorensen *et al.* 2009]. However, deconvolution methods are highly sensitive to arterial input function (AIF) selection, i.e. location and acquisition type[Bleeker *et al.* 2009a]. Indeed even using deconvolution methods, additional improvements are necessary to reach absolute quantification of perfusion, especially in brain-lesioned patients[Calamante *et al.* 2009].

In fact, relative estimation of brain perfusion using interhemispheric ratios on perfusion maps calculated without AIF selection, is a well-known method, demonstrated to be robust and reproducible[Wetzel *et al.* 2002]. In clinical practice and to our knowledge, all MR manufacturers still provide this method on their workstation, although new softwares based on deconvolution techniques are now appearing. Moreover, many clinical

studies in neuro-oncology were conducted using gamma-variate fitting correction, even recently[Law *et al.* 2008]. Then, relative CBV estimation remains daily used to better diagnose and care patients with brain tumors in most groups.

In fMRI literature, very few articles addressed the relationships between perfusion and BOLD activation in patients with brain tumors, both deconvolution[Ludemann *et al.* 2006] and gamma-variate fitting were used[Hou *et al.* 2006]. Finally in our study, we have tested the relationships between relative parameters based on interhemispheric ratios. We agree that absolute quantification would better describe perfusion, and even the range of interhemispheric ratios. However, significant changes in our correlation analyses conducted using non-parametric method based on value ranking, are unlikely.

3.4.4 BOLD responses to motor and carbogen inhalation

To estimate the BOLD signal independently of sensorimotor neural activity, we conducted BOLD acquisition during carbogen inhalation for each patient after having extracted an empirical regressor from healthy subjects. BOLD signal related to carbogen was mainly located in the gray matter, in accordance with previous studies[Vesely *et al.* 2001; Rauscher *et al.* 2005; van der Zande *et al.* 2005]. Despite competing effects of CO_2 and O_2 on the CBF via the cerebral vasoreactivity (CVR), it was shown that CBF increases from 10 to 20%[An *et al.* 2003; Ashkanian *et al.* 2008]. Although CVR, autoregulation, and neurovascular coupling are different properties that react to distinct stimuli, these mechanisms elicit a vasomotor response that relies on common structural characteristics of the microvasculature. Indeed, imaging of CVR using BOLD signal to carbogen and CO_2 inhalation has been proposed to explore perfusion changes, especially in patients with vascular disorders and false negative fMRI results[Rother *et al.* 2002; Hamzei *et al.* 2003].

Here, we observed that almost 95% of all motor activations overlapped significant BOLD response to carbogen inhalation, suggesting that the underlying structures involved in the BOLD signal during neural stimuli are also elicited by carbogen inhalation. The amplitudes of BOLD signals to carbogen and motor tasks were similar but time courses

were different (Figure III-2). In fact, no direct correlation between both BOLD signals could be detected at the voxel level, when analyzed using dedicated regressors for each task tested by the general linear model. However using a semi-quantitative analysis with interhemispheric ratios, rBOLD-motor and rBOLD-carbogen were correlated. The regression analysis even showed that rBOLD-carbogen was the best quantitative predictor to explain the variance of rBOLD-motor across patients. These results are in line with those obtained in patients after stroke, despite several methodological differences including: 1) the estimation of vasoreactivity, that was obtained during hyperventilation that led to hypocapnia and vasoconstriction, and 2°) BOLD signals analyses which were conducted on percentage of signal change[Krainik *et al.* 2005]. Although common anatomical components produce BOLD signals, the absence of direct correlation between vasoreactivity and motor tasks at the voxel level reflects, at least, physiological differences regarding evoked vasomotor and cerebral blood oxygenation (CBO) changes. However in brain-lesioned patients, significant relationships between interhemispheric ratios of vasoreactivity and motor tasks suggest common pathophysiological disorders.

3.4.4.1 The oxygenation hypothesis

The oxygenation hypothesis was proposed after combined fMRI-NIRS studies in brain-lesioned patients[Sakatani *et al.* 2007]. In patients with primary brain neoplasms and during motor tasks, NIRS showed CBV increase in eloquent SM1. Whereas the concentration of deoxyhemoglobin (deoxy-Hb) decreased as expected in the healthy hemisphere, NIRS identified two groups of patients on the basis of the evoked deoxy-Hb changes in the ipsitumoral hemisphere, the “deoxy-Hb decrease” group and the “deoxy-Hb increase” group[Fujiwara *et al.* 2004]. Deoxy-Hb increase in patients after stroke was also reported[Murata *et al.* 2002]. Main hypotheses were: 1°) a decreased oxygen delivery, 2°) an increased oxygen extraction that may due to impaired hemodynamics including an increased blood transit time[Murata *et al.* 2002; Sakatani *et al.* 2007], and 3°) changes in venous oxygenation and blood volume [Hoshi *et al.* 2001]. In fact, some normal adults and newborn infants did also have deoxy-Hb increase in eloquent cortex[Sakatani *et al.* 1999a;

Sakatani *et al.* 1999b]. No histological data could still help to further understand these results. Thus, deoxy-Hb increase should not be interpreted as an abnormal evoked-CBO change, rather atypical[Fujiwara *et al.* 2004]. Considering plausible heterogeneous evoked-CBO changes within the eloquent cortex, spatial resolution of the NIRS may fail to identify small foci of deoxy-Hb decrease related to neural activity, whereas using BOLD-fMRI activation areas are smaller than they really are[Sakatani *et al.* 2007].

Finally, a combined hypothesis could be advanced considering atypical evoked-CBO changes and impaired vascular response to neural activity in the vicinity of the tumor[Fujiwara *et al.* 2004]. Such hypothesis could be further studied using combined fMRI-NIRS during vasoreactivity and motor tasks.

Besides oxygenation disorders in the vicinity of brain lesions, impaired vasomotor responses have been previously proposed to explain BOLD discrepancies[Arthurs and Boniface 2002]. Schematically, pathophysiological alterations might be secondary to changes in: 1°) the functional mechanisms that link a specific stimulus and a vasomotor response (neurovascular coupling in response to neural activity, vasoreactivity to circulating gases, and autoregulation to perfusion pressure); 2°) the quality of the hemodynamic responses that might be affected by loco-regional changes in basal perfusion and structural abnormalities of the vasculature.

3.4.4.2 The functional hypothesis

The functional hypothesis would rely on selective dysfunction of the physiological properties of the brain vessels. In spite of the lack of direct estimation of the autoregulation, our data showed correlated abnormalities between neural and gaseous stimuli. This result could suggest both functional and hemodynamic disorders. Although partially elucidated, neurovascular coupling and vasoreactivity are mediated by common metabolic changes, such as NO and H^+, and both properties rely on the integrity of the BBB[Xu *et al.* 2004; Girouard and Iadecola 2006; Lavi *et al.* 2006]. In HGG with BBB disruption, the vasomotor properties of the surrounding parenchyma are likely impaired. To our knowledge, no data is available in patients to show how far these impairments could be

detected from the BBB disruption. Here, we choose to measure such effects in the peritumoral parenchyma that seemed normal on conventional anatomical images. Thus, our results could suggest both remote effects of the BBB disruption as previously suggested in stroke[D'Esposito *et al.* 2003; Rossini *et al.* 2004; Krainik *et al.* 2005], and local structural abnormalities like edema or BBB disorder invisible to conventional MRI. Precious information could be expected from DTI and permeability imaging to better know how far BBB impairment could be detected from the tumoral core.

In meningiomas, BBB is usually respected, except in case of cortical adherence and malignancy. In such lesions, peritumoral edema is present[Bitzer *et al.* 1997; Vaz *et al.* 1998]. Here, no frank cortical adherence was detected during surgery and all meningiomas were benign. Meningiomas were located at from 7 to 29 mm to SM1. Adjacent peritumoral edema was detected in 6 out of 10 patients, and involving SM1 in 2 patients, only. Thus, impaired functional properties of the vasculature due to a BBB disruption seem unlikely in such patients.

3.4.4.3 The hemodynamic hypothesis

The hemodynamic hypothesis would be supported by regional perfusion changes whether due to the tumoral vascularisation, whether to structural alterations of the surrounding brain vessels.

The regional effects of the hypervascularisation of meningiomas and of neo-angiogenesis in HGG have been previously reported to explain decreased fMRI activations [Hou *et al.* 2006; Ludemann *et al.* 2006]. During hemodynamic responses to vasomotor stimuli, the functional hyperperfusion would be partially absorbed by the surrounding hyperperfusion of the tumor, mimicking a functional steal phenomenon.

In our group of HGG, this hypothesis seems unlikely because of the absence of major neo-angiogenesis, despite an obvious underestimation of the tumoral CBV in necrotized tumor as mentioned above. Actually, rCBV in SM1 was rather decreased contrary to previous studies[Ludemann *et al.* 2006; Chen *et al.* 2008]. Such differences could be likely due to the absence of tumoral infiltration of the SM1 in our series.

In meningiomas, this hypothesis seems interesting because of the strong tumoral hypervascularisation. Although no significant change in CBF and CBV was detected in eloquent cortex, MTT tended to increase. This effect could be explained by a preserved autoregulation, which maintains perfusion pressure by compensating the decrease in the mean arterial pressure due to a subtle steal phenomenon. This effect could maintain basal perfusion but the compensatory vasodilatation would be partially exhausted. Thus, the range of potential perfusion increase would be reduced and evoked BOLD signals as well. Beside arteriolar disorders, impaired venous drainage and stasis induced by meningiomas and the involvement of cortical veins, bridging veins and dural sinuses have been previously reported, especially in patients with edema [Bitzer *et al.* 1998; Bitzer *et al.* 2000]. As BOLD contrast relies, at least partially, on venous dilatation[Lee *et al.* 2001; Buxton *et al.* 2004], it could be impaired whatever the functional stimulus used. Finally, increased MTT in meningiomas could also be responsible of a decrease in BOLD signal secondary to an increase in oxygen extraction and deoxy-Hb concentration as previously advocated[Murata *et al.* 2002; Sakatani *et al.* 2007].

Structural alterations of brain vessels might also impair morphological changes elicited by functional stimuli. In such case, one may expect that all functional properties could be affected whatever functional stimuli used. These alterations could be due to an increase in vascular stiffness that might lead to a chronic hypoperfusion. It has been previously suggested in patients with cerebrovascular disorders including stroke, diabetes mellitus, chronic hypertension and ageing[Rother *et al.* 2002; D'Esposito *et al.* 2003; Hamzei *et al.* 2003; Rossini *et al.* 2004; Krainik *et al.* 2005; Girouard and Iadecola 2006], and even in patients with neurodegenerative disorders such as Alzheimer disease[Farkas *et al.* 2001; Girouard and Iadecola 2006; Silvestrini *et al.* 2006].

In patients with tumors, structural abnormalities of the microvessels were described in case of brain edema[Coomber *et al.* 1987; Vaz *et al.* 1998]. In HGG, morphological changes such as occasional fenestration of peritumoral vessels support an increase in permeability[Vaz *et al.* 1996]. In meningiomas, edema occurs in case of cortico-pial

adherence and pial blood supply, especially in secretory and malignant meningiomas[Bitzer *et al.* 1997]. Basal perfusion changes are commonly associated [Bitzer *et al.* 2002; Uematsu *et al.* 2003; Lehmann *et al.* 2009]. In our study, we did not obtain histological data of peritumoral brain parenchyma and its vasculature, thus we could not rule out subtle edema and regional structural changes of vessels. However our results do not support a major effect of structural abnormalities of parenchymal vessels to explain BOLD impairments in SM1 considering, with the methodological reserves mentioned above, the absence of edema in all patients but two meningiomas, the absence of obvious BBB disruption, and the slight perfusion changes.

3.5 Conclusion

To summarize, our results suggest that peritumoral BOLD fMRI is affected by the distance and the pathology. In case of LGG, a pathological condition which may have a benefit of complete surgical resection even in functional areas[Duffau *et al.* 2005], BOLD signals elicited by motor tasks and carbogen inhalation were normal. However, obvious impairments were detected in HGG, that might have been due to a vasomotor disorder, common to both neural and CO_2 stimuli. While CBV was decreased in the ipsitumoral SM1 in HGG contrary to meningiomas, a loss of autoregulation was likely as previously suggested[Holodny *et al.* 2000; Ludemann *et al.* 2006; Chen *et al.* 2008]. Thus in HGG, a loco-regional dysfunction of the BBB could be advanced because common functional properties of brain perfusion, which rely on the BBB integrity, seemed altered. In meningiomas, abnormal but uncorrelated responses to neural and CO_2 stimuli associated with a maintained perfusion in the ipsitumoral SM1 that might correspond to a compensatory vasodilatation, preserved vascular properties are likely but, at least, partially exhausted to compensate the mass effect and a potential steal phenomenon of these hypervascularized lesions[Holodny *et al.* 2000; Ludemann *et al.* 2006; Chen *et al.* 2008].

Both functional and hemodynamic hypotheses could also be associated with evoked

CBO changes, as a cause or consequence. Indeed, these physiological properties are closely related with numerous interactions, explaining why independent studies of each phenomenon are highly challenging. As BOLD fMRI aggregates evoked CBO and functional changes in brain perfusion, the data interpretation might remain equivoqual, especially in case of focal lesion that modify these parameters. Multimodal advanced imaging, including DTI to better detect peritumoral infiltration and edema, perfusion study with permeability and vessel size imaging, functional imaging of the perfusion using arterial spin labeling during vasomotor challenge, oxygenation imaging using MRI or NIRS, could be proposed to better interpret fMRI data in patients, and to better characterize and understand structural and functional changes in the vicinity of brain lesions.

Chapter IV Perspectives of MR Imaging of brain tumors – CONCLUSION

As far as diagnostic, prognostic, pre-therapeutic and treatment follow-up are concerned, MR imaging has become an important tool owing to its approving spatial and temporal resolution, and to combining with the approaches of morphology, metabolism, and bio-function, some of these being already available on clinical machines, but others are being currently developed in laboratories.

In comparison with other imaging techniques, MR imaging shows a notable advantage that it allows transferring the new approaches and new scanning sequences, which are developed and tested on animal models or experimental equipments, in clinical application immediately. A bunch of articles have been already published on this subject, and in particular on brain tumors, due to some of these developments enabling ones to test new molecules that likely intend anti-angiogenesis in animal model, for instance[Jain *et al.* 2007; Jouanneau 2008]. Further investigations are necessary to understand the tumoral neo-angiogenesis phenomenon and its evolution in vivo. This tumoral neo-angiogenesis is known as a factor linked with the tumoral growth and its aggressiveness[Leon *et al.* 1996; Zagzag *et al.* 2000; Vajkoczy *et al.* 2002]. Although the necessary processes to create the neo blood vessels and the regulation of the pros- and anti-angiogenic molecule are complex, a number of classes of molecules are implied in the tumoral angiogenesis [Jouanneau 2008]. Today, a lot of important researches are done to create new drugs for the angiogenesis target, either during pre-clinical animal testing, or in clinical testing.

In this context, biomarkers are expected to better predict the response or the resistance to the treatment. Moreover, monitoring the anti-angiogenic effects is necessary. The imaging techniques, especially the modern MR imaging techniques should play an important role in this area[Batchelor *et al.* 2007] (Figure IV-1).

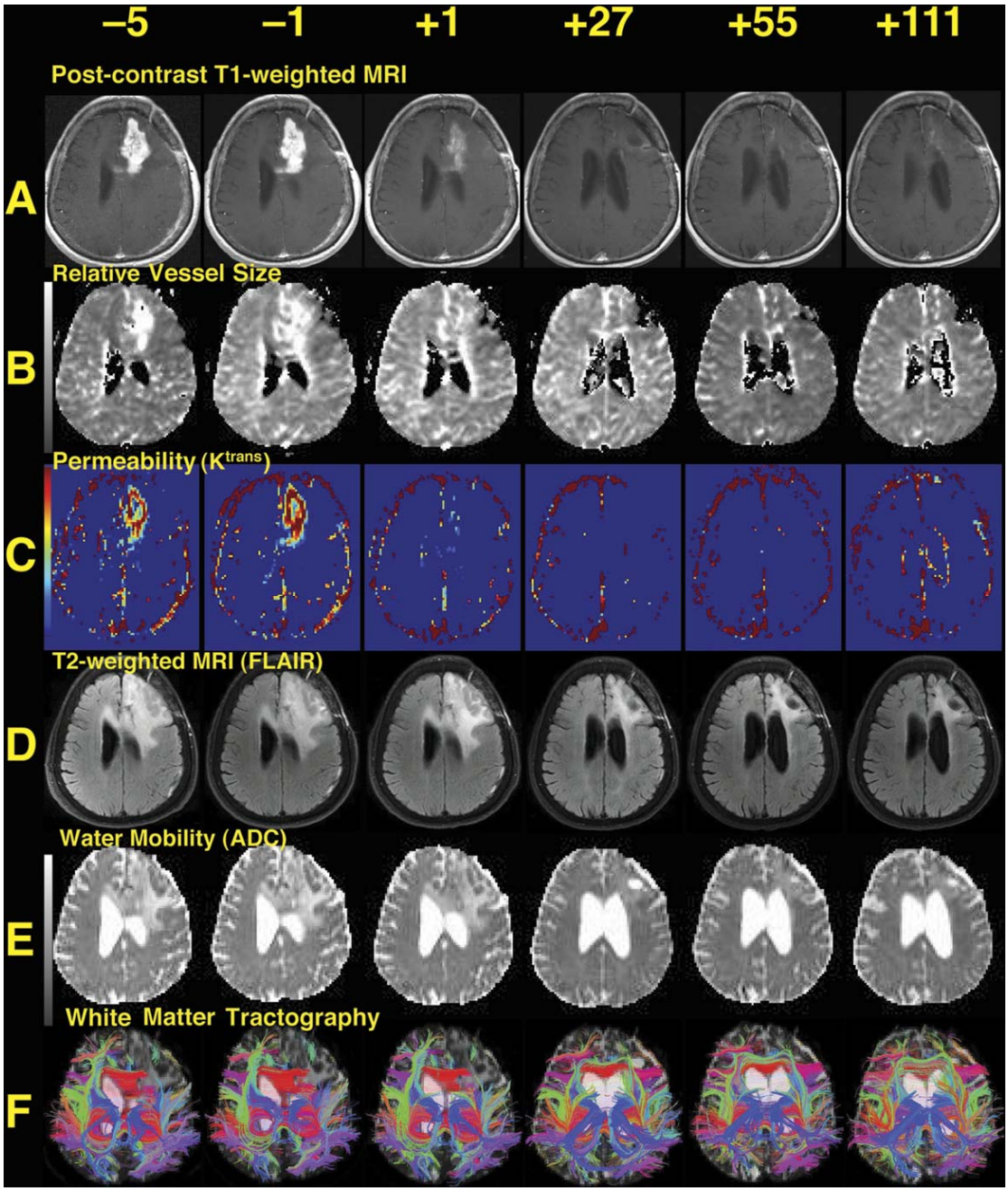

Figure IV-1: Multi-parameter MRI for estimating the response of anti-angiogenetic agent in gliobalstoma patients. *A) T_1-weighted images after administration of gadolinium-DTPA, demonstrating a glioblastoma in the left frontal lobe shrinking over time. B) Map of relative microvessel size, also showing decrease over time. C) Maps of K^{trans} showing deceased permeability over time. D) FLAIR images and E) ADC images showing the edema surrounding the tumor also reducing over time. F) Tractography demonstrating the white matter tracts recovering more evident along with the decrease of vasogenic edema and of the mass effect. ADC, apparent diffusion coefficient; DTPA, diethylenetriamine pentaacetic acid; FLAIR, fluid-attenuated inversion recovery sequence; GBM, glioblastoma.[Batchelor et al. 2007]***.

4.1 Multi-parameteric MRI

4.1.1 Cerebral blood volume variations

Cerebral blood volume variations rely on both vascular density changes and vascular caliber changes. The DSC MRI technique with gadolinium injection, as used in this work, gives priority to the temporal resolution, at the expense of spatial resolution. Besides, the leakage of gadolinium due to damaged BBB results in under-estimation of CBV[Paulson and Schmainda 2008].

A steady-state MRI technique has been developed to determine absolute blood volume, using ultra small super paramagnetic iron oxide (USPIO), an intravascular contrast agent whose plasmatic half-life is enough long and remaining intravascular even if the BBB is damaged[Beaumont *et al.* 2009]. The disturbed magnetic field induced by intravascular USPIO extends into adjacent tissues, leading to an increase of transversal relaxation velocity of R_2* (R_2*=1/T_2*). Measuring R_2* before and after injection enables one to calculate the variation of R_2* (ΔR_2*), and then the CBV[Tropres *et al.* 2001].

In comparison with the dynamic technique of bolus tracing, the steady-state measurement using USPIO has a increased signal-to-noise ratio, thus providing a better spatial resolution. Unlike the former, this technique has no requirement to determine the AIF during quantitative measurements.

4.1.2 Measurement of the vessel size index

Some MRI techniques have been developed to estimate the distribution of microvessel radii, which is represented as an approximation of the mean vessel size index (VSI) in cerebral tumors.

The measure of VSI is, like the CBV measurement mentioned above, based on the changes in the magnetic susceptibility induced by the presence (or the passage) of a contrast agent in the blood vessels. Besides increasing in transverse relaxation time R_2*, the presence of intravascular contrast agent induces also an increase in R_2 (R_2=1/ T_2). The increase in R_2 is principally due to the diffusion effects of water molecules into vessel

surrounding tissues. By combining sequences of gradient echo and spin echo before and after injection, ΔR_2^* and ΔR_2 measurements are carried out using either dynamic method[Kiselev *et al.* 2005] or steady-state method[Tropres *et al.* 2001; Tropres *et al.* 2004]. Then the VSI can be calculated from the ratio of $(\Delta R_2^* / \Delta R_2)^{3/2}$, and from a coefficient of the water diffusion and the concentration of intravascular contrast agent according to a deduced equation.

Similar to the measurement of CBV, the steady-state method needs a contrast agent that should strictly remain into the intravascular compartment during image data acquisition, which is quite slower than that using dynamic method. In comparison with the dynamic method, the estimation of AIF is not required and it allows an absolute quantification of VSI with a better spatial resolution.

4.1.3 Measurement of vascular permeability

Measuring the degree of permeability of the BBB in brain tumors has exhibited its promising value both in tumoral diagnosis and treatment follow-up. Increased vascular permeability has been correlated with higher grades of tumor which has more aggressive property[Roberts *et al.* 2000; Provenzale *et al.* 2002; Law *et al.* 2004]. Thus, targeting biopsy sites to more permeable areas may improve tumor grading, particularly in patients with a recurrent low-grade tumor that might transform into a high grade tumor. In the patients receiving anti-angiogenic treatment using recent developed drugs, measurement of permeability allows monitoring the decrease vascular permeability to test the therapeutic effect of these new drugs as well as their clinical scenarios[Batchelor *et al.* 2007].

The marker of vascular permeability is the leakage of paramagnetic contrast agent - most frequently, gadolinium, which may induce a gradient of local magnetic field leading to the modification of the T_1 relaxation time. Using dynamic contrast-enhanced (DCE) MRI, the models called “pharmacokinetic” have been developed to quantify the leakage of contrast across the BBB[Tofts *et al.* 1991]. Calculating from DCE MR imaging, several parameters are used to measure permeability, including K^{trans}, the volume transfer constant

reflecting the rate of flux of contrast agent into the extracellular extravascular space, and V_e, the fractional volume of the extracellular extravascular space.

4.1.4 Measurement of diffusion coefficient

The diffusion-weighted imaging (DWI) is able to measure the diffusivity of water molecules in brain tissue. The apparent diffusion coefficient (ADC) maps calculated upon this imaging technique, which is widely available on present-day MRI machines, can provide information on cell density.

Combined with DWI, histological investigations on both animal and human have indicated that low ADC values correlated with increased cell density and proliferation in brain tumors[Chenevert *et al.* 2000; Higano *et al.* 2006]. Besides, regional increased ADC value within the tumor has been concerned as positive response to radiation therapy[Chenevert *et al.* 2000; Mardor *et al.* 2003; Moffat *et al.* 2005]. A recent study showed that, combined with radiologic response, quantification of ADC changes provided a more accurate prediction of survival in patients with high-grade gliomas[Hamstra *et al.* 2008].

Some preclinical studies showed that gliomas can escape the action of anti-angiogenic agents in terms of co-opting native brain blood vessels to infiltrate surrounding normal appearing tissue[Rubenstein *et al.* 2000; Kunkel *et al.* 2001]. As the areas where tumor cells co-opted with blood vessels with intact BBB, the growth of tumor is unlikely detected by conventional contrast MRI. In this instance, ADC has the potential to detect infiltrating tumor owing to sensitivity of increased cell density, which hold promise as a marker of tumor growth in response to treatments.

4.1.5 Local saturation of blood oxygen (lSO_2)

The tumor vessels induced by angiogenesis are often dilated and tortuous, with chaotic function in blood supply. This abnormal tumor vasculature leads to heterogeneity in tumor blood flow with some areas receiving high blood flow whereas others receive very little, so the existence of abnormal vasculature can not guarantee a favorable

oxygenation in tumoral tissue. In contrast to normal brain tissue, only 50% to 70% of newly formed glioma vessels are red blood cell perfused and that rate of perfusion falls below 25% in central areas of large tumors[Vajkoczy *et al.* 2004]. In addition, with a highly proliferation faster than vascularization, tumor cells likely meet up with an avascular environment deficient in oxygen rapidly. All these events suggest that hypoxia occurs frequently within tumoral tissue, which has been actually confirmed by quite a number of studies. Moreover, the hypoxia is in association with the aggressive phenotype promoting the tumoral progression and metastatic possibility, as well as the chemo- and radio-therapeutic resistant[Vaupel *et al.* 2001; Tatum *et al.* 2006; Brahimi-Horn *et al.* 2007; Jensen 2009]. Hence the measurements of lSO2 are necessary for optimizing tumor treatments.

The lSO2 measured by MRI is based on magnetic susceptibility (T_2*). The contrast agent used here is endogenous one: haemoglobin, because the oxygenated haemoglobin is less paramagnetic than deoxygenated haemoglobin. The method developed in laboratory to estimate the lSO_2 is based on measuring quantitative BOLD signal (qBOLD)[He *et al.* 2007; He *et al.* 2008]. The general opinion of this technique is that, if the macroscopic effects of magnetic field on the T_2* maps (T_2*_{corr}, corrected T_2* maps using a map of magnetic field of B_0) are exempted, the difference between the T_2 and T_2*_{corr} is principally due to the presence of blood deoxygenated haemoglobin.

4.1.6 ^{1}H-Magnetic resonance spectroscopy (^{1}H-MRS)

Although ^{1}H-MRS has a limited spatial resolution, it provides useful metabolic information for brain tumor diagnosis and glioma grading[Poptani *et al.* 1995; Kaminogo *et al.* 2001]. Lipids and lactates are two metabolites that have been mainly investigated as hypoxia markers. Increased lipids not only correlate to tumoral necrosis, but also represent an early response to tumor-cells bearing hypoxic stress[Barba *et al.* 1999; Li *et al.* 2005]. The correlation between lipids and grade in gliomas has been well established[Fayed *et al.* 2006]. As the end product of anaerobic metabolism, the increased lactates are considered

due to hypoxia occurring in tissue, but its significance in grading remains debatable[Howe *et al.* 2003; Walecki *et al.* 2003; Fayed *et al.* 2006]. Results from previous study indicated that the increased ratio of choline / NAA (N-Acetyl-Aspartate) with / or the presence of lipids or lactates makes suspicions of a rapid evolution or a transformation undergoing in low grade glioma [Law *et al.* 2003]. Because either lipid or lactate have been identified in hypoxic areas and have been correlated with the rCBV in malignant gliomas[Li *et al.* 2005], the ^{1}H-MRS is likely able to be used as a complementary method for checking brain tumor treatment.

4.1.7 BOLD functional MRI

The functional MRI based on the BOLD signal analysis, enables to imaging non-invasively active brain regions via measuring the assumed hemodynamic response correlated indirectly with neuronal activity. This technique has been widely used to ascertain functional areas before surgical intervention[Atlas *et al.* 1996; Maldjian *et al.* 1997; Schulder *et al.* 1998; Roux *et al.* 1999] and to estimate lesion-induced cortical function reorganization[Krainik *et al.* 2003; Krainik *et al.* 2004] in last two decades.

Imaging of vascular reactivity using fMRI during carbogen inhalation, which is developed in this work, is able to investigate the common structural characteristics of microvasculature, and to explore perfusion changes in adjacent tissue of cerebral lesion. This technique enables ones to better interpreter the false negative fMRI activation in patients with cerebral pathological changes at an individual level[Krainik *et al.* 2005; Jiang *et al.* 2009]. In addition, owing to the capability of the evaluation of microvasculature structure, this technique is likely to investigate the correlation between vascular reactivity and hypoxia in brain tumors, which may predict the chemo- and radio-therapeutic resistance. This issue is undergoing in our laboratory.

4.2 Multimodal Imaging Approach

MRI is not the only means to know the lesion vascularization. Two other main

complementary or concurrent methods can be used for some measurement.

4.2.1 Perfusion computed tomography (PCT)

The widespread clinical practice of perfusion computed tomography (PCT) was allowed by the recent introduction of rapid, large-coverage multi-slice spiral CT scanners. PCT is an imaging technique that permits a timely, quantitative evaluation of cerebral perfusion by generating parametric maps of perfusion, including that of CBV, CBF, and MTT[Wintermark *et al.* 2005]. With Patlak modeling to first-pass data, PCT enables one to calculate the maps of BBB permeability surface product (BBBP) reflecting the extent of BBB damage[Cianfoni *et al.* 2006; Bisdas *et al.* 2007; Goh *et al.* 2007; Lin *et al.* 2007].

In a similar way as it is done with DSC MRI, PCT uses also first-pass tracer methodology. The data are obtained by monitoring the signal (X-ray absorption coefficient) changes due to the first pass of an iodinated contrast agent bolus, which is injected intravenously by an automatic injector, through the cerebral vasculature. Generally speaking, the PCT data acquisition takes approximately in 1 minute[Wintermark *et al.* 2005].

The central volume principle is applied as the theoretical basis for PCT imaging. The linear relationship between contrast agent concentration and attenuation is used to calculate the amount of contrast agent in a given region from the degree of transient increase in attenuation. Time versus contrast-concentration curves are for each pixel of the scan, as well as for an arterial and a venous region of interest. The MTT map is then calculated from deconvolution of arterial and tissue enhancement curves. CBV is calculated as the area under the curve in a parenchymal pixel divided by the area under the curve in the venous pixel. Based on central volume principle, the CBF can be calculated with the equation CBF=CBV/MTT[Wintermark *et al.* 2001].

Deconvolution analysis not only gives quantitatively accurate results, but also allows much lower contrast material injection rates, which are more practical and tolerable for patients, without impairment of analysis accuracy[Wintermark *et al.* 2001].

Previous studies showed that microvascular permeability increases with increasing biologic aggressiveness of tumors, while a reduction in permeability in response to anti-angiogenic treatment associated with decreased tumor growth[Roberts *et al.* 2000; Provenzale *et al.* 2002; Law *et al.* 2004; Batchelor *et al.* 2007]. As indicating by the results from an initial study, a measurement of microvascular permeability performed by PCT (BBBP) showed to be predictive of pathologic agrade and to correlate with tumor mitotic activity[Cenic *et al.* 2000]. High BBBP values were located in the tumor only, and not in the surrounding tissues[Roberts *et al.* 2002a; Roberts *et al.* 2002b]. In addiction, PCT is likely to help in distinguishing glial neoplasms from extra-axial tumors and metastases[Cianfoni *et al.* 2006].

In comparison with MR imaging, PCT has more advantages in the assessment of tumor angiogenesis, given the linear relationship between contrast agent concentration and attenuation changes, the lack of sensitivity to flow, the high spatial resolution, and the absence of susceptibility artifacts. Nevertheless, compared with MR, there are some limitations for microvasculature evaluation using PCT, such as the exposure to ionizing radiation, the potential for adverse reaction to the contrast agent, and the limited anatomic coverage[Roberts *et al.* 2002a; Roberts *et al.* 2002b]. Whereas, some efforts have been explored to improve PCT clinical practice, including optimizing the PCT protocol by developing low kV and mAs technique for data acquisition, using low rate of injection of contrast agent, as well as optimizing the data post-processing technique[Wintermark *et al.* 2000; Wintermark *et al.* 2001; Josephson *et al.* 2005].

4.2.2 Nuclear medicine techniques (SPECT or PET)

Nuclear medicine techniques, such as single-photon emission-computed tomography (SPECT) and positron emission tomography (PET), can also explore metabolic and functional parameters of brain tumor.

4.2.2.1 SPECT

The tumoral uptake of TI-201 or Sestamibi Tc-99m on SPECT has been correlated with proliferative activity[Higa *et al.* 2001; Le Jeune *et al.* 2006]. The level of uptake

index, calculated by tumoral uptake/contralateral normal tissue uptake, is likely to help in glioma grading[Comte *et al.* 2006].

4.2.2.2 PET

18F-fluorodeoxyglucose (FDG) uptake is generally high in high-grade brain tumors. The prognostic value of FDG uptake is well established owing to early diagnosis of anaplastic transformation in a previously known low-grade glioma with high FDG uptake[De Witte *et al.* 1996; Padma *et al.* 2003]. However, with the high physiological glucose metabolic rate of normal brain tissue, FDG-PET is hardly able to detect tumors with modest increases in glucose metabolism such as low-grade tumors and, in some cases, recurrent high-grade tumors[Olivero *et al.* 1995; Ricci *et al.* 1998].

New PET tracers going beyond FDG are being developed, for instance, 3'-deoxy-3'-18F-fluorothymidine (FLT) and 18F-fluoromisonidazole (FMISO).

In gliomas, studies indicated that elevated FLT uptake is associated with elevated Ki-67 labeling that represents mitotic activity[Chen *et al.* 2005; Ullrich *et al.* 2008]. Thus, as a marker of proliferation, FLT-PET has potential for assessing glioma growth when conventional imaging measures are unreliable such as in the setting of anti-angiogenic or cytostatic therapies[Chen *et al.* 2007].

FMISO-PET is a means of evaluation hypoxic areas within brain tumors [Tochon-Danguy *et al.* 2002]. Because hypoxia is not only an important factor for angiogenesis, but also a barrier to the efficacy of chemotherapy and radiotherapy, investigation of the extent of tumor hypoxia is likely to guide treatment. Recent studies on patients with glioma have shown that FMISO uptake was correlated with Ki-67 and VEGFR-1 expression, and elevated volume of FMISO uptake was also related to a shorter survival in this population[Cher *et al.* 2006; Spence *et al.* 2008].

4.2.2.3 Nuclear images fusion with conventional images

After coregistration and fusion PET images with high resolution 3D volume MRI images, the complementary metabolic information is able to improve diagnostic accuracy of biopsy specimens representing the more active areas within tumors [Sabbah *et al.* 2002;

Floeth *et al.* 2005; Pauleit *et al.* 2005] and to increase survival by more accurately defining radiation fields[Grosu *et al.* 2005].

4.3 Advantages of an integrated approach combining tumoral cytogenetic, serum biologic, and imaging parameters

Since the codeletion of chromosome 1p and19q is observed and then being suggested as a genetic biomarker associated with a better chemosensibility as well as a better clinical outcome in patients with oligodendroglial tumors[Reifenberger *et al.* 1994; Cairncross *et al.* 1998; Kujas *et al.* 2005; Cairncross *et al.* 2006; van den Bent *et al.* 2006], cytogenetics has nowadays an important role in the glioma characterization and its treatments.

The HIPK gene and BRAF gene, which locate on chromosome 7q, are recently identified as the significant genes in association with the oncogenesis in low grade astrocytomas, particularly in pilocytic astrocytomas [Bar *et al.* 2008; Deshmukh *et al.* 2008; Jones *et al.* 2008; Pfister *et al.* 2008]. In the glioblastomas, using multi technologic approaches, the mutation of IDH1 gene is firstly observed in about 10% cases and is correlated with young patients and with a favorable prognostic [Parsons *et al.* 2008]. The further investigations identified that the mutations of IDH1 and IDH2 occur in grade II, III and IV gliomas[Balss *et al.* 2008; Bleeker *et al.* 2009b; Yan *et al.* 2009]. In the grade III gliomas without 1p/19q deletion, the occurred mutation of IDH1 is likely to be associated with a better prognostic[Sanson *et al.* 2009; Yan *et al.* 2009]. All of these cytogenetic findings may provide a therapeutic target in future. In fact, results from previous studies have indicated the relationship between temozolomide therapy and the methylation of promoter of MGMT gene in glioblastomas[Hegi *et al.* 2005; Stupp *et al.* 2005; anonymity 2008; Project 2008]. Thus, it is more than likely that future individualization of a patient's treatment should be based on the patients' molecular signature.

Recently, the measure of the circulating collagen IV combined with imaging parameters including microvessel CBV and Ktrans is utilized to monitor anti-angiogenic

treatment efficacy in recurrent glioblastoma patients[Sorensen *et al.* 2009]. Interestingly, a composite statistic index calculated from these three parameters is more closely associated with survival than either metric alone.

As widely known today, the conventional MRI with contrast administration is routinely used as the simplest method for monitoring response to glioma therapy in clinical practice. The morphological information, such as the size of a lesion determined with either visual or more formal volumetry, is no longer enough to characterize timely the tumor progression, and to judge precisely the new therapeutic efficacies.

Because of applicable to a wide range of tumors as well as complement existing therapies, anti-angiogenesis therapy comes with the hope of major advance in the fight against cancer. The most crucial key in the development of anti-angiogenesis therapy for gliomas consists in identifying and validating clinically applicable surrogate markers of angiogenesis as well as the events referring angiogenic mechanisms. Besides, the development of the tumor is a dynamic process. At each step of the tumor cell division, some genetic alterations that control cellular multiplication as well as undergoing pathogenesis are likely to occur. Several molecules resulting from the tumor progression can be chosen as new pro- or anti-angiogenic targets. Up to now, more than 70 individual drugs and 30 treatment combinations have been tested on gliomas, some of which are in clinical trials[Gagner *et al.* 2005]. The further research endeavor considering the association of multi approaches could make real progress in this issue.

References

Akella, N. S., D. B. Twieg, T. Mikkelsen, F. H. Hochberg, S. Grossman*, et al.* "Assessment of brain tumor angiogenesis inhibitors using perfusion magnetic resonance imaging: quality and analysis results of a phase I trial." *J Magn Reson Imaging* 2004; 20(6): 913-22.

An, H. and W. Lin "Impact of intravascular signal on quantitative measures of cerebral oxygen extraction and blood volume under normo- and hypercapnic conditions using an asymmetric spin echo approach." *Magn Reson Med* 2003; 50(4): 708-16.

anonymity "The Cancer Genome Atlas Network Project. "Comprehensive genomic characterization defines human glioblastoma genes and core pathways."." *Nature* 2008; 455(7216): 1061-8.

Aronen, H. J., I. E. Gazit, D. N. Louis, B. R. Buchbinder, F. S. Pardo*, et al.* "Cerebral blood volume maps of gliomas: comparison with tumor grade and histologic findings." *Radiology* 1994; 191(1): 41-51.

Aronen, H. J., F. S. Pardo, D. N. Kennedy, J. W. Belliveau, S. D. Packard*, et al.* "High microvascular blood volume is associated with high glucose uptake and tumor angiogenesis in human gliomas." *Clin Cancer Res* 2000; 6(6): 2189-200.

Arthurs, O. J. and S. Boniface "How well do we understand the neural origins of the fMRI BOLD signal?" *Trends Neurosci* 2002; 25(1): 27-31.

Ashkanian, M., P. Borghammer, A. Gjedde, L. Ostergaard and M. Vafaee "Improvement of brain tissue oxygenation by inhalation of carbogen." *Neuroscience* 2008; 156(4): 932-8.

Atlas, S. W., R. S. Howard, 2nd, J. Maldjian, D. Alsop, J. A. Detre*, et al.* "Functional magnetic resonance imaging of regional brain activity in patients with intracerebral gliomas: findings and implications for clinical management." *Neurosurgery* 1996; 38(2): 329-38.

Attwell, D. and C. Iadecola "The neural basis of functional brain imaging signals." *Trends Neurosci* 2002; 25(12): 621-5.

Balss, J., J. Meyer, W. Mueller, A. Korshunov, C. Hartmann*, et al.* "Analysis of the IDH1 codon 132 mutation in brain tumors." *Acta Neuropathol* 2008; 116(6): 597-602.

Bar, E. E., A. Lin, T. Tihan, P. C. Burger and C. G. Eberhart "Frequent gains at chromosome 7q34 involving BRAF in pilocytic astrocytoma." *J Neuropathol Exp Neurol* 2008; 67(9): 878-87.

Barba, I., M. E. Cabanas and C. Arus "The relationship between nuclear magnetic resonance-visible lipids, lipid droplets, and cell proliferation in cultured C6 cells." *Cancer Res* 1999; 59(8): 1861-8.

Barbier, E. L., J. A. den Boer, A. R. Peters, A. R. Rozeboom, J. Sau*, et al.* "A model of the dual effect of gadopentetate dimeglumine on dynamic brain MR images." *J Magn Reson Imaging* 1999; 10(3): 242-53.

Barbier, E. L., L. Lamalle and M. Decorps "Methodology of brain perfusion imaging." *J Magn Reson Imaging* 2001; 13(4): 496-520.

Batchelor, T. T., A. G. Sorensen, E. di Tomaso, W. T. Zhang, D. G. Duda*, et al.* "AZD2171, a pan-VEGF receptor tyrosine kinase inhibitor, normalizes tumor vasculature and alleviates edema in glioblastoma patients." *Cancer Cell* 2007; 11(1): 83-95.

Bauchet, L., V. Rigau, H. Mathieu-Daude, D. Figarella-Branger, D. Hugues*, et al.* "French brain tumor data bank: methodology and first results on 10,000 cases." *J Neurooncol* 2007; 84(2): 189-99.

Beaumont, M., B. Lemasson, R. Farion, C. Segebarth, C. Remy, *et al.* "Characterization of tumor angiogenesis in rat brain using iron-based vessel size index MRI in combination with gadolinium-based dynamic contrast-enhanced MRI." *J Cereb Blood Flow Metab* 2009; 29(10): 1714-26.

Behin, A., K. Hoang-Xuan, A. F. Carpentier and J. Y. Delattre "Primary brain tumours in adults." *Lancet* 2003; 361(9354): 323-31.

Bisdas, S., M. Hartel, L. H. Cheong, T. S. Koh and T. J. Vogl "Prediction of subsequent hemorrhage in acute ischemic stroke using permeability CT imaging and a distributed parameter tracer kinetic model." *J Neuroradiol* 2007; 34(2): 101-8.

Bitzer, M., U. Klose, B. Geist-Barth, T. Nagele, F. Schick, *et al.* "Alterations in diffusion and perfusion in the pathogenesis of peritumoral brain edema in meningiomas." *Eur Radiol* 2002; 12(8): 2062-76.

Bitzer, M., T. Nagele, B. Geist-Barth, U. Klose, E. Gronewaller, *et al.* "Role of hydrodynamic processes in the pathogenesis of peritumoral brain edema in meningiomas." *J Neurosurg* 2000; 93(4): 594-604.

Bitzer, M., H. Topka, M. Morgalla, S. Friese, L. Wockel, *et al.* "Tumor-related venous obstruction and development of peritumoral brain edema in meningiomas." *Neurosurgery* 1998; 42(4): 730-7.

Bitzer, M., L. Wockel, A. R. Luft, A. K. Wakhloo, D. Petersen, *et al.* "The importance of pial blood supply to the development of peritumoral brain edema in meningiomas." *J Neurosurg* 1997; 87(3): 368-73.

Bleeker, E. J., M. A. van Buchem and M. J. van Osch "Optimal location for arterial input function measurements near the middle cerebral artery in first-pass perfusion MRI." *J Cereb Blood Flow Metab* 2009a; 29(4): 840-52.

Bleeker, F. E., S. Lamba, S. Leenstra, D. Troost, T. Hulsebos, *et al.* "IDH1 mutations at residue p.R132 (IDH1(R132)) occur frequently in high-grade gliomas but not in other solid tumors." *Hum Mutat* 2009b; 30(1): 7-11.

Boxerman, J. L., K. M. Schmainda and R. M. Weisskoff "Relative cerebral blood volume maps corrected for contrast agent extravasation significantly correlate with glioma tumor grade, whereas uncorrected maps do not." *AJNR Am J Neuroradiol* 2006; 27(4): 859-67.

Brahimi-Horn, M. C., J. Chiche and J. Pouyssegur "Hypoxia and cancer." *J Mol Med* 2007; 85(12): 1301-7.

Brami-Zylberberg, F., S. Grand, J. F. Le Bas and J. F. Meder "[MRI for oligodendrogliomas]." *Neurochirurgie* 2005; 51(3-4 Pt 2): 273-85.

Brasil Caseiras, G., O. Ciccarelli, D. R. Altmann, C. E. Benton, D. J. Tozer, *et al.* "Low-grade gliomas: six-month tumor growth predicts patient outcome better than admission tumor volume, relative cerebral blood volume, and apparent diffusion coefficient." *Radiology* 2009; 253(2): 505-12.

Brown, G. G., L. T. Eyler Zorrilla, B. Georgy, S. S. Kindermann, E. C. Wong, *et al.* "BOLD and perfusion response to finger-thumb apposition after acetazolamide administration: differential relationship to global perfusion." *J Cereb Blood Flow Metab* 2003; 23(7): 829-37.

Burton, E. C., K. R. Lamborn, P. Forsyth, J. Scott, J. O'Campo, *et al.* "Aberrant p53, mdm2, and proliferation differ in glioblastomas from long-term compared with typical survivors." *Clin Cancer Res* 2002; 8(1): 180-7.

Buxton, R. B., K. Uludag, D. J. Dubowitz and T. T. Liu "Modeling the hemodynamic response to brain activation." *Neuroimage* 2004; 23 Suppl 1: S220-33.

Cairncross, G., B. Berkey, E. Shaw, R. Jenkins, B. Scheithauer, *et al.* "Phase III trial of chemotherapy plus

radiotherapy compared with radiotherapy alone for pure and mixed anaplastic oligodendroglioma: Intergroup Radiation Therapy Oncology Group Trial 9402." *J Clin Oncol* 2006; 24(18): 2707-14.

Cairncross, J. G., K. Ueki, M. C. Zlatescu, D. K. Lisle, D. M. Finkelstein*, et al.* "Specific genetic predictors of chemotherapeutic response and survival in patients with anaplastic oligodendrogliomas." *J Natl Cancer Inst* 1998; 90(19): 1473-9.

Calamante, F., A. Connelly and M. J. van Osch "Nonlinear DeltaR*2 effects in perfusion quantification using bolus-tracking MRI." *Magn Reson Med* 2009; 61(2): 486-92.

Carmeliet, P. "Mechanisms of angiogenesis and arteriogenesis." *Nat Med* 2000; 6(4): 389-95.

Carmeliet, P. and R. K. Jain "Angiogenesis in cancer and other diseases." *Nature* 2000; 407(6801): 249-57.

Cenic, A., D. G. Nabavi, R. A. Craen, A. W. Gelb and T. Y. Lee "A CT method to measure hemodynamics in brain tumors: validation and application of cerebral blood flow maps." *AJNR Am J Neuroradiol* 2000; 21(3): 462-70.

Cha, S., E. A. Knopp, G. Johnson, S. G. Wetzel, A. W. Litt*, et al.* "Intracranial mass lesions: dynamic contrast-enhanced susceptibility-weighted echo-planar perfusion MR imaging." *Radiology* 2002; 223(1): 11-29.

Cha, S., T. Tihan, F. Crawford, N. J. Fischbein, S. Chang*, et al.* "Differentiation of low-grade oligodendrogliomas from low-grade astrocytomas by using quantitative blood-volume measurements derived from dynamic susceptibility contrast-enhanced MR imaging." *AJNR Am J Neuroradiol* 2005; 26(2): 266-73.

Chakrabarti, I., M. Cockburn, W. Cozen, Y. P. Wang and S. Preston-Martin "A population-based description of glioblastoma multiforme in Los Angeles County, 1974-1999." *Cancer* 2005; 104(12): 2798-806.

Chen, C. M., B. L. Hou and A. I. Holodny "Effect of age and tumor grade on BOLD functional MR imaging in preoperative assessment of patients with glioma." *Radiology* 2008; 248(3): 971-8.

Chen, W., T. Cloughesy, N. Kamdar, N. Satyamurthy, M. Bergsneider*, et al.* "Imaging proliferation in brain tumors with 18F-FLT PET: comparison with 18F-FDG." *J Nucl Med* 2005; 46(6): 945-52.

Chen, W., S. Delaloye, D. H. Silverman, C. Geist, J. Czernin*, et al.* "Predicting treatment response of malignant gliomas to bevacizumab and irinotecan by imaging proliferation with [18F] fluorothymidine positron emission tomography: a pilot study." *J Clin Oncol* 2007; 25(30): 4714-21.

Chenevert, T. L., L. D. Stegman, J. M. Taylor, P. L. Robertson, H. S. Greenberg*, et al.* "Diffusion magnetic resonance imaging: an early surrogate marker of therapeutic efficacy in brain tumors." *J Natl Cancer Inst* 2000; 92(24): 2029-36.

Cher, L. M., C. Murone, N. Lawrentschuk, S. Ramdave, A. Papenfuss*, et al.* "Correlation of hypoxic cell fraction and angiogenesis with glucose metabolic rate in gliomas using 18F-fluoromisonidazole, 18F-FDG PET, and immunohistochemical studies." *J Nucl Med* 2006; 47(3): 410-8.

Chiarelli, P. A., D. P. Bulte, R. Wise, D. Gallichan and P. Jezzard "A calibration method for quantitative BOLD fMRI based on hyperoxia." *Neuroimage* 2007; 37(3): 808-20.

Cianfoni, A., S. Cha, W. G. Bradley, W. P. Dillon and M. Wintermark "Quantitative measurement of blood-brain barrier permeability using perfusion-CT in extra-axial brain tumors." *J Neuroradiol* 2006; 33(3): 164-8.

Cohen, E. R., K. Ugurbil and S. G. Kim "Effect of basal conditions on the magnitude and dynamics of the Blood Oxygenation Level–Dependent fMRI response." *J Cereb Blood Flow Metab* 2002; 22(9):

1042-53.

Comte, F., L. Bauchet, V. Rigau, J. R. Hauet, M. Fabbro*, et al.* "Correlation of preoperative thallium SPECT with histological grading and overall survival in adult gliomas." *Nucl Med Commun* 2006; 27(2): 137-42.

Coomber, B., P. Stewart, K. Hayakawa, C. Farrel and R. Del Maestro "Quantitative morphology of human glioblastoma multiforme microvessels: structural basis of blood-brain barrier defect." *J Neurooncol* 1987; 5: 299-307.

D'Esposito, M., L. Y. Deouell and A. Gazzaley "Alterations in the BOLD fMRI signal with ageing and disease: a challenge for neuroimaging " *Nat Rev Neurosci* 2003; 4(11): 863-72.

Daumas-Duport, C., M. L. Tucker, H. Kolles, P. Cervera, F. Beuvon*, et al.* "Oligodendrogliomas. Part II: A new grading system based on morphological and imaging criteria." *J Neurooncol* 1997a; 34(1): 61-78.

Daumas-Duport, C., P. Varlet, M. L. Tucker, F. Beuvon, P. Cervera*, et al.* "Oligodendrogliomas. Part I: Patterns of growth, histological diagnosis, clinical and imaging correlations: a study of 153 cases." *J Neurooncol* 1997b; 34(1): 37-59.

De Witte, O., M. Levivier, P. Violon, I. Salmon, P. Damhaut*, et al.* "Prognostic value positron emission tomography with [18F]fluoro-2-deoxy-D-glucose in the low-grade glioma." *Neurosurgery* 1996; 39(3): 470-6; discussion 476-7.

Dennie, J., J. B. Mandeville, J. L. Boxerman, S. D. Packard, B. R. Rosen*, et al.* "NMR imaging of changes in vascular morphology due to tumor angiogenesis." *Magn Reson Med* 1998; 40(6): 793-9.

Deshmukh, H., T. H. Yeh, J. Yu, M. K. Sharma, A. Perry*, et al.* "High-resolution, dual-platform aCGH analysis reveals frequent HIPK2 amplification and increased expression in pilocytic astrocytomas." *Oncogene* 2008; 27(34): 4745-51.

Donahue, K. M., H. G. Krouwer, S. D. Rand, A. P. Pathak, C. S. Marszalkowski*, et al.* "Utility of simultaneously acquired gradient-echo and spin-echo cerebral blood volume and morphology maps in brain tumor patients." *Magn Reson Med* 2000; 43(6): 845-53.

Drake, C. T. and C. Iadecola "The role of neuronal signaling in controlling cerebral blood flow." *Brain Lang* 2007; 102(2): 141-52.

Ducray, F., G. Dutertre, D. Ricard, E. Gontier, A. Idbaih*, et al.* "[Advances in adults' gliomas biology, imaging and treatment]." *Bull Cancer* 2010; 97(1): 17-36.

Duffau, H., M. Lopes, F. Arthuis, A. Bitar, J. P. Sichez*, et al.* "Contribution of intraoperative electrical stimulations in surgery of low grade gliomas: a comparative study between two series without (1985-96) and with (1996-2003) functional mapping in the same institution." *J Neurol Neurosurg Psychiatry* 2005; 76(6): 845-51.

Engelhard, H. H., A. Stelea and A. Mundt "Oligodendroglioma and anaplastic oligodendroglioma: clinical features, treatment, and prognosis." *Surg Neurol* 2003; 60(5): 443-56.

Farkas, E. and P. G. Luiten "Cerebral microvascular pathology in aging and Alzheimer's disease." *Prog Neurobiol* 2001; 64(6): 575-611.

Fayed, N., H. Morales, P. J. Modrego and M. A. Pina "Contrast/Noise ratio on conventional MRI and choline/creatine ratio on proton MRI spectroscopy accurately discriminate low-grade from high-grade cerebral gliomas." *Acad Radiol* 2006; 13(6): 728-37.

Fisel, C. R., J. L. Ackerman, R. B. Buxton, L. Garrido, J. W. Belliveau, *et al.* "MR contrast due to microscopically heterogeneous magnetic susceptibility: numerical simulations and applications to cerebral physiology." *Magn Reson Med* 1991; 17(2): 336-47.

Floeth, F. W., D. Pauleit, H. J. Wittsack, K. J. Langen, G. Reifenberger, *et al.* "Multimodal metabolic imaging of cerebral gliomas: positron emission tomography with [18F]fluoroethyl-L-tyrosine and magnetic resonance spectroscopy." *J Neurosurg* 2005; 102(2): 318-27.

Friedlander, D. R., D. Zagzag, B. Shiff, H. Cohen, J. C. Allen, *et al.* "Migration of brain tumor cells on extracellular matrix proteins in vitro correlates with tumor type and grade and involves alphaV and beta1 integrins." *Cancer Res* 1996; 56(8): 1939-47.

Fujiwara, N., K. Sakatani, Y. Katayama, Y. Murata, T. Hoshino, *et al.* "Evoked-cerebral blood oxygenation changes in false-negative activations in BOLD contrast functional MRI of patients with brain tumors." *Neuroimage* 2004; 21(4): 1464-71.

Gagner, J. P., M. Law, I. Fischer, E. W. Newcomb and D. Zagzag "Angiogenesis in gliomas: imaging and experimental therapeutics." *Brain Pathol* 2005; 15(4): 342-63.

Gerstner, E. R., A. G. Sorensen, R. K. Jain and T. T. Batchelor "Advances in neuroimaging techniques for the evaluation of tumor growth, vascular permeability, and angiogenesis in gliomas." *Curr Opin Neurol* 2008; 21(6): 728-35.

Giese, A. and M. Westphal "Glioma invasion in the central nervous system." *Neurosurgery* 1996; 39(2): 235-50; discussion 250-2.

Ginsberg, L. E., G. N. Fuller, M. Hashmi, N. E. Leeds and D. F. Schomer "The significance of lack of MR contrast enhancement of supratentorial brain tumors in adults: histopathological evaluation of a series." *Surg Neurol* 1998; 49(4): 436-40.

Girouard, H. and C. Iadecola "Neurovascular coupling in the normal brain and in hypertension, stroke, and Alzheimer disease." *J Appl Physiol* 2006; 100(1): 328-35.

Goh, V., S. Halligan and C. I. Bartram "Quantitative tumor perfusion assessment with multidetector CT: are measurements from two commercial software packages interchangeable?" *Radiology* 2007; 242(3): 777-82.

Grandin, C. B. "Assessment of brain perfusion with MRI: methodology and application to acute stroke." *Neuroradiology* 2003; 45(11): 755-66.

Grandin, C. B., A. Bol, A. M. Smith, C. Michel and G. Cosnard "Absolute CBF and CBV measurements by MRI bolus tracking before and after acetazolamide challenge: repeatabilily and comparison with PET in humans." *Neuroimage* 2005; 26(2): 525-35.

Grosu, A. L., W. A. Weber, M. Franz, S. Stark, M. Piert, *et al.* "Reirradiation of recurrent high-grade gliomas using amino acid PET (SPECT)/CT/MRI image fusion to determine gross tumor volume for stereotactic fractionated radiotherapy." *Int J Radiat Oncol Biol Phys* 2005; 63(2): 511-9.

Haller, S., L. H. Bonati, J. Rick, M. Klarhofer, O. Speck, *et al.* "Reduced cerebrovascular reserve at CO2 BOLD MR imaging is associated with increased risk of periinterventional ischemic lesions during carotid endarterectomy or stent placement: preliminary results." *Radiology* 2008; 249(1): 251-8.

Hamel, E. "Perivascular nerves and the regulation of cerebrovascular tone." *J Appl Physiol* 2006; 100(3): 1059-64.

Hamstra, D. A., C. J. Galban, C. R. Meyer, T. D. Johnson, P. C. Sundgren, *et al.* "Functional diffusion map as

an early imaging biomarker for high-grade glioma: correlation with conventional radiologic response and overall survival." *J Clin Oncol* 2008; 26(20): 3387-94.

Hamzei, F., R. Knab, C. Weiller and J. Rother "The influence of extra- and intracranial artery disease on the BOLD signal in FMRI." *Neuroimage* 2003; 20(2): 1393-9.

He, J., K. Mokhtari, M. Sanson, Y. Marie, M. Kujas*, et al.* "Glioblastomas with an oligodendroglial component: a pathological and molecular study." *J Neuropathol Exp Neurol* 2001; 60(9): 863-71.

He, X. and D. A. Yablonskiy "Quantitative BOLD: mapping of human cerebral deoxygenated blood volume and oxygen extraction fraction: default state." *Magn Reson Med* 2007; 57(1): 115-26.

He, X., M. Zhu and D. A. Yablonskiy "Validation of oxygen extraction fraction measurement by qBOLD technique." *Magn Reson Med* 2008; 60(4): 882-8.

Hegi, M. E., A. C. Diserens, T. Gorlia, M. F. Hamou, N. de Tribolet*, et al.* "MGMT gene silencing and benefit from temozolomide in glioblastoma." *N Engl J Med* 2005; 352(10): 997-1003.

Hesselmann, V., O. Zaro Weber, C. Wedekind, T. Krings, O. Schulte*, et al.* "Age related signal decrease in functional magnetic resonance imaging during motor stimulation in humans." *Neurosci Lett* 2001; 308(3): 141-4.

Higa, T., S. Maetani, K. Yoichiro and S. Nabeshima "TI-201 SPECT compared with histopathologic grade in the prognostic assessment of cerebral gliomas." *Clin Nucl Med* 2001; 26(2): 119-24.

Higano, S., X. Yun, T. Kumabe, M. Watanabe, S. Mugikura*, et al.* "Malignant astrocytic tumors: clinical importance of apparent diffusion coefficient in prediction of grade and prognosis." *Radiology* 2006; 241(3): 839-46.

Hirai, T., R. Murakami, H. Nakamura, M. Kitajima, H. Fukuoka*, et al.* "Prognostic value of perfusion MR imaging of high-grade astrocytomas: long-term follow-up study." *AJNR Am J Neuroradiol* 2008; 29(8): 1505-10.

Hoge, R. D., J. Atkinson, B. Gill, G. R. Crelier, S. Marrett*, et al.* "Investigation of BOLD signal dependence on cerebral blood flow and oxygen consumption: the deoxyhemoglobin dilution model." *Magn Reson Med* 1999; 42(5): 849-63.

Holash, J., P. C. Maisonpierre, D. Compton, P. Boland, C. R. Alexander*, et al.* "Vessel cooption, regression, and growth in tumors mediated by angiopoietins and VEGF." *Science* 1999; 284(5422): 1994-8.

Holmes, T. M., J. R. Petrella and J. M. Provenzale "Distinction between cerebral abscesses and high-grade neoplasms by dynamic susceptibility contrast perfusion MRI." *AJR Am J Roentgenol* 2004; 183(5): 1247-52.

Holodny, A. I., M. Schulder, W. C. Liu, J. Wolko, J. A. Maldjian*, et al.* "The effect of brain tumors on BOLD functional MR imaging activation in the adjacent motor cortex: implications for image-guided neurosurgery." *AJNR Am J Neuroradiol* 2000; 21(8): 1415-22.

Hoshi, Y., N. Kobayashi and M. Tamura "Interpretation of near-infrared spectroscopy signals: a study with a newly developed perfused rat brain model." *J Appl Physiol* 2001; 90(5): 1657-62.

Hou, B. L., M. Bradbury, K. K. Peck, N. M. Petrovich, P. H. Gutin*, et al.* "Effect of brain tumor neovasculature defined by rCBV on BOLD fMRI activation volume in the primary motor cortex." *Neuroimage* 2006; 32(2): 489-97.

Howe, F. A., S. J. Barton, S. A. Cudlip, M. Stubbs, D. E. Saunders*, et al.* "Metabolic profiles of human brain tumors using quantitative in vivo 1H magnetic resonance spectroscopy." *Magn Reson Med* 2003;

49(2): 223-32.

Hund-Georgiadis, M., S. Zysset, S. Naganawa, D. G. Norris and D. Y. Von Cramon "Determination of cerebrovascular reactivity by means of FMRI signal changes in cerebral microangiopathy: a correlation with morphological abnormalities." *Cerebrovasc Dis* 2003; 16(2): 158-65.

Iadecola, C. "Neurovascular regulation in the normal brain and in Alzheimer's disease." *Nat Rev Neurosci* 2004; 5(5): 347-60.

Inoue, T., H. Shimizu, N. Nakasato, T. Kumabe and T. Yoshimoto "Accuracy and limitation of functional magnetic resonance imaging for identification of the central sulcus: comparison with magnetoencephalography in patients with brain tumors." *Neuroimage* 1999; 10(6): 738-48.

Ito, H., I. Kanno, M. Ibaraki, J. Hatazawa and S. Miura "Changes in human cerebral blood flow and cerebral blood volume during hypercapnia and hypocapnia measured by positron emission tomography." *Journal of Cerebral Blood Flow & Metabolism* 2003; 23(6): 665-70.

Jackson, R. J., G. N. Fuller, D. Abi-Said, F. F. Lang, Z. L. Gokaslan*, et al.* "Limitations of stereotactic biopsy in the initial management of gliomas." *Neuro Oncol* 2001; 3(3): 193-200.

Jain, R. K., E. di Tomaso, D. G. Duda, J. S. Loeffler, A. G. Sorensen*, et al.* "Angiogenesis in brain tumours." *Nat Rev Neurosci* 2007; 8(8): 610-22.

Jensen, D., L. A. Wolfe, D. E. O'Donnell and G. A. Davies "Chemoreflex control of breathing during wakefulness in healthy men and women." *J Appl Physiol* 2005; 98(3): 822-8.

Jensen, R. L. "Brain tumor hypoxia: tumorigenesis, angiogenesis, imaging, pseudoprogression, and as a therapeutic target." *J Neurooncol* 2009; 92(3): 317-35.

Jiang, Z., E. Ramos-Bombin, E. Barbier, I. Tropres, D. Hoffmann*, et al.* (2009). Impaired peritumoral BOLD signal using cerebral fMRI. European Congress of Radiology 2009. E. R. 2009. Vienna - Austria, Eur Radiol 2009. **19:** S210.

Jones, D. T., S. Kocialkowski, L. Liu, D. M. Pearson, L. M. Backlund*, et al.* "Tandem duplication producing a novel oncogenic BRAF fusion gene defines the majority of pilocytic astrocytomas." *Cancer Res* 2008; 68(21): 8673-7.

Josephson, S. A., W. P. Dillon and W. S. Smith "Incidence of contrast nephropathy from cerebral CT angiography and CT perfusion imaging." *NEUROLOGY* 2005; 64(10): 1805-6.

Jouanneau, E. "Angiogenesis and gliomas: current issues and development of surrogate markers." *Neurosurgery* 2008; 62(1): 31-50; discussion 50-2.

Kalaria, R. N. "Cerebral vessels in ageing and Alzheimer's disease." *Pharmacol Ther* 1996; 72(3): 193-214.

Kaminogo, M., H. Ishimaru, M. Morikawa, M. Ochi, R. Ushijima*, et al.* "Diagnostic potential of short echo time MR spectroscopy of gliomas with single-voxel and point-resolved spatially localised proton spectroscopy of brain." *Neuroradiology* 2001; 43(5): 353-63.

Kastrup, A., G. Kruger, G. H. Glover and M. E. Moseley "Assessment of cerebral oxidative metabolism with breath holding and fMRI." *Magn Reson Med* 1999a; 42(3): 608-11.

Kastrup, A., G. Kruger, G. H. Glover, T. Neumann-Haefelin and M. E. Moseley "Regional variability of cerebral blood oxygenation response to hypercapnia." *Neuroimage* 1999b; 10(6): 675-81.

Kastrup, A., G. Kruger, T. Neumann-Haefelin and M. E. Moseley "Assessment of cerebrovascular reactivity with functional magnetic resonance imaging: comparison of CO(2) and breath holding." *Magn Reson Imaging* 2001; 19(1): 13-20.

Kastrup, A., T. Q. Li, G. H. Glover, G. Kruger and M. E. Moseley "Gender differences in cerebral blood flow and oxygenation response during focal physiologic neural activity." *J Cereb Blood Flow Metab* 1999c; 19(10): 1066-71.

Kim, M. J., A. I. Holodny, B. L. Hou, K. K. Peck, C. S. Moskowitz*, et al.* "The effect of prior surgery on blood oxygen level-dependent functional MR imaging in the preoperative assessment of brain tumors." *AJNR Am J Neuroradiol* 2005; 26(8): 1980-5.

Kim, S. G., E. Rostrup, H. B. Larsson, S. Ogawa and O. B. Paulson "Determination of relative CMRO2 from CBF and BOLD changes: significant increase of oxygen consumption rate during visual stimulation." *Magn Reson Med* 1999; 41(6): 1152-61.

Kiselev, V. G., R. Strecker, S. Ziyeh, O. Speck and J. Hennig "Vessel size imaging in humans." *Magn Reson Med* 2005; 53(3): 553-63.

Krainik, A., H. Duffau, L. Capelle, P. Cornu, A. L. Boch*, et al.* "Role of the healthy hemisphere in recovery after resection of the supplementary motor area." *Neurology* 2004; 62(8): 1323-32.

Krainik, A., M. Hund-Georgiadis, S. Zysset and D. Y. von Cramon "Regional impairment of cerebrovascular reactivity and BOLD signal in adults after stroke." *Stroke* 2005; 36(6): 1146-52.

Krainik, A., S. Lehericy, H. Duffau, L. Capelle, H. Chainay*, et al.* "Postoperative speech disorder after medial frontal surgery: role of the supplementary motor area." *Neurology* 2003; 60(4): 587-94.

Krainik, A., S. Lehericy, H. Duffau, M. Vlaicu, F. Poupon*, et al.* "Role of the supplementary motor area in motor deficit following medial frontal lobe surgery." *Neurology* 2001; 57(5): 871-8.

Kremer, S., S. Grand, C. Remy, F. Esteve, V. Lefournier*, et al.* "Cerebral blood volume mapping by MR imaging in the initial evaluation of brain tumors." *J Neuroradiol* 2002; 29(2): 105-13.

Kujas, M., J. Lejeune, A. Benouaich-Amiel, E. Criniere, F. Laigle-Donadey*, et al.* "Chromosome 1p loss: a favorable prognostic factor in low-grade gliomas." *Ann Neurol* 2005; 58(2): 322-6.

Kunkel, P., U. Ulbricht, P. Bohlen, M. A. Brockmann, R. Fillbrandt*, et al.* "Inhibition of glioma angiogenesis and growth in vivo by systemic treatment with a monoclonal antibody against vascular endothelial growth factor receptor-2." *Cancer Res* 2001; 61(18): 6624-8.

Lacombe, P., C. Oligo, V. Domenga, E. Tournier-Lasserve and A. Joutel "Impaired cerebral vasoreactivity in a transgenic mouse model of cerebral autosomal dominant arteriopathy with subcortical infarcts and leukoencephalopathy arteriopathy." *Stroke* 2005; 36(5): 1053-8.

Lavi, S., D. Gaitini, V. Milloul and G. Jacob "Impaired cerebral CO2 vasoreactivity: association with endothelial dysfunction." *Am J Physiol Heart Circ Physiol* 2006; 291(4): H1856-61.

Law, M., S. Oh, J. S. Babb, E. Wang, M. Inglese*, et al.* "Low-grade gliomas: dynamic susceptibility-weighted contrast-enhanced perfusion MR imaging--prediction of patient clinical response." *Radiology* 2006a; 238(2): 658-67.

Law, M., S. Oh, G. Johnson, J. S. Babb, D. Zagzag*, et al.* "Perfusion magnetic resonance imaging predicts patient outcome as an adjunct to histopathology: a second reference standard in the surgical and nonsurgical treatment of low-grade gliomas." *Neurosurgery* 2006b; 58(6): 1099-107; discussion 1099-107.

Law, M., S. Yang, J. S. Babb, E. A. Knopp, J. G. Golfinos*, et al.* "Comparison of cerebral blood volume and vascular permeability from dynamic susceptibility contrast-enhanced perfusion MR imaging with glioma grade." *AJNR Am J Neuroradiol* 2004; 25(5): 746-55.

Law, M., S. Yang, H. Wang, J. S. Babb, G. Johnson, *et al.* "Glioma grading: sensitivity, specificity, and predictive values of perfusion MR imaging and proton MR spectroscopic imaging compared with conventional MR imaging." *AJNR Am J Neuroradiol* 2003; 24(10): 1989-98.

Law, M., R. J. Young, J. S. Babb, N. Peccerelli, S. Chheang, *et al.* "Gliomas: predicting time to progression or survival with cerebral blood volume measurements at dynamic susceptibility-weighted contrast-enhanced perfusion MR imaging." *Radiology* 2008; 247(2): 490-8.

Le Bas, J. F., S. Grand, A. Krainik, V. Lefournier, I. Tropres, *et al.* "[Perfusion MR imaging in brain tumors]." *J Radiol* 2006; 87(6 Pt 2): 807-21.

Le Bas, J. F., S. Grand, S. Kremer, I. Tropres, Z. Jiang, *et al.* "[Perfusion MR imaging for initial diagnosis and follow-up of brain tumors]." *Neurochirurgie* 2005; 51(3-4 Pt 2): 287-98.

Le Jeune, F. P., F. Dubois, S. Blond and M. Steinling "Sestamibi technetium-99m brain single-photon emission computed tomography to identify recurrent glioma in adults: 201 studies." *J Neurooncol* 2006; 77(2): 177-83.

Lee, S. P., T. Q. Duong, G. Yang, C. Iadecola and S. G. Kim "Relative changes of cerebral arterial and venous blood volumes during increased cerebral blood flow: implications for BOLD fMRI." *Magn Reson Med* 2001; 45(5): 791-800.

Lehericy, S., H. Duffau, P. Cornu, L. Capelle, B. Pidoux, *et al.* "Correspondence between functional magnetic resonance imaging somatotopy and individual brain anatomy of the central region: comparison with intraoperative stimulation in patients with brain tumors." *J Neurosurg* 2000; 92(4): 589-98.

Lehmann, P., J. N. Vallee, G. Saliou, P. Monet, A. Bruniau, *et al.* "Dynamic contrast-enhanced T2*-weighted MR imaging: a peritumoral brain oedema study." *J Neuroradiol* 2009; 36(2): 88-92.

Leon, S. P., R. D. Folkerth and P. M. Black "Microvessel density is a prognostic indicator for patients with astroglial brain tumors." *Cancer* 1996; 77(2): 362-72.

Lev, M. H., Y. Ozsunar, J. W. Henson, A. A. Rasheed, G. D. Barest, *et al.* "Glial tumor grading and outcome prediction using dynamic spin-echo MR susceptibility mapping compared with conventional contrast-enhanced MR: confounding effect of elevated rCBV of oligodendrogliomas [corrected]." *AJNR Am J Neuroradiol* 2004; 25(2): 214-21.

Levenberg, K. "A Method for the Solution of Certain Problems in Least Squares." *Quart. Appl. Math* 1944; 2: 164-168.

Li, X., D. B. Vigneron, S. Cha, E. E. Graves, F. Crawford, *et al.* "Relationship of MR-derived lactate, mobile lipids, and relative blood volume for gliomas in vivo." *AJNR Am J Neuroradiol* 2005; 26(4): 760-9.

Lin, K., K. S. Kazmi, M. Law, J. Babb, N. Peccerelli, *et al.* "Measuring elevated microvascular permeability and predicting hemorrhagic transformation in acute ischemic stroke using first-pass dynamic perfusion CT imaging." *AJNR Am J Neuroradiol* 2007; 28(7): 1292-8.

Liu, H. L., J. C. Huang, C. T. Wu and Y. Y. Hsu "Detectability of blood oxygenation level-dependent signal changes during short breath hold duration." *Magn Reson Imaging* 2002; 20(9): 643-8.

Liu, T. T., Y. Behzadi, K. Restom, K. Uludag, K. Lu, *et al.* "Caffeine alters the temporal dynamics of the visual BOLD response." *NeuroImage* 2004; 23(4): 1402-13.

Liu, W. C., S. C. Feldman, M. Schulder, A. J. Kalnin, A. I. Holodny, *et al.* "The effect of tumour type and distance on activation in the motor cortex." *Neuroradiology* 2005; 47(11): 813-9.

Logothetis, N. K., J. Pauls, M. Augath, T. Trinath and A. Oeltermann "Neurophysiological investigation of

the basis of the fMRI signal." *Nature* 2001; 412(6843): 150-7.

Logothetis, N. K. and B. A. Wandell "Interpreting the BOLD signal." *Annu Rev Physiol* 2004; 66: 735-69.

Lorenz, C., T. Benner, C. J. Lopez, H. Ay, M. W. Zhu*, et al.* "Effect of using local arterial input functions on cerebral blood flow estimation." *J Magn Reson Imaging* 2006; 24(1): 57-65.

Louis, D. N., H. Ohgaki, O. D. Wiestler and W. K. Cavenee WHO classification of Tumours of the Central Nervous System. 2007a. Lyon, IARC.

Louis, D. N., H. Ohgaki, O. D. Wiestler, W. K. Cavenee, P. C. Burger*, et al.* "The 2007 WHO classification of tumours of the central nervous system." *Acta Neuropathol* 2007b; 114(2): 97-109.

Ludemann, L., A. Forschler, W. Grieger and C. Zimmer "BOLD signal in the motor cortex shows a correlation with the blood volume of brain tumors." *J Magn Reson Imaging* 2006; 23(4): 435-43.

Maia, A. C., Jr., S. M. Malheiros, A. J. da Rocha, C. J. da Silva, A. A. Gabbai*, et al.* "MR cerebral blood volume maps correlated with vascular endothelial growth factor expression and tumor grade in nonenhancing gliomas." *AJNR Am J Neuroradiol* 2005; 26(4): 777-83.

Maldjian, J. A., M. Schulder, W. C. Liu, I. K. Mun, D. Hirschorn*, et al.* "Intraoperative functional MRI using a real-time neurosurgical navigation system." *J Comput Assist Tomogr* 1997; 21(6): 910-2.

Mardor, Y., R. Pfeffer, R. Spiegelmann, Y. Roth, S. E. Maier*, et al.* "Early detection of response to radiation therapy in patients with brain malignancies using conventional and high b-value diffusion-weighted magnetic resonance imaging." *J Clin Oncol* 2003; 21(6): 1094-100.

Marquardt, D. "An Algorithm for Least-Squares Estimation of Nonlinear Parameters." *SIAM J. Appl. Math* 1963; 11: 431-441.

Mills, S. J., T. A. Patankar, H. A. Haroon, D. Baleriaux, R. Swindell*, et al.* "Do cerebral blood volume and contrast transfer coefficient predict prognosis in human glioma?" *AJNR Am J Neuroradiol* 2006; 27(4): 853-8.

Miyati, T., T. Banno, M. Mase, H. Kasai, H. Shundo*, et al.* "Dual dynamic contrast-enhanced MR imaging." *J Magn Reson Imaging* 1997; 7(1): 230-5.

Moffat, B. A., T. L. Chenevert, T. S. Lawrence, C. R. Meyer, T. D. Johnson*, et al.* "Functional diffusion map: a noninvasive MRI biomarker for early stratification of clinical brain tumor response." *Proc Natl Acad Sci U S A* 2005; 102(15): 5524-9.

Murata, Y., K. Sakatani, Y. Katayama and C. Fukaya "Increase in focal concentration of deoxyhaemoglobin during neuronal activity in cerebral ischaemic patients." *J Neurol Neurosurg Psychiatry* 2002; 73(2): 182-4.

Naganawa, S., D. G. Norris, S. Zysset and T. Mildner "Regional differences of fMR signal changes induced by hyperventilation: comparison between SE-EPI and GE-EPI at 3-T." *J Magn Reson Imaging* 2002; 15(1): 23-30.

Nasseri, K. and J. R. Mills "Epidemiology of primary brain tumors in the Middle Eastern population in California, USA 2001-2005." *Cancer Detect Prev* 2009; 32(5-6): 363-71.

Ogawa, S., T. M. Lee, A. R. Kay and D. W. Tank "Brain magnetic resonance imaging with contrast dependent on blood oxygenation." *Proc Natl Acad Sci U S A* 1990; 87(24): 9868-72.

Ogawa, S., D. W. Tank, R. Menon, J. M. Ellermann, S. G. Kim*, et al.* "Intrinsic signal changes accompanying sensory stimulation: functional brain mapping with magnetic resonance imaging." *Proc Natl Acad Sci U S A* 1992; 89(13): 5951-5.

Olivero, W. C., S. C. Dulebohn and J. R. Lister "The use of PET in evaluating patients with primary brain tumours: is it useful?" *J Neurol Neurosurg Psychiatry* 1995; 58(2): 250-2.

Ostergaard, L., A. G. Sorensen, K. K. Kwong, R. M. Weisskoff, C. Gyldensted*, et al.* "High resolution measurement of cerebral blood flow using intravascular tracer bolus passages. Part II: Experimental comparison and preliminary results." *Magn Reson Med* 1996; 36(5): 726-36.

Padera, T. P., B. R. Stoll, J. B. Tooredman, D. Capen, E. di Tomaso*, et al.* "Pathology: cancer cells compress intratumour vessels." *Nature* 2004; 427(6976): 695.

Padma, M. V., S. Said, M. Jacobs, D. R. Hwang, K. Dunigan*, et al.* "Prediction of pathology and survival by FDG PET in gliomas." *J Neurooncol* 2003; 64(3): 227-37.

Parsons, D. W., S. Jones, X. Zhang, J. C. Lin, R. J. Leary*, et al.* "An integrated genomic analysis of human glioblastoma multiforme." *Science* 2008; 321(5897): 1807-12.

Pathak, A. P., K. M. Schmainda, B. D. Ward, J. R. Linderman, K. J. Rebro*, et al.* "MR-derived cerebral blood volume maps: issues regarding histological validation and assessment of tumor angiogenesis." *Magn Reson Med* 2001; 46(4): 735-47.

Pauleit, D., F. Floeth, K. Hamacher, M. J. Riemenschneider, G. Reifenberger*, et al.* "O-(2-[18F]fluoroethyl)-L-tyrosine PET combined with MRI improves the diagnostic assessment of cerebral gliomas." *Brain* 2005; 128(Pt 3): 678-87.

Paulson, E. S. and K. M. Schmainda "Comparison of dynamic susceptibility-weighted contrast-enhanced MR methods: recommendations for measuring relative cerebral blood volume in brain tumors." *Radiology* 2008; 249(2): 601-13.

Pfister, S., W. G. Janzarik, M. Remke, A. Ernst, W. Werft*, et al.* "BRAF gene duplication constitutes a mechanism of MAPK pathway activation in low-grade astrocytomas." *J Clin Invest* 2008; 118(5): 1739-49.

Poptani, H., R. K. Gupta, R. Roy, R. Pandey, V. K. Jain*, et al.* "Characterization of intracranial mass lesions with in vivo proton MR spectroscopy." *AJNR Am J Neuroradiol* 1995; 16(8): 1593-603.

Project "The Cancer Genome Atlas Network Project. "Comprehensive genomic characterization defines human glioblastoma genes and core pathways."." *Nature* 2008; 455(7216): 1061-8.

Provenzale, J. M., P. McGraw, P. Mhatre, A. C. Guo and D. Delong "Peritumoral brain regions in gliomas and meningiomas: investigation with isotropic diffusion-weighted MR imaging and diffusion-tensor MR imaging." *Radiology* 2004; 232(2): 451-60.

Provenzale, J. M., G. R. Wang, T. Brenner, J. R. Petrella and A. G. Sorensen "Comparison of permeability in high-grade and low-grade brain tumors using dynamic susceptibility contrast MR imaging." *AJR Am J Roentgenol* 2002; 178(3): 711-6.

Rauscher, A., J. Sedlacik, M. Barth, E. M. Haacke and J. R. Reichenbach "Nonnvasive assessment of vascular architecture and function during modulated blood oxygenation using susceptibility weighted magnetic resonance imaging." *Magn Reson Med* 2005; 54(1): 87-95.

Rebeles, F., J. Fink, Y. Anzai and K. R. Maravilla "Blood-brain barrier imaging and therapeutic potentials." *Top Magn Reson Imaging* 2006; 17(2): 107-16.

Reifenberger, J., G. Reifenberger, L. Liu, C. D. James, W. Wechsler*, et al.* "Molecular genetic analysis of oligodendroglial tumors shows preferential allelic deletions on 19q and 1p." *Am J Pathol* 1994; 145(5): 1175-90.

Restom, K., K. J. Bangen, M. W. Bondi, J. E. Perthen and T. T. Liu "Cerebral blood flow and BOLD responses to a memory encoding task: a comparison between healthy young and elderly adults." *NeuroImage* 2007; 37(2): 430-9.

Ricci, P. E., J. P. Karis, J. E. Heiserman, E. K. Fram, A. N. Bice*, et al.* "Differentiating recurrent tumor from radiation necrosis: time for re-evaluation of positron emission tomography?" *AJNR Am J Neuroradiol* 1998; 19(3): 407-13.

Riecker, A., W. Grodd, U. Klose, J. B. Schulz, K. Groschel*, et al.* "Relation between regional functional MRI activation and vascular reactivity to carbon dioxide during normal aging." *J Cereb Blood Flow Metab* 2003; 23(5): 565-73.

Roberts, H. C., T. P. Roberts, R. C. Brasch and W. P. Dillon "Quantitative measurement of microvascular permeability in human brain tumors achieved using dynamic contrast-enhanced MR imaging: correlation with histologic grade." *AJNR Am J Neuroradiol* 2000; 21(5): 891-9.

Roberts, H. C., T. P. Roberts, T. Y. Lee and W. P. Dillon "Dynamic contrast-enhanced computed tomography (CT) for quantitative estimation of microvascular permeability in human brain tumors." *Acad Radiol* 2002a; 9 Suppl 2: S364-7.

Roberts, H. C., T. P. Roberts, T. Y. Lee and W. P. Dillon "Dynamic, contrast-enhanced CT of human brain tumors: quantitative assessment of blood volume, blood flow, and microvascular permeability: report of two cases." *AJNR Am J Neuroradiol* 2002b; 23(5): 828-32.

Rosen, B. R., J. W. Belliveau, J. M. Vevea and T. J. Brady "Perfusion imaging with NMR contrast agents." *Magn Reson Med* 1990; 14(2): 249-65.

Rossini, P. M., C. Altamura, A. Ferretti, F. Vernieri, F. Zappasodi*, et al.* "Does cerebrovascular disease affect the coupling between neuronal activity and local haemodynamics?" *Brain* 2004; 127(Pt 1): 99-110.

Rossini, P. M., C. Calautti, F. Pauri and J. C. Baron "Post-stroke plastic reorganisation in the adult brain." *Lancet Neurol* 2003; 2(8): 493-502.

Rostrup, E., G. M. Knudsen, I. Law, S. Holm, H. B. Larsson*, et al.* "The relationship between cerebral blood flow and volume in humans." *NeuroImage* 2005; 24(1): 1-11.

Rostrup, E., I. Law, F. Pott, K. Ide and G. M. Knudsen "Cerebral hemodynamics measured with simultaneous PET and near-infrared spectroscopy in humans." *Brain Res* 2002; 954(2): 183-93.

Rother, J., R. Knab, F. Hamzei, J. Fiehler, J. R. Reichenbach*, et al.* "Negative dip in BOLD fMRI is caused by blood flow--oxygen consumption uncoupling in humans." *Neuroimage* 2002; 15(1): 98-102.

Roux, F. E., K. Boulanouar, J. P. Ranjeva, M. Tremoulet, P. Henry*, et al.* "Usefulness of motor functional MRI correlated to cortical mapping in Rolandic low-grade astrocytomas." *Acta Neurochir (Wien)* 1999; 141(1): 71-9.

Rubenstein, J. L., J. Kim, T. Ozawa, M. Zhang, M. Westphal*, et al.* "Anti-VEGF antibody treatment of glioblastoma prolongs survival but results in increased vascular cooption." *Neoplasia* 2000; 2(4): 306-14.

Sabbah, P., H. Foehrenbach, G. Dutertre, C. Nioche, O. DeDreuille*, et al.* "Multimodal anatomic, functional, and metabolic brain imaging for tumor resection." *Clin Imaging* 2002; 26(1): 6-12.

Sakatani, K., S. Chen, W. Lichty, H. Zuo and Y. P. Wang "Cerebral blood oxygenation changes induced by auditory stimulation in newborn infants measured by near infrared spectroscopy." *Early Hum Dev* 1999a; 55(3): 229-36.

Sakatani, K., Y. Katayama, T. Yamamoto and S. Suzuki "Changes in cerebral blood oxygenation of the frontal lobe induced by direct electrical stimulation of thalamus and globus pallidus: a near infrared spectroscopy study." *J Neurol Neurosurg Psychiatry* 1999b; 67(6): 769-73.

Sakatani, K., Y. Murata, N. Fujiwara, T. Hoshino, S. Nakamura*, et al.* "Comparison of blood-oxygen-level-dependent functional magnetic resonance imaging and near-infrared spectroscopy recording during functional brain activation in patients with stroke and brain tumors." *J Biomed Opt* 2007; 12(6): 062110.

Sanson, M., Y. Marie, S. Paris, A. Idbaih, J. Laffaire*, et al.* "Isocitrate dehydrogenase 1 codon 132 mutation is an important prognostic biomarker in gliomas." *J Clin Oncol* 2009; 27(25): 4150-4.

Schiffer, D., P. Cavalla, A. Dutto and L. Borsotti "Cell proliferation and invasion in malignant gliomas." *Anticancer Res* 1997; 17(1A): 61-9.

Schreiber, A., U. Hubbe, S. Ziyeh and J. Hennig "The influence of gliomas and nonglial space-occupying lesions on Blood-oxygen-level-dependent contrast enhancement." *AJNR Am J Neuroradiol* 2000; 21(6): 1055-63.

Schulder, M., J. A. Maldjian, W. C. Liu, A. I. Holodny, A. T. Kalnin*, et al.* "Functional image-guided surgery of intracranial tumors located in or near the sensorimotor cortex." *J Neurosurg* 1998; 89(3): 412-8.

Seifritz, E., D. Bilecen, D. Hanggi, R. Haselhorst, E. W. Radu*, et al.* "Effect of ethanol on BOLD response to acoustic stimulation: implications for neuropharmacological fMRI." *Psychiatry Res* 2000; 99(1): 1-13.

Shinojima, N., M. Kochi, J. Hamada, H. Nakamura, S. Yano*, et al.* "The influence of sex and the presence of giant cells on postoperative long-term survival in adult patients with supratentorial glioblastoma multiforme." *J Neurosurg* 2004; 101(2): 219-26.

Silvestrini, M., P. Pasqualetti, R. Baruffaldi, M. Bartolini, Y. Handouk*, et al.* "Cerebrovascular reactivity and cognitive decline in patients with Alzheimer disease." *Stroke* 2006; 37(4): 1010-5.

Sorensen, A. G., T. T. Batchelor, W. T. Zhang, P. J. Chen, P. Yeo*, et al.* "A "vascular normalization index" as potential mechanistic biomarker to predict survival after a single dose of cediranib in recurrent glioblastoma patients." *Cancer Res* 2009; 69(13): 5296-300.

Spampinato, M. V., C. Wooten, M. Dorlon, N. Besenski and Z. Rumboldt "Comparison of first-pass and second-bolus dynamic susceptibility perfusion MRI in brain tumors." *Neuroradiology* 2006; 48(12): 867-74.

Spence, A. M., M. Muzi, K. R. Swanson, F. O'Sullivan, J. K. Rockhill*, et al.* "Regional hypoxia in glioblastoma multiforme quantified with [18F]fluoromisonidazole positron emission tomography before radiotherapy: correlation with time to progression and survival." *Clin Cancer Res* 2008; 14(9): 2623-30.

Stefanovic, B., J. M. Warnking, E. Kobayashi, A. P. Bagshaw, C. Hawco*, et al.* "Hemodynamic and metabolic responses to activation, deactivation and epileptic discharges." *Neuroimage* 2005; 28(1): 205-15.

Stefanovic, B., J. M. Warnking and G. B. Pike "Hemodynamic and metabolic responses to neuronal inhibition." *NeuroImage* 2004; 22(2): 771-8.

Stefanovic, B., J. M. Warnking, K. M. Rylander and G. B. Pike "The effect of global cerebral vasodilation on focal activation hemodynamics." *Neuroimage* 2006; 30(3): 726-34.

Stippich, C., P. Freitag, J. Kassubek, P. Soros, K. Kamada*, et al.* "Motor, somatosensory and auditory cortex

localization by fMRI and MEG." *Neuroreport* 1998; 9(9): 1953-7.

Stupp, R., W. P. Mason, M. J. van den Bent, M. Weller, B. Fisher*, et al.* "Radiotherapy plus concomitant and adjuvant temozolomide for glioblastoma." *N Engl J Med* 2005; 352(10): 987-96.

Sugahara, T., Y. Korogi, M. Kochi, I. Ikushima, T. Hirai*, et al.* "Correlation of MR imaging-determined cerebral blood volume maps with histologic and angiographic determination of vascularity of gliomas." *AJR Am J Roentgenol* 1998; 171(6): 1479-86.

Tatum, J. L., G. J. Kelloff, R. J. Gillies, J. M. Arbeit, J. M. Brown*, et al.* "Hypoxia: importance in tumor biology, noninvasive measurement by imaging, and value of its measurement in the management of cancer therapy." *Int J Radiat Biol* 2006; 82(10): 699-757.

Tochon-Danguy, H. J., J. I. Sachinidis, F. Chan, J. G. Chan, C. Hall*, et al.* "Imaging and quantitation of the hypoxic cell fraction of viable tumor in an animal model of intracerebral high grade glioma using [18F]fluoromisonidazole (FMISO)." *Nucl Med Biol* 2002; 29(2): 191-7.

Tofts, P. S. and A. G. Kermode "Measurement of the blood-brain barrier permeability and leakage space using dynamic MR imaging. 1. Fundamental concepts." *Magn Reson Med* 1991; 17(2): 357-67.

Tropres, I., S. Grimault, A. Vaeth, E. Grillon, C. Julien*, et al.* "Vessel size imaging." *Magn Reson Med* 2001; 45(3): 397-408.

Tropres, I., L. Lamalle, M. Peoc'h, R. Farion, Y. Usson*, et al.* "In vivo assessment of tumoral angiogenesis." *Magn Reson Med* 2004; 51(3): 533-41.

Uematsu, H., M. Maeda and H. Itoh "Peritumoral brain edema in intracranial meningiomas evaluated by dynamic perfusion-weighted MR imaging: a preliminary study." *Eur Radiol* 2003; 13(4): 758-62.

Ullrich, R., H. Backes, H. Li, L. Kracht, H. Miletic*, et al.* "Glioma proliferation as assessed by 3'-fluoro-3'-deoxy-L-thymidine positron emission tomography in patients with newly diagnosed high-grade glioma." *Clin Cancer Res* 2008; 14(7): 2049-55.

Ulmer, J. L., L. Hacein-Bey, V. P. Mathews, W. M. Mueller, E. A. DeYoe*, et al.* "Lesion-induced pseudo-dominance at functional magnetic resonance imaging: implications for preoperative assessments " *Neurosurgery* 2004; 55(3): 569-79; discussion 580-1.

Ulmer, J. L., H. G. Krouwer, W. M. Mueller, M. S. Ugurel, M. Kocak*, et al.* "Pseudo-reorganization of language cortical function at fMR imaging: a consequence of tumor-Induced neurovascular uncoupling." *AJNR Am J Neuroradiol* 2003; 24(2): 213-7.

Vajkoczy, P., M. Farhadi, A. Gaumann, R. Heidenreich, R. Erber*, et al.* "Microtumor growth initiates angiogenic sprouting with simultaneous expression of VEGF, VEGF receptor-2, and angiopoietin-2." *J Clin Invest* 2002; 109(6): 777-85.

Vajkoczy, P. and M. D. Menger "Vascular microenvironment in gliomas." *Cancer Treat Res* 2004; 117: 249-62.

van den Bent, M. J., A. F. Carpentier, A. A. Brandes, M. Sanson, M. J. Taphoorn*, et al.* "Adjuvant procarbazine, lomustine, and vincristine improves progression-free survival but not overall survival in newly diagnosed anaplastic oligodendrogliomas and oligoastrocytomas: a randomized European Organisation for Research and Treatment of Cancer phase III trial." *J Clin Oncol* 2006; 24(18): 2715-22.

van der Zande, F. H., P. A. Hofman and W. H. Backes "Mapping hypercapnia-induced cerebrovascular reactivity using BOLD MRI." *Neuroradiology* 2005; 47(2): 114-20.

van Zijl, P. C., S. M. Eleff, J. A. Ulatowski, J. M. Oja, A. M. Ulug, *et al.* "Quantitative assessment of blood flow, blood volume and blood oxygenation effects in functional magnetic resonance imaging." *Nat Med* 1998; 4(2): 159-67.

Vaupel, P., O. Thews and M. Hoeckel "Treatment resistance of solid tumors: role of hypoxia and anemia." *Med Oncol* 2001; 18(4): 243-59.

Vaz, R., N. Borges, C. Cruz and I. Azevedo "Cerebral edema associated with meningiomas: the role of peritumoral brain tissue." *J Neurooncol* 1998; 36(3): 285-91.

Vaz, R., N. Borges, A. Sarmento and I. Azevedo "Reversion of phenotype of endothelial cells in brain tissue around glioblastomas." *J Neurooncol* 1996; 27: 127-132.

Vesely, A., H. Sasano, G. Volgyesi, R. Somogyi, J. Tesler, *et al.* "MRI mapping of cerebrovascular reactivity using square wave changes in end-tidal PCO2." *Magn Reson Med* 2001; 45(6): 1011-3.

von Deimling, A., K. von Ammon, D. Schoenfeld, O. D. Wiestler, B. R. Seizinger, *et al.* "Subsets of glioblastoma multiforme defined by molecular genetic analysis." *Brain Pathol* 1993; 3(1): 19-26.

Walecki, J., E. Tarasow, B. Kubas, Z. Czemicki, J. Lewko, *et al.* "Hydrogen-1 MR spectroscopy of the peritumoral zone in patients with cerebral glioma: assessment of the value of the method." *Acad Radiol* 2003; 10(2): 145-53.

Weisskoff, R. M., C. S. Zuo, J. L. Boxerman and B. R. Rosen "Microscopic susceptibility variation and transverse relaxation: theory and experiment." *Magn Reson Med* 1994; 31(6): 601-10.

Wetzel, S. G., S. Cha, G. Johnson, P. Lee, M. Law, *et al.* "Relative cerebral blood volume measurements in intracranial mass lesions: interobserver and intraobserver reproducibility study." *Radiology* 2002; 224(3): 797-803.

Wintermark, M., P. Maeder, J. P. Thiran, P. Schnyder and R. Meuli "Quantitative assessment of regional cerebral blood flows by perfusion CT studies at low injection rates: a critical review of the underlying theoretical models." *Eur Radiol* 2001; 11(7): 1220-30.

Wintermark, M., P. Maeder, F. R. Verdun, J. P. Thiran, J. F. Valley, *et al.* "Using 80 kVp versus 120 kVp in perfusion CT measurement of regional cerebral blood flow." *AJNR Am J Neuroradiol* 2000; 21(10): 1881-4.

Wintermark, M., M. Sesay, E. Barbier, K. Borbely, W. P. Dillon, *et al.* "Comparative overview of brain perfusion imaging techniques." *J. Neuroradiol* 2005; 32(5): 294-314.

Wirestam, R., L. Andersson, L. Ostergaard, M. Bolling, J. P. Aunola, *et al.* "Assessment of regional cerebral blood flow by dynamic susceptibility contrast MRI using different deconvolution techniques." *Magn Reson Med* 2000; 43(5): 691-700.

Wrensch, M., Y. Minn, T. Chew, M. Bondy and M. S. Berger "Epidemiology of primary brain tumors: current concepts and review of the literature." *Neuro Oncol* 2002; 4(4): 278-99.

Xu, H. L., H. M. Koenig, S. Ye, D. L. Feinstein and D. A. Pelligrino "Influence of the glia limitans on pial arteriolar relaxation in the rat." *Am J Physiol Heart Circ Physiol* 2004; 287(1): H331-9.

Yan, H., D. W. Parsons, G. Jin, R. McLendon, B. A. Rasheed, *et al.* "IDH1 and IDH2 mutations in gliomas." *N Engl J Med* 2009; 360(8): 765-73.

Young, G. S. "Advanced MRI of adult brain tumors." *Neurol Clin* 2007; 25(4): 947-73, viii.

Yousry, T. A., U. D. Schmid, H. Alkadhi, D. Schmidt, A. Peraud, *et al.* "Localization of the motor hand area to a knob on the precentral gyrus. A new landmark." *Brain* 1997; 120 (Pt 1): 141-57.

Zagzag, D., R. Amirnovin, M. A. Greco, H. Yee, J. Holash*, et al.* "Vascular apoptosis and involution in gliomas precede neovascularization: a novel concept for glioma growth and angiogenesis." *Lab Invest* 2000; 80(6): 837-49.

Zaharchuk, G., J. B. Mandeville, A. A. Bogdanov, Jr., R. Weissleder, B. R. Rosen*, et al.* "Cerebrovascular dynamics of autoregulation and hypoperfusion. An MRI study of CBF and changes in total and microvascular cerebral blood volume during hemorrhagic hypotension." *Stroke* 1999; 30(10): 2197-204; discussion 2204-5.

Zaharchuk, G., M. Yamada, M. Sasamata, B. G. Jenkins, M. A. Moskowitz*, et al.* "Is all perfusion-weighted magnetic resonance imaging for stroke equal? The temporal evolution of multiple hemodynamic parameters after focal ischemia in rats correlated with evidence of infarction." *J Cereb Blood Flow Metab* 2000; 20(9): 1341-51.

宋冰冰, 刘巍, 何惠, 孙喜文, 吴树龄, *et al.* "哈尔滨市南岗区脑瘤发病率时间趋势分析及预测." *哈尔滨医科大学学报* 2008; 42(4): 437-8.

翟秀伟, 邵永祥, 孙立红, 邢立举, 邹冬梅, et al. "大庆地区原发脑肿瘤流行病学研究." *齐齐哈尔医学院学报* 2008; 29(22): 2750-2.

Annexes

Production scientifique du Dr Zhen JIANG au cours de sa thèse (2007-2010)

Article dans des revues a comite de lecture :

Jiang Z, Le Bas JF, Grand S, Salon C, Pasteris C, Hoffmann D, Bing F, Berger F, Liu C, Krainik A. "Prognostic value of perfusion MR imaging in patients with oligodendroglioma: a survival study", ***Journal of Neuroradiology, 2010,*** à paraître

Jiang Z, Krainik A, David O, Salon C, Barbier E, Troprès I, Hoffmann D, Warnking J, Chabardes S, Berger F, Pasteris C, Grand S, Segebarth C, Gay E, Le Bas JF. "Impaired fMRI Activation in Patients with Primary Brain Tumors." ***Neuroimage, 2010,*** à paraître

Communications orales avec résumé publié :

Jiang Z, Krainik A, Barbier E, Troprès I, Hoffmann D, Chabardes S, Seigneuret E, Bing F, Grand S, Le Bas JF. "Altérations des activations péritumorales en IRM fonctionnelle." 56èmes Journées Françaises de Radiologie 2008, Paris – France. ***J Radiol 2008;89:p1232***

Jiang Z, Ramos-Bombin E, Barbier E, Tropres I, Hoffmann D, Grand S, Berger F, Le Bas JF, Krainik A. Impaired peritumoral BOLD signal using cerebral fMRI. European Congress of Radiology 2009, Vienna – Austria. ***Eur Radiol 2009;19:S210***

Le Bas JF, Grand S, **Jiang Z**, Remy C, Salon C, Krainik A, Berger F. Suivi en imagerie RMN de l'angiogénèse : un élément clé dans les gliomes. Journées de Neurologie de Langue Française 2009, Lille – France. ***Rev Neurol 2009;165:p159***

Posters avec résumé publié:

Jiang Z, Krainik A, Barbier E, Tropres I, Hoffmann D, Chabardes S, Seigneuret E, Bing F, Grand S, Le Bas JF. Altérations des activations péritumorales en IRM fonctionnelle. 56èmes Journées Françaises de Radiologie 2008, Paris – France. ***J Radiol 2008;89:p1580***

Krainik A, **Jiang Z**, Barbier E, Chabardes S, David O, Touvier J, Pasteris C, Grand S,

Berger F, Le Bas JF. IRM de perfusion et IRM BOLD au carbogène en neuro-oncologie : étude préliminaire. XXXVème congrès annuel de la Société Française de Neuroradiologie 2008; Paris – France. ***J Neuroradiol 2008;35:p8***

Jiang Z, Le Bas JF, Grand S, Salon C, Pasteris C, Berger F, Chabardes S, Remy C, Krainik A. Valeur pronositque de l'imagerie IRM de perfusion chez des patients porteurs d'oligodendrogliomes : étude de survie. 5èmes Journées scientifiques du CLARA 2010, Lyon– France. ***Bulletin du Cancer 2010;97:pS12***

Approche par IRM de la vascularisation tumorale et peri-tumorale en Neuro-Oncologie

Les plus fréquentes tumeurs cérébrales primitives chez l'adulte sont les gliomes. Depuis qu'il est établi que la néo-angiogenèse est liée fortement au mécanisme de croissance des gliomes, plusieurs drogues à visée anti-angiogénique ont étés développées et testés comme un traitement complémentaire en plus de radio- et chimiothérapie. De nouvelles approches par IRM ont été développées pour estimer non-invasivement la néo-angiogenèse tumorale in vivo et étudier son retentissement sur la vascularisation du tissu peritumoral. La première partie de cette thèse a permis d'évaluer la valeur pronostique de la mesure du volume sanguin cérébral (VSC) par l'IRM de perfusion pour la survie des patients qui portent un oligodendrogliome ou une tumeur mixte oligoastrocytaire. Les résultats montraient que le relatif VSC mesuré en IRM de perfusion de premier passage apparaissant comme un facteur pronostique pour la suive des patients. La deuxième partie de cette thèse vise à estimer la perfusion basale peri-tumorale par la technique de premier passage ainsi que la vasoréactivité peri-tumorale par la technique de l'IRMf lors d'inhalation de carbogène, pour évaluer les mécanismes patho-physiologique des altérations du signal BOLD à proximité des tumeurs cérébrales primitives. Les résultats indiquent que l'altération de perfusion basale ne peut pas expliquer le déficit de l'activation motrice au niveau du cortex moteur primaire. La réponse BOLD au carbogène était le meilleur facteur pour expliquer l'asymétrie de l'activation motrice.

Mots Clés : IRM de perfusion, Tumeur cérébrale, oligodendrogliome, facteur pronostique, vasoréactivité cérébrale, IRMf BOLD

Key words : perfusion MRI, brain tumor, oligodendroglioma, prognostic factor, cerebral vasoreactivity, BOLD fMRI

脑肿瘤及瘤周血管的磁共振成像研究

胶质瘤是最常见的成人原发性脑肿瘤。肿瘤性血管形成不仅与胶质瘤的增殖密切相关，同时也被视为抗肿瘤治疗的途径之一，越来越多的抑制肿瘤血管形成的药物被研发出来，并陆续进入临床前期试验。现代磁共振成像（MRI）技术能无创检测活体内的血管形成情况，因此在胶质瘤的诊治与新药物疗效评价中受到广泛关注。本论文的第一部分，即利用顺磁性造影剂首过效应的MRI 灌注成像技术，检测少突胶质细胞瘤的血流灌注情况，以此评价其在预测患者生存预后中的价值。研究结果显示，MRI 灌注成像技术检测肿瘤 CBV 能较好的预测该类患者的生存预后；同时提示，利用该技术得到的肿瘤 rCBV 值能为该类肿瘤恶性程度分级提供影像学参考指标。本论文的第二部分，即联合运用 MRI 灌注成像技术及 Carbogen 吸入的血氧水平依赖功能磁共振成像技术（BOLD fMRI），分别检测脑肿瘤患者肿瘤周围脑组织的局部血流灌注情况以及组织内的血管反应性，用以较精确地分析其与肿瘤侧脑功能区 BOLD 信号减弱之间的关系。研究结果表明，脑肿瘤患者肿瘤侧主动运动区 BOLD 信号的降低与局部脑血流灌注无明显显著性相关，却与局部脑组织血管反应性的改变呈显著正相关关系。这两项研究结果均显示，MRI 技术在检测与评价脑肿瘤的血管形成具有良好的应用前景。

关键词：磁共振灌注成像，脑肿瘤，少突胶质细胞瘤，预测因子，脑血管反应性，血氧水平依赖功能磁共振成像